Proceedings of the I·R·E

FEBRUARY 1940

VOLUME 28 NUMBER 2

Institute of Radio Engineers

Joint Meeting with American Section, International Scientific Radio Union

Washington, D. C., April 26 and 27, 1940

Fifteenth Annual Convention

Boston, Mass., June 27, 28, and 29, 1940

Pacific Coast Convention

Los Angeles, Calif., August 27 and 28, 1940

New York Meeting—Engineering Societies Building—March 6, 1940

33 West 39th Street, New York, N. Y.

SECTION MEETINGS

DETROIT
March 15

ATLANTA
March 15

LOS ANGELES
March 19

PITTSBURGH
March 19

CLEVELAND
March 28

PHILADELPHIA
March 7

WASHINGTON
March 11

SECTIONS

ATLANTA—Chairman, Ben Akerman; Secretary, J. G. Preston, 125 Vance Cir., Marietta, Ga.

BALTIMORE—Chairman, C. A. Ellert; Secretary, Alexander Whitney, 105 Shady Nook Ct., Catonsville, Md.

BOSTON—Chairman, W. L. Barrow; Secretary, P. K. McElroy, General Radio Co., 30 State St., Cambridge, Mass.

BUENOS AIRES—Chairman, A. M. Stevens; Secretary, E. E. Kapus, Bolivar 1743, Buenos Aires, Argentina.

BUFFALO-NIAGARA—Chairman, K. B. Hoffman; Secretary, E. C. Waud, 235 Huntington Ave., Buffalo, N. Y.

CHICAGO—Chairman, E. H. Kohler; Secretary, P. C. Sandretto, United Air Lines Transport Co., 5936 S. Cicero Ave., Chicago, Ill.

CINCINNATI—Chairman, C. H. Topmiller; Secretary, W. L. Schwesinger, Radio Station WSAI, Cincinnati, Ohio.

CLEVELAND—Chairman, R. L. Kline; Secretary, J. D. Woodward, WGAR, Hotel Statler, Cleveland, Ohio

CONNECTICUT VALLEY—Chairman, E. R. Sanders; Secretary, W. R. G. Baker, General Electric Co., Bridgeport, Conn.

DETROIT—Chairman, J. D. Kraus; Secretary, Paul Frincke, WJBK, 6559 Hamilton Ave., Detroit, Mich.

EMPORIUM—Chairman, C. R. Smith; Secretary, H. L. Ratchford, Hygrade Sylvania Corp., Emporium, Pa.

INDIANAPOLIS—Chairman, I. M. Slater; Secretary, B. V. K. French, P. R. Mallory & Co., E. Washington St., Indianapolis, Ind.

LOS ANGELES—Chairman, A. C. Packard; Secretary, J. N. A. Hawkins, 3239 Laclede Ave., Los Angeles, Calif.

MONTREAL—Chairman, A. B. Oxley; Secretary, W. A. Nichols, Canadian Broadcasting Corp., 1012 Keefer Bldg., Montreal, Que.

NEW ORLEANS—Chairman, G. H. Peirce; Secretary, D. W. Bowman, 8327 Sycamore St., New Orleans, La.

PHILADELPHIA—Chairman, R. S. Hayes; Secretary, R. L. Snyder, 103 Franklin Rd., Glassboro, N. J.

PITTSBURGH—Chairman, Joseph Baudino; Secretary, Gary Muffly, Gulf Research and Development Corp., Drawer 2038, Pittsburgh, Penna.

PORTLAND—Chairman, Marcus O'Day; Secretary, Earl Schoenfeld, 1627 S. E. Elliott Ave., Portland, Ore.

ROCHESTER—Chairman, W. F. Cotter; Secretary, H. C. Sheve, Stromberg-Carlson Telephone Manufacturing Co., Rochester, N. Y.

SAN FRANCISCO—Chairman, Carl Penther; Secretary, H. E. Held, 420 Market St., San Francisco, Calif.

SEATTLE—Chairman, R. M. Walker; Secretary, L. B. Cochran, University of Washington, Seattle, Wash.

TORONTO—Chairman, G. J. Irwin; Secretary, N. Potter, Canadian National Carbon Co., Ltd., 805 Davenport Rd., Toronto, Ont.

WASHINGTON—Chairman, L. C. Young; Secretary, E. M. Webster, Federal Communications Commission, Rm. 5319, New Post Office Bldg., Washington, D. C.

Proceedings of the I·R·E

Published Monthly by
The Institute of Radio Engineers, Inc.

VOLUME 28 — *February, 1940* — NUMBER 2

Entered as second-class matter October 26, 1927, at the post office at Menasha, Wisconsin, under the Act of February 28, 1925, embodied in Paragraph 4, Section 412 of the Postal Laws and Regulations. Publication office, 450 Ahnaip Street, Menasha, Wisconsin. Subscription, $10.00 per year; foreign, $11.00.

THE INSTITUTE

The Institute of Radio Engineers serves those interested in radio and allied electrical-communication fields through the presentation and publication of technical material. In 1913 the first issue of the PROCEEDINGS appeared; it has been published uninterruptedly since then. Over 1800 technical papers have been included in its pages and portray a currently written history of developments in both theory and practice.

STANDARDS

In addition to the publication of submitted papers, many thousands of man-hours have been devoted to the preparation of standards useful to engineers. These comprise the general fields of terminology, graphical and literal symbols, and methods of testing and rating apparatus. Members received a copy of each report. A list of the current issues of these reports follows:

Standards on Electroacoustics, 1938
Standards on Electronics, 1938
Standards on Radio Receivers, 1938
Standards on Radio Transmitters and Antennas, 1938.

MEETINGS

Meetings at which technical papers are presented are held in the twenty-three cities in the United States, Canada, and Argentina listed on the inside front cover of this issue. A number of special meetings are held annually and include one in Washington, D. C., in co-operation with the American Section of the International Scientific Radio Union (U.R.S.I.) in April, which is devoted to the general problems of wave propagation and measurement technique, the Rochester Fall Meeting in co-operation with the Radio Manufacturers Association in November, which is devoted chiefly to the problems of broadcast-receiver design, and the Annual Convention, the location and date of which are not fixed.

MEMBERSHIP

Membership has grown from a few dozen in 1912 to more than five thousand. Practically every country in the world in which radio engineers may be found is represented in our membership roster. Approximately a quarter of the membership is located outside of the United States. There are several grades of membership, depending on the qualifications of the applicant. Dues range between $3.00 per year for Students and $10.00 per year for Members. PROCEEDINGS are sent to each member without further payment.

PROCEEDINGS

The contents of each paper published in the PROCEEDINGS are the responsibility of the author and are not binding on the Institute or its members. Material appearing in the PROCEEDINGS may be reprinted or abstracted in other publications on the express condition that specific reference shall be made to its original appearance in the PROCEEDINGS. Illustrations of any variety may not be reproduced, however, without specific permission from the Institute.

Papers submitted to the Institute for publication shall be regarded as no longer confidential. They will be examined by the Papers Committee and Board of Editors to determine their suitability for publication. Suggestions on the mechanical form in which manuscripts should be prepared may be obtained from the Secretary.

SUBSCRIPTIONS

Annual subscription rates for the United States of America, its possessions, and Canada, $10.00; to college and public libraries when ordering direct, $5.00. Other countries, $1.00 additional.

The Institute of Radio Engineers, Inc.
Harold P. Westman, Secretary
330 West 42nd Street
New York, N.Y.

The Impetus Which Aviation Has Given to the Application of Ultra-High Frequencies*

W. E. JACKSON†, MEMBER, I.R.E.

Summary—*This paper briefly mentions some of the most important applications of ultra-high frequencies in the field of aeronautics and describes one of them in some detail. This is the ultra-high-frequency radio range, a short-wave counterpart of the conventional long-wave radio range which now provides directional guidance along the Federal Airways of the United States. A direct comparison is made between the two by means of graphs based on signal recordings made during flight tests of a standard long-wave range and an ultra-high-frequency range operating under the same conditions and at the same location near Pittsburgh, Pa. The advantages of ultra-high frequencies over low frequencies are strikingly illustrated.*

MODERN air transport relies upon radio to perform two very important jobs which are essential to regular dependable and safe flight operations. The importance and magnitude of these jobs have increased tremendously with the advent of larger aircraft, higher speeds, maintenance of rigid day and night schedules, and regular dependence upon instrument navigation. Those two jobs are to provide navigation guidance and to furnish instantaneous and reliable communications particularly while in flight and especially during bad weather or emergencies.

Until recently, almost all Government-operated navigational and telephone radio facilities have operated at low frequencies, chiefly between 200 and 400 kilocycles. Two-way radiotelephone transmissions from aircraft have been conducted almost entirely at medium high frequencies which may be segregated into two general groups; one in the neighborhood of 3000 kilocycles for night operations and the other centered about 5000 kilocycles for daylight use.

Any form of radio communication is subject to interruptions when atmospheric electrical disturbances become sufficiently violent. Communications at the lower radio frequencies are inherently more vulnerable to such disturbances. In addition to these atmospheric disturbances, there are still further difficulties created by high-speed flight of aircraft through electrically charged areas of nonuniform potentials usually associated with certain types of cloud formations, rain, snow, sleet, and dust.

The development and use of various types of shielded antennas and static-discharge devices have minimized to a considerable degree the possibility of interruptions due to precipitation electrical disturbances. The results of these developments have improved reliability, but it has not yet been possible to overcome completely all the limitations inherent in the relatively low frequencies. It has been recognized for several years that even a supplemental use of the ultra-high frequencies offered definite promise of a more complete solution to at least one of the most serious limitations of the lower frequencies, namely, interruptions of communications due to atmospheric interference. Experience has not only confirmed this, but has also indicated that there is a decided reduction in precipitation static although this improvement is not as great as with atmospheric disturbances. In pursuing this promise, numerous other advantages became apparent. Before enumerating some of these advantages, consider first the peculiar adaptability of aircraft at normal flight altitudes and their ability to use efficiently ultra-high frequencies which on the ground are more or less restricted to line-of-sight communications.

Some of the advantages of ultra-high frequencies for aircraft use are as follows:

1. Marked decrease of atmospheric static.
2. Diminution of precipitation static.
3. Reduction of multiple-course and bent-course phenomena in radio ranges.
4. Availability of frequencies in the ultra-high-frequency bands which may be used to relieve congestion in the lower frequency bands.
5. Permits the use of more efficient antennas on the aircraft with less aerodynamic drag.
6. More economical ground installations due primarily to smaller physical dimensions of antennas.
7. Permits the use of frequency modulation which possibly may give greatly improved signal-to-noise ratio.
8. Permits the operation of many stations on the same frequency without interference.

Some of the disadvantages of ultra-high frequencies for aircraft are:

1. Signal attenuates rapidly below line of sight.
2. Noise level of engine-ignition system in airplane at ultra-high frequencies is higher, thus requiring good shielding and bonding.
3. Directional effects of receiving antenna on aircraft.
4. Propeller modulation.

It is only possible here to discuss briefly one of the several advantages mentioned, that is, the reduction of multiple courses from an ultra-high-frequency range as compared to a low-frequency radio range[1] with

* Decimal classification: R520. Original manuscript received by the Institute, September 16, 1939; revised manuscript received, January 10, 1940. Presented, I.R.E.-U.R.S.I. meeting, Washington, D.C., April 29, 1939.

† Civil Aeronautics Authority, Washington, D.C.

[1] W. E. Jackson and D. M. Stuart, "Simultaneous radio range and telephone transmission," PROC. I.R.E., vol. 25, pp. 314–326; March, (1937).

which our national system of airways is now generally equipped.

The presence of multiple courses on low-frequency radio ranges has been found to be more pronounced when the station is located in mountainous terrain. A typical installation of this type is the station located

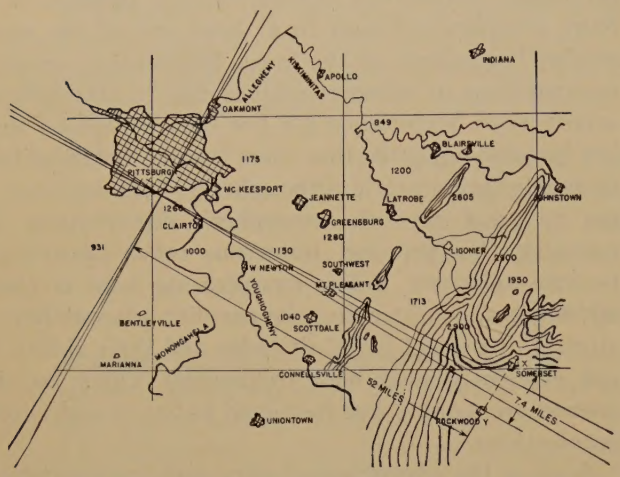

Fig. 1—Course orientation of both Pittsburgh range stations. (254 and 63,000 kilocycles.)

at Pittsburgh, Pa. This station operates at a frequency of 254 kilocycles.

Its geographical location with respect to Pittsburgh is shown on the map reproduced as Fig. 1, and is the point from which range courses are indicated as radiating at 90-degree intervals in four directions.

The courses are formed by two crossed figure-of-eight field patterns alternately produced to give *A* and *N* signals of equal amplitude at any point along the lines where adjacent patterns intersect. The ratio of these signals at any given point may be determined theoretically by scaling off the amplitude of the *N* and *A* field-strength patterns. It is therefore apparent that when *N* and *A* signals are equal and alternated without interruption, they will produce a steady continuous tone.

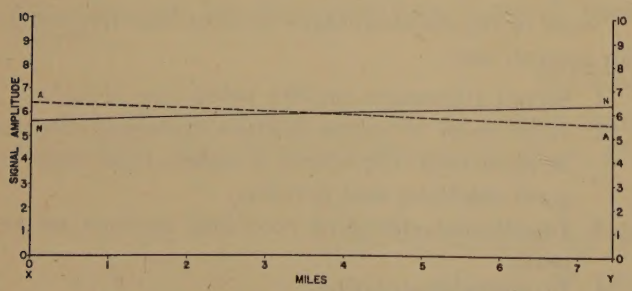

Fig. 2—Sector *X–Y* of *A* and *N* field-strength contours 52 miles from the range transmitter. (Theoretical.)

Let us now consider the sector included between the points $X - Y$ and determine the relative amplitude of the *A* and *N* signals. Fig. 2 graphically represents the theoretical signal amplitudes between the points *X* and *Y*. The abscissa has been magnified several times in order to indicate clearly the presence of multiple courses in actual recordings. Now compare this with Fig. 3, which is a graph made from the actual continuous recording of received signal amplitude.

Fig. 3 represents a recording of the 254-kilocycle range signals. In order to determine the actual signal amplitudes on 254 kilocycles, a recording of received signals was made in an airplane flying from point *X* to *Y* at a constant speed and altitude across the southeast course of the Pittsburgh range at a distance of 52 miles from the transmitter.

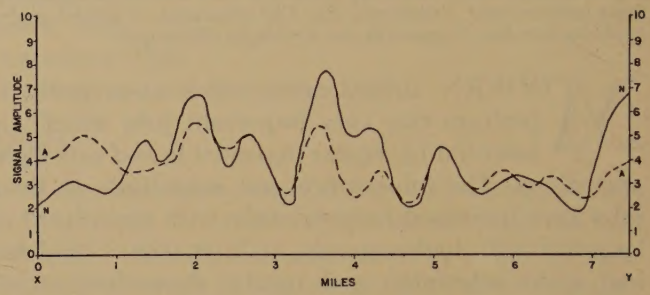

Fig. 3—Sector *X–Y* of *A* and *N* field-strength contours 52 miles from the 254-kilocycle transmitter. (Actual.)

In attempting to reconcile this actual recording with the theoretical and mentally translating it into the signals which the pilot heard while the recording was being made, it is obvious that the aircraft successively passed over several points where signals were of equal intensity. In other words, there was not just one course, or equisignal zone, but several.

At first thought, it might seem that courses with multiples of this magnitude would not be flyable. Actually, however, it is possible to follow with difficulty one of the very sharp multiples or a group of

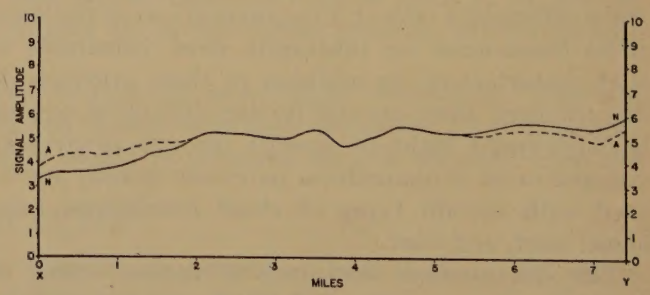

Fig. 4—Sector *X–Y* of *A* and *N* field-strength contours 52 miles from the 63,000-kilocycle transmitter. (Actual.)

multiple courses by aural integration. Multiple courses are therefore still considered a serious problem to air navigation by radio. The persistent search for a solution has probably given as great impetus to aeronautical application of the ultra-high frequencies as any other one factor, with the possible exception of the demand for additional frequencies for aviation and the need for frequencies inherently less vulnerable to atmospheric interference.

In order to obtain a direct comparison of the multiple-course phenomenon on 254 kilocycles as against 63,000 kilocycles, an ultra-high-frequency range was installed at Pittsburgh near the existing

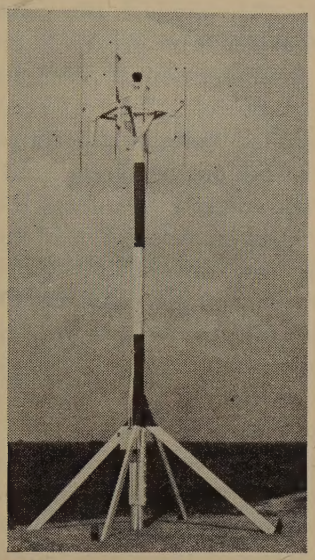

Fig. 5—Preliminary design of the ultra-high-frequency radio-range transmitting antenna.

low-frequency station. Courses were oriented to coincide with the low-frequency station as illustrated in Fig. 1. Identically, the same flight tests and recordings were made in checking the ultra-high-frequency range courses for multiples as were used in checking the low-frequency range. Fig. 4 shows a recording made on the 63-megacycle range under the same conditions and at the same place. It will be noted that this recording more nearly approaches the theoretical rela-

Fig. 6—Field in a vertical plane radiated from a 63-megacycle range antenna array $3\lambda/2$ above a typical earth.

tive amplitudes previously illustrated. The practical result is a clean-cut on-course signal on 63 megacycles free of multiple courses.

The next illustration, Fig. 5, shows one of the earlier 63-megacycle range antennas.[2] The height above ground was $1\frac{1}{2}$ wavelengths. It will be noted that vertical polarization is employed. The relative advantages and disadvantages of vertical and horizontal polarization cannot be adequately treated in this paper. Considerable work has been accomplished on a study of this phase of the development and a report probably will be published at a later date.

Fig. 6 shows the radiated field pattern in the vertical plane from the antenna illustrated in Fig. 5. The practical difficulties of flying a range course through several lobes are apparent; however, this is essentially the pattern produced by the 32- to 38-megacycle range equipment installed in Australia.

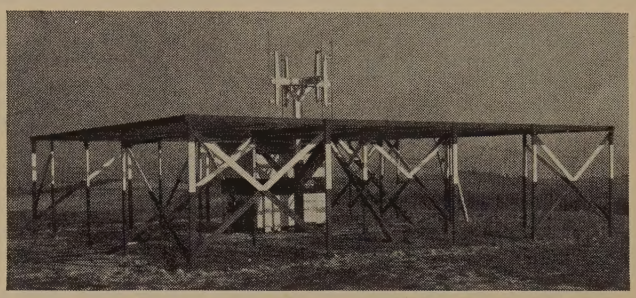

Fig. 7—Final design of the ultra-high-frequency radio-range station.

In this country, the advantages of eliminating the smaller spurious lobes were considered to be so important that experiments were continued, finally resulting in the antenna and ground-screen array illustrated in Fig. 7. This is the antenna arrangement used for the comparative tests at Pittsburgh.

The theoretical pattern in the vertical plane of an antenna $\frac{1}{4}$ wavelength above typical earth is shown in Fig. 8. The pattern obtained with the antenna above a counterpoise closely approaches this pattern.

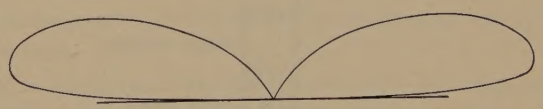

Fig. 8—Field in a vertical plane radiated from a 63-megacycle range antenna array $\lambda/4$ above a typical earth.

Many other aeronautical applications of the ultra-high frequencies could be described. Each would, however, justify separate treatment and therefore only mention has been made of a few of the more important applications which have added momentum to the really remarkable development on the very short waves.

[2] J. C. Hromada, "Preliminary Report on a Four Course Ultra-High-Frequency Radio Range," Bureau of Air Commerce Report No. 3, January, 1938.

Surface-Controlled Mercury-Pool Rectifier*

T. M. Libby†, member, I.R.E.

Summary—*A vertical water-jacketed pyrex cylinder having an anode at the upper end, a mercury-pool cathode in the lower end, and a high vapor pressure in the region of the cathode constitutes a new type of controlled high-voltage rectifier or switch.*

A boiler and deflector or nozzle system maintains a relatively high vapor pressure and corresponding low sparking potential in the region of the cathode while the water jacket maintains a low potential gradient and corresponding high sparking potential in the region of the anode.

When the water jacket is electrically connected to the cathode, its shielding action prevents the establishment by the anode potential of significant potential gradients through the high-pressure region resulting in high sparking potential. When a moderate alternating voltage is impressed between the water jacket and cathode, the high-pressure vapor is ionized periodically and the rectifier passes current during the positive half cycle of anode voltage. The value of the average current is limited by the voltage, circuit resistance, and duration of the conducting period. By varying the phase relation between the voltages impressed upon the water jacket and the anode, the instantaneous value of the anode voltage at which the arc is initiated for each cycle can be varied at will over approximately the entire positive half cycle of anode voltage.

When the water jacket is electrically connected to the anode, the rectifier passes current during the positive half cycle of anode voltage and effectively shields the anode from significant potential gradients during the negative half cycle. This shielding action greatly reduces the probability of inverse discharges, and permits the use of greater vapor pressure.

The device has been used for rectifying voltages from 3000 to 105,000 volts and currents up to the capacity of the available power supply.

Introduction

THE greatest obstacle in the development of high-voltage rectifiers has been the failure to obtain current capacities greater than a few amperes, together with a satisfactorily low probability of inverse discharge, or backfire, for applied voltages in excess of about 20,000 volts. This paper describes a new type of large-current rectifier in which the voltage required to produce backfire has been greatly increased as compared to that of conventionally designed rectifiers.

The inverse peak voltage across a rectifier consists of the peak applied voltage superimposed upon the direct voltage of the output circuit and is usually two or three times the value of the effective supply voltage. This inverse voltage may be greatly increased by unavoidable transients, and the ability of the rectifier to withstand inverse voltage may be lowered by the presence of high-frequency voltage in the rectifier circuit. In determining the voltage rating of a rectifier, it is necessary to provide a large overvoltage factor for the inverse voltage.

The voltage across the rectifier during the conducting period is simply the equivalent *IR* voltage drop and since this represents wasted power it should be only a small fraction of the applied voltage.

The hot-cathode high-vacuum type of rectifier is the only type that has been used commercially on supply voltages in excess of about 20,000. The current capacity of this type is limited to the electron emission of its hot cathode and its voltage drop is very high. Hence, this type is very inefficient compared to other electric devices. Such rectifiers cannot be economically used for the production of high-voltage direct current for power applications.

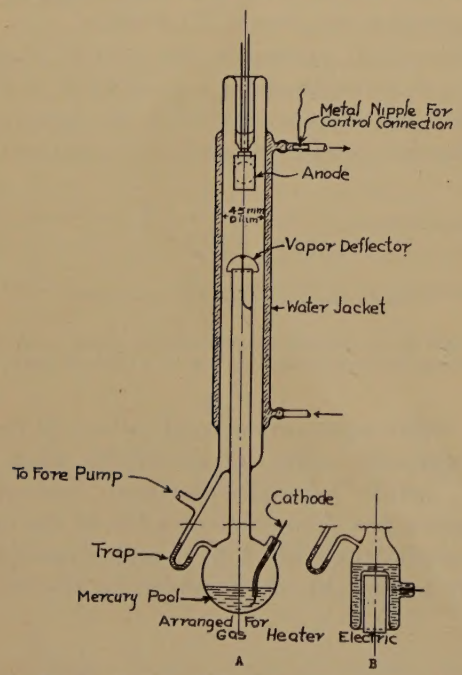

Fig. 1—Sectional view of Cordes-type surface-controlled mercury-pool rectifier.
A. Arrangement for gas heater.
B. Arrangement for electric heater.

Description

The new type of rectifier discussed herein consists essentially of an elongated cylindrical envelope of insulating material, such as pyrex, having a mercury-pool cathode at its lower end, an iron or graphite anode in the upper end, and a water jacket around the envelope for temperature control which also serves as a control electrode as later described and is referred to as the control surface.

The lower end of the device is adapted for heating the mercury pool by an externally applied electric or gas heater. The region between the anode and cathode, surrounded by the control surface, contains mercury vapor. This region is divided into two parts by a vapor-pressure interface. The low-pressure part adjacent to the anode is called the anode chamber, and the high-pressure part adjacent to the cathode is called the cathode chamber.

Several models have been tested with encouraging results. One of these models[1] is shown in section in Fig. 1. All of the models described herein conform to the specifications and claims of this patent. In the model of Fig. 1, the upper end of the cathode chamber

* Decimal classification: R356.3. Original manuscript received by the Institute, August 7, 1939. Presented, Pacific Coast Convention, San Francisco, Calif., June 28, 1939.

† Seattle, Washington.

[1] This model was developed by H. G. Cordes, Patent No. 2,105,463.

supports a vapor deflector, and the mercury container is adapted for heating by an external gas flame or electric heater. When the mercury is maintained at a temperature exceeding 120 degrees centigrade, the vapor pressure in the cathode chamber exceeds 1 millimeter of mercury. Mercury vapor from the cathode chamber is deflected outward and downward to the cooled side walls where it condenses, thence returns to the mercury pool via a mercury trap. In this manner the device functions as an efficient diffusion pump and maintains a very low foreign gas pressure in the anode chamber. A mechanical fore pump is required to reduce the back pressure against the diffusion pump.

The water jacket is electrically insulated from the grounded water supply and sink by 8 feet of pure rubber tubing.

Operating Characteristics

After outgassing the tube by passing a direct current of 10 amperes for about 8 hours, high voltages may be applied. With a mercury temperature of 140 degrees centigrade, a cooling-water supply temperature of 20 degrees centigrade and the control electrode free (see Fig. 2), gradually increasing the alternating voltage between the anode and the cathode produces no visible change in the rectifier until at 20,000 volts effective a diffused faint-green-colored glow fills the cathode chamber. A stroboscopic examination shows that this glow exists for only a portion of each half cycle of the applied voltage. This glow in the cathode chamber exists for all voltages up to the maximum tried which was 105,000 peak volts. The anode chamber remains dark for this range of voltages so long as the control electrode is isolated or connected to ground via the cooling-water connections.

When the control electrode is connected to the cathode, no visible change occurs in the rectifier as the anode voltage is varied over the above range, other than occasional threadlike discharges over the inner walls of the anode chamber.

With the anode isolated, gradually increasing the voltage between the control and cathode results in the formation of a green glow in the cathode chamber at an effective alternating voltage of 500. As the voltage on the control electrode is increased to 105,000, the glow in the cathode chamber becomes more intense but the anode chamber remains dark. As the control voltage is increased, the period during which the cathode-chamber glow exists is increased, but a dark period occurs at the zero voltage part of the applied voltage wave.

When the control electrode is connected to the anode, an arc is initiated each positive half cycle of the supply voltage. When the supply voltage is less than about 5000 volts effective, the instantaneous value of supply voltage at which the arc is initiated varies erratically from cycle to cycle between 750 and 1150 volts, as estimated with a cathode-ray oscilloscope. When the supply voltage is in the order of 10,000 or greater, the arc is initiated regularly at about 700 volts instantaneous value.

When the rectifier is delivering a very small direct current, in the order of 10 to 100 milliamperes, the cathode chamber is filled with a green glow, an intense white glow covers the surface of the mercury pool, the anode chamber is diffused with a pale blue or gray glow. The voltage drop across the rectifier is several hundred volts. When the current is increased to values greater than 100 milliamperes, cathode spots form on the surface of the mercury, the glow in the anode chamber does not change, but the glow in the cathode chamber increases greatly in intensity and whiteness. With 10 amperes direct current flowing, the cathode glow is so intense that observers must wear smoked glasses and a myriad of cathode spots dance about on the mercury pool. This intense glow extends up to the lower edge of the vapor deflector, clearly demarking the interface between the low and the high vapor pressures, or between the anode and the cathode chambers.

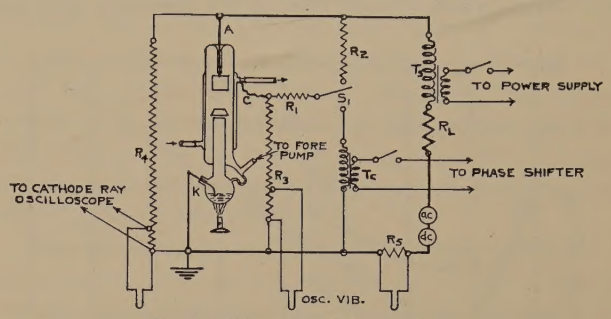

Fig. 2—Diagram of connections.
A = anode
K = cathode
C = control electrode
T_s = high-voltage supply transformer
T_c = control transformer, luminant-tube type
R_L = load resistance or filter input
R_1, R_2 = protection resistors, 1-megohm low wattage
R_3, R_4, R_5 = voltage divider resistors for oscillograph

The current-conducting capacity of mercury-arc rectifiers, for a given vapor pressure, is limited to that value of current at which a large percentage of all the atoms of vapor have been ionized. When about 50 per cent of the atoms of the vapor have been ionized a sharp rise in the voltage drop through the device occurs for further increases of current. This is thought to be due to a limitation in the number of positive ions, hence positive space charge, and the negative space charge then rapidly rises with slight increases of current. Also, when the current through the rectifier exceeds the value of current at which the voltage drop suddenly rises, the probability of inverse discharges increases greatly. An abrupt rise in the voltage drop, with increasing current, is accepted as the maximum value of current which the device can safely handle. This criterion assumes stable temperature control, freedom from foreign gas, and other conditions which might otherwise limit the sparking potential.

Referring to Fig. 3, the voltage-current characteristics of the rectifier shown in Fig. 1 are shown for two different temperatures of the mercury boiler. These temperatures were determined by a thermometer on the upper wall of the boiler and are not the actual temperatures of the mercury pool. Since this thermometer temperature lagged that of the mercury pool and

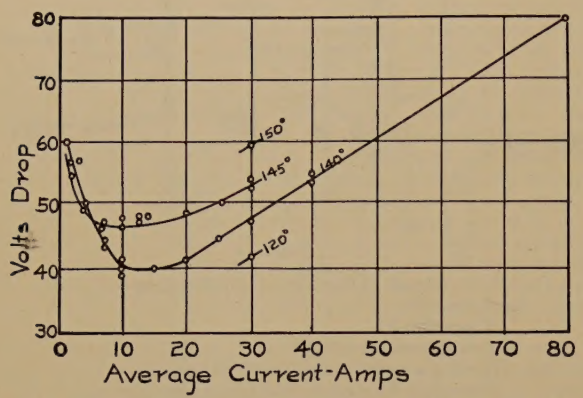

Fig. 3—Voltage drop through the rectifier of Fig. 1 versus average current for several boiler temperatures.

since the temperature of the pool varied with time, several different values of voltage drop were obtained for the same current and temperature as measured.

It will be noted that the voltage drop through the rectifier is a linear function of the current, on the positive characteristic, up to eighty amperes, at which value of current the cathode lead-in failed. This voltage-current characteristic indicates that for the particular tube tested the peak instantaneous value of current is equal to 80 amperes or more. While adequate anode-current capacity and cooling of the cathode were not provided in the test model for any such value of current, the characteristic shown indicates the current-carrying capacity of the limited cross-sectional area of arc path at the interface of the vapor pressures. When the rectifier of Fig. 1A has a boiler temperature of 140 degrees, thermometer, and a current of 11.5 amperes flowing, the gas heater may be removed and the boiler temperature remains constant. The boiler temperature of the rectifier, Fig. 1B, has a boiler temperature in equilibrium with the air temperature when a current of 20 amperes is flowing and the external heater is turned off. This difference in current for boiler-temperature equilibrium is due to the difference in the radiating surfaces of the two types of cathodes. For larger values of current these cathodes require cooling, and, conversely for smaller values of current external heat must be applied.

The voltage drop through the tube was measured as a function of boiler temperature for a constant current of 30 amperes average. The results of this test are shown in Fig. 4 which indicates that the voltage drop decreases with decreasing boiler temperature. This is at variance with the characteristics of the conventional mercury-arc rectifiers, and is probably due to the gradient in both vapor pressure and potential at the edge of the vapor deflector.

While the data of Fig. 4 indicate the desirability of decreasing the boiler temperature, the minimum temperature is fixed by a consideration of the pumping action and the arc-initiation voltage requirements. These will be discussed later.

Throughout the above-described tests, the cooling-water supply temperature was held between 20 and 23 degrees centigrade. The discharge-water temperature increased with increasing values of current.

Arc Initiation

When the boiler temperature is 110 degrees centigrade or greater, and a moderate alternating or rectified alternating voltage is applied between the control surface and cathode, the vapor in the cathode chamber is ionized, although no change occurs in the low-pressure anode chamber if the anode potential is zero or negative with respect to the cathode. When the potentials of the control surface and the anode are simultaneously positive with respect to the cathode, and the anode voltage exceeds about 200 volts, the ionization of the mercury vapor is accompanied by the formation of a large number of cathode spots on the surface of the mercury pool and an arc discharge between the cathode and anode. These cathode spots are the most copious electron emitters known, one spot furnishing as much as 30 amperes. The diffusion of the spots, probably caused by the high vapor pressure, is a distinct advantage in heavy-current rectifiers, since it

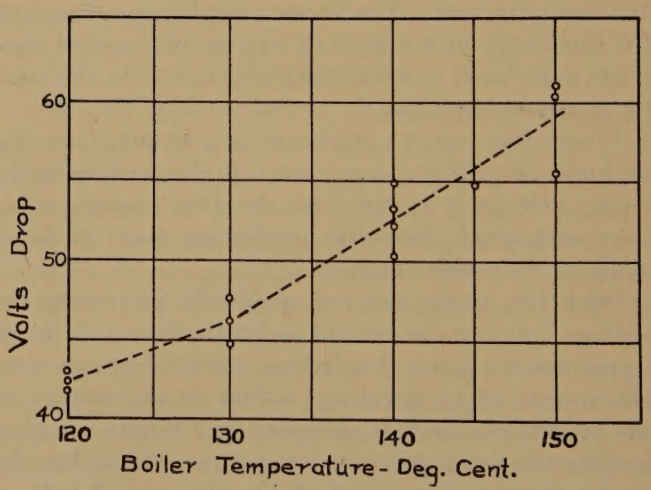

Fig. 4—Voltage drop versus boiler temperature for average current of 30 amperes, rectifier of Fig. 1.

avoids the formation of a large cathode spot at the interface of the mercury and the pyrex container, which would shorten the life of the device.

The voltage applied to the control surface for initiation of a new cathode for each conducting period may be obtained from the anode when conduction for the entire positive half cycle of anode voltage is desired. When control of the power output is desired, the control voltage is supplied by a small transformer and a

phase shifter. By adjusting the phase shifter, the arc may be initiated at any point on the positive half cycle of anode voltage, as shown in Fig. 5.

The high voltage gradient and high vapor pressure in the cathode chamber, made possible by the control surface as explained later, are ideal for ionization of

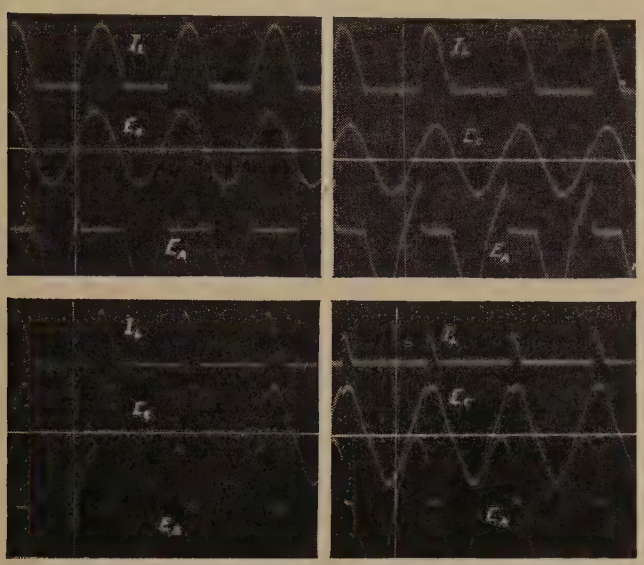

Fig. 5—Oscillograms of voltage and current relations. I_L=average current through rectifier. E_C=control voltage. E_A=voltage across rectifier.

the vapor in the region of the cathode. When the voltage of the control surface and the anode are both positive with respect to the cathode, electrons are probably accelerated toward the walls and the anode, and positive ions drift toward the cathode. As accumulative ionization progresses upward through the cathode chamber, the voltage gradient to the anode continuously increases, thereby further accelerating electrons to the anode, i.e., the gradient over the nonionized region increases progressively with accumulative ionization in the high-pressure region, until the arc is formed. In the high-pressure high-gradient region over the cathode, positive ions are formed in abundance and accelerated to the cathode, a condition conducive to rapid arc formation. An examination of the first oscillogram in Fig. 5 discloses that the arc formed when the instantaneous anode voltage was about 700, although when the control voltage is not applied, 105,000 volts, 60 cycles, between anode and cathode, fail to produce even a glow in the tube.

The separate control transformer used throughout the described tests was a luminant-tube transformer rated at 15 milliamperes, 6000 volts. As the boiler temperature is increased from 110 to 175 degrees centigrade, the control voltage required for initiating the arc decreases. However, for a rectifier having a fixed length and radius, there seems to be a minimum anode voltage which will initiate an arc, regardless of how great the control voltage may be.

The sparking potentials of many gases are lower than that of pure mercury vapor and the sparking potential of a mixture of several gases is lower than that of the component gas having the lowest individual sparking potential. The test data taken by the author strongly indicate that the presence of foreign gases may be one of the principal causes of high-voltage backfires. In the model shown in Fig. 1, the probability of backfire due to the presence of foreign gases is greatly reduced by the inclusion of the diffusion pump directly below the anode.

The presence of a hot cathode, keep-alive arc, or other continuous source of electrons in a rectifier will reduce the inverse sparking voltage to about one half of its value when no electron source is present. The models shown herein do not contain a continuous electron emitter, a new cathode being formed on the mercury pool for each conducting period.

Control Surface

The effect of the control surface during the conducting period is not known. Certainly the charge distribution on the side walls of the anode chamber is influenced by the potential impressed upon the control surface. Since this potential is positive during the conducting period, probably a larger number of electrons and fewer positive ions are collected on the side walls than would be if the control surface were free. The ratio of the positive space charge to negative space charge for a given current should therefore be greater than exists in a conventional rectifier having no control surface. This effect reduces the voltage drop for a given value of current.

The positive column of the arc is probably a plasma so that nearly all the ions in the anode chamber vanish due to recombination in about 10^{-4} seconds after the anode voltage passes through zero. Neutralization of the remaining space charge is probably accelerated by the high negative voltage on the control surface upon the reversal of the anode voltage.

The important functions of the control surface are performed during the nonconducting periods, when no space charges are present in the device. In the absence of space charges, Laplace's equation may be applied to determine the potential gradients established by the electrode potentials.

By means of Laplace's equation it may be shown that for a cylindrical container which is long compared to its radius, with zero wall potential, and having electrodes at opposite ends similar to the rectifier herein described, the potential of any point P within the cylinder may be expressed by

$$V_p = V_0 J_0\left(2.405\frac{a}{r}\right)\left(\exp -2.405\,\frac{d}{r}\right) \qquad (1)$$

where V_0 is the potential of one electrode, r is the radius of the cylinder, a is the distance of point P

from the axis of the cylinder, d is the distance from the end of the cylinder having the charged electrode to the point P, and $J_0(\ )$ is the Bessel function of the first kind.

By means of this expression, the equipotentials in a cylinder have been calculated and are shown on the

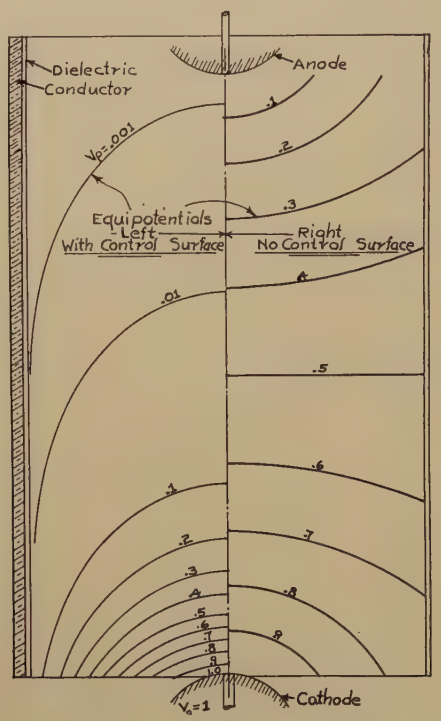

Fig. 6—Equipotentials in cylinder-plane section on axis; right of center line, no control surface. Left of center line, with control surface.

left side of Fig. 6, where the distance between anode and cathode is three times the radius. By contrast, the equipotentials without the cylindrical control surface are shown on the right side of the figure. These equipotentials as shown in Fig. 6 are cross-sectional views of equipotential surfaces where the section is taken in a plane through the axis of the cylinder. Referring to the above solution, or to the left side of Fig. 6, which embodies the control surface, it is seen that as the distance d from the charged cathode increases, the voltage gradient rapidly diminishes. For each increment of d equal to 0.96 r, this gradient is reduced to one tenth of its value at the point from which the increment was taken. At $d=3r$ (at the anode in Fig. 6) the potential is practically zero and if the anode be connected to the control surface the gradients would not differ appreciably from those shown. Without a cylindrical control surface (right side of Fig. 6), the potential gradient is almost uniform. Comparing the potential gradients for the two conditions, it is seen that the gradient over the upper two thirds of the distance between the electrodes, with the control surface, is only one sixth of that without the control surface. The gradient over the upper one third of the distance between the electrodes, with a control surface, is only one fortieth of that without the control surface.

Fig. 6 illustrates the degree in which the potential gradients in the vicinity of the anode may be greatly reduced, whereas in the vicinity of the cathode the gradients are increased approximately fourfold by the application of the control surface.

This increase in potential gradient at the cathode facilitates the initiation of a new arc for each conducting period of the rectifier. The effect of the decreased potential gradient in the vicinity of the anode will be discussed later.

Sparking Potentials

The sparking potentials of gases and vapors are theoretically defined by Paschen's law and have been determined experimentally by a large number of investigators. The sparking potential of mercury vapor as experimentally determined by Smede and Hull is shown in Fig. 7 for voltages up to 40,000. These experimental data agree very well with Paschen's law and if the sparking potential versus pressure times distance follows Paschen's law for voltages in excess of 40,000, the characteristic above this voltage would be as as shown by the broken line in Fig. 7.

For a rectifier having a fixed electrode separation, the vapor pressure for a given sparking potential may be determined from Fig. 7. The data of Fig. 7 is applicable only where neither sidewall effects nor a continuous source of electrons are present. This figure shows that

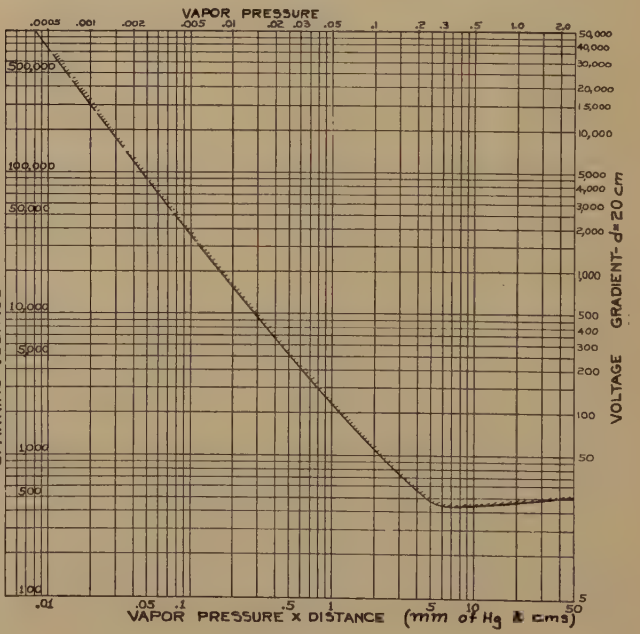

Fig. 7

for a given electrode separation d there is a vapor pressure at which the sparking voltage is a minimum. This pressure corresponding to the minimum sparking voltage is the pressure which should preferably be maintained in the cathode chamber of the rectifier herein described. Note that as the product pd increases from its value for minimum sparking voltage, the sparking voltage rises gradually, whereas, if the value pd de-

creases from its value for minimum sparking voltage, the sparking voltage rises very rapidly. It is seen from these relations, that the normal operating pressure in the cathode chamber of this rectifier should be somewhat in excess of the *pd* for minimum sparking voltage in order that stability of arc initiation will persist over a wide range of cathode temperatures, or cathode-chamber vapor pressures.

Fig. 7 discloses that for a given electrode separation *d*, as the sparking voltage is increased to large values, the pressure diminishes to extremely small values and with sufficiently large sparking voltage this pressure approaches that of the best commercially obtainable vacuum. With diminishing pressure, or diminishing vapor density, the number of positive ions that may be formed in the arc stream are also diminished and for the limiting sparking voltage the number of positive ions are negligible in comparison with the electrons. For this condition, the electron space charge determines the voltage drop which is, for very high voltages and correspondingly low pressures, about twenty-five per cent of the supply voltage. The current in such a pure electron stream is altogether too small for economic applications in the commercial power field.

The foregoing indicates how current-carrying capacity and efficiency are greatly reduced in present high-voltage rectifiers wherein high sparking voltage is obtained by the use of very low vapor pressures.

In Fig. 7, for a given separation of electrodes *d* the sparking voltage ordinate divided by *d* gives gradient. Also, if the abscissas *pd* be divided by *d* we get *p*. These ratios have been taken for an electrode separation of 20 centimeters and the new co-ordinates of pressure and gradient are marked at the top and the right side, respectively, of Fig. 7. This derived relation between voltage gradient and vapor pressure, so simply obtained arithmetically, holds only for a constant value of *d*.

Decreasing the separation of the anode and cathode in an arc-discharge device with no control surface increases the sparking voltage for values of *pd* less than about 6. Advantage of this relation is taken in the design of hot-cathode rectifiers, but the current capacity of this type is limited to the emission of the hot cathode. In mercury-pool rectifiers, a minimum electrode separation is determined by the problems of shielding the anode from the high-velocity vapor leaving the cathode, cooling, and the provision of large anodes having sufficient current capacity. For a rectifier of the type shown in Fig. 1 having a rated current capacity of 20 amperes direct current, and peak backfire voltage in excess of 1000,000, the minimum separation between anode and cathode is about 20 centimeters.

Selecting 20 centimeters as the minimum electrode separation, and referring to the *pd* versus sparking voltage curve of Fig. 7, which applies to a rectifier having no control surface, it is seen that for a sparking voltage of 100,000 the *pd* must not exceed 0.046 or the vapor pressure must not exceed 0.0023 millimeter of mercury. Referring to the voltage-gradient scale on the right, the gradient is found to be 5000. By applying a properly connected control surface over two thirds of the tube length measured from the anode and by making the radius of the tube equal to the electrode separation divided by 4.2 (for 20-centimeter separation the radius will be 4.75 centimeters, the voltage gradient may be decreased to one per cent of its former value. Again referring to the voltage-gradient scale in Fig. 7, a reduction of the original gradient of 5000 to one per cent, or 50, results in a vapor pressure of 0.11 millimeter of mercury. This is an increase in pressure of 48 fold, hence, in current-carrying capacity, for the same sparking voltage.

The writer wishes to emphasize that the method used in this illustration has not been experimentally verified but is offered as an explanation for the fact that rectifiers which had no surface control, backfired constantly at 6000 peak volts, and after applying a control surface the same rectifiers have not backfired at 105,000 peak volts. Also, the sparking voltage of some commercial types of low-voltage rectifiers may be increased tenfold by applying a metallic control surface over the outside of the anode arms.

As shown by equation (1) and Fig. 6, the voltage gradient in the anode region is diminished 90 per cent for each increment, equal to the radius, in the axial length of the control surface. As the gradient is decreased in this manner, i.e., by increasing the ratio of length to radius, the sparking voltage increases. Contrary to past designs, the sparking voltage increases with increasing separation of the anode and cathode in the surface-controlled type. The limitations imposed upon mercury-pool rectifiers of past design, in regard to diminishing electrode separation to obtain higher sparking voltages, are nonexistent in the surface-control type, since there are no restrictions to increasing the separation, within practical limits, in this type of rectifier.

It has been suggested by several authorities in this field that backfires may be caused by positive-ion bombardment of the anode at the beginning of the nonconducting period. In the surface-controlled rectifier this positive-ion bombardment is greatly reduced by the diminished voltage gradient at the anode and by the increased gradient to the control surface upon which a negative potential is impressed during the critical period.

The principle functions of the control surface may be summarized as follows:

(a) Reduce the potential gradient in the region of the anode, which permits the use of higher vapor pressures and correspondingly higher current, for a given backfire voltage.

(b) Accelerate the deionization of the anode cham-

ber at the end of the conducting period, thereby decreasing the probability of emission caused by positive-ion bombardment of the anode at the beginning of the nonconducting period.

(c) Provide positive control of the arc initiation.

Current and Voltage Limits

The current and voltage limits of vapor rectifiers are interdependent, and, with the facilities available, the writer has been unable to determine the interrelated limits. For a supply of 6000 volts effective, 60 cycles, with a resistive load, the thin napkin-ring anodes or the small tungsten-wire lead-ins failed before the current saturation of the vapor was reached.

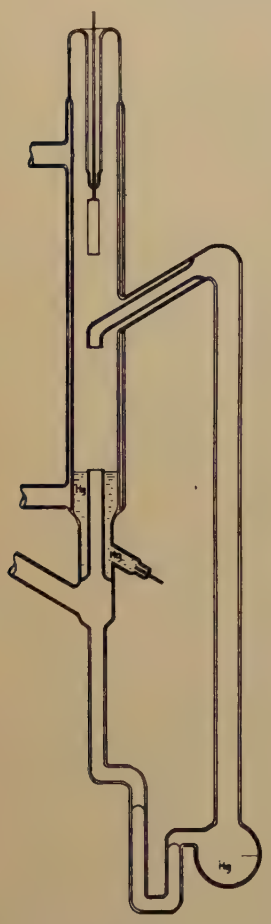

Fig. 8—Sectional view of jet-type surface-controlled rectifier.

On the maximum supply voltage available, which was 75,000 volts effective, 60 cycles, the maximum current was 2 amperes average. The rectifier of Fig. 1 showed no indications of failure during 100 hours of operation at this current and voltage. Previously, this rectifier operated for more than 100 hours with a filtered load and a peak inverse voltage of 80,000.

The only backfires that have occurred were produced by starting the rectifier without a fore pump after an idle period of six days, or upon admitting a very small amount of air into the rectifier. After thoroughly outgasing a rectifier it was sealed off and placed on test. Seven days later the positive column of the arc showed colors of foreign gas and soon afterward backfired continuously.

During the high-voltage tests, external flashovers necessitated the application of external gradient shields, and it was always apparent that the commercial-design problem resided on the outside of the device rather than on the inside.

The current capacity is limited by the cross-sectional area of the arc path at the deflector restriction. By increasing the diameter of the tube to 10 centimeters, this restricted cross-sectional area may be increased to ten times the corresponding area of the rectifier shown in Fig. 1. The current capacity would be increased a like amount if adequate cooling were also provided.

Other Types of Surface-Controlled Mercury-Pool Rectifiers

When several rectifiers are used in the same location, for instance, such as in a multiphase rectifier, one diffusion pump may serve several rectifier tubes. It is then economical to use a simpler type of tube which does not incorporate a diffusion pump and to supply a separate pump for the battery of tubes. Several different types of tubes for application in multiphase rectifiers have been developed and two of them will be briefly described.

The model shown in Fig. 8 is small and easily built with limited facilities. In this model the high vapor pressure in the region of the cathode is obtained by the jet of vapor entering the envelope midway between the two main electrodes. When this model is operated with its anode connected to its water jacket, the supply voltage is limited to about 10,000 volts, since voltages in excess of this value may cause failure of the pyrex wall which separates the mercury pool and the water near the surface of the mercury. When it is desired to operate this model on voltages in excess of 10,000, a separate control transformer of moderate voltage may be provided. A 6000-volt neon-sign transformer of the smallest size has been used for this purpose. Such a transformer should be energized by the low-voltage source of the anode supply voltage, the control transformer being poled so that the control and anode voltages are in phase. By providing a small

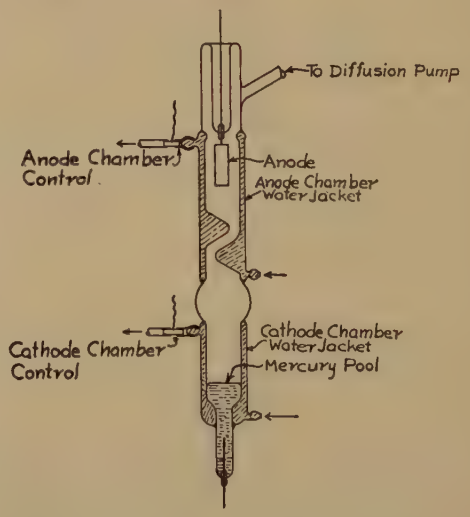

Fig. 9—Sectional view of surface-controlled rectifier having independent temperature control of anode and cathode chambers.

phase shifter in the supply circuit of the control transformer, the direct-current power output of the rectifier may be varied from zero to full power.

A third type of rectifier, having a slight restriction between the anode and cathode chambers, is provided with separate water jackets on the two chambers. This permits independent temperature control of the anode and cathode chambers and eliminates the use of a gas or electric heater. The restriction between the chambers of the tube, shown in Fig. 9, lies diagonally across

the arc path and prevents mercury, sputtered from the cathode, reaching the anode. The cross-sectional area of the restriction is large, hence, provides a high current-carrying capacity.

In starting the rectifier it is necessary to preheat the cathode with a flame. After the tube has been placed in operation, the heat liberated at the cathode may be sufficient to maintain the correct cathode temperature. The circulating water in the cathode water jacket is provided either to heat or cool the cathode chamber, the requirements in this respect being fixed by the effective current through the rectifier.

For supply voltages not exceeding 10,000 the water in the cathode water jacket may be connected to the anode. For higher supply voltages, a separate control transformer should be provided.

In all of the models described, contact with the water in the water jacket has been made by inserting a short metal nipple in the rubber tubing near the water jacket. A 6-foot length of tubing has offered a sufficiently higher resistance to insulate the water jacket from a grounded water supply or another rectifier tube, when using ordinary tap water. When several adjacent rectifier tubes are used, as in a multiphase rectifier, the cooling water is circulated through all tubes in a series connection, 6-foot lengths of rubber tubing coiled on insulated spindles being used for the interconnection of the rectifier tubes.

High-Voltage Switch Application

The new rectifier has been used as a switch on the highest alternating voltage available, namely 75,000 volts effective. To close the mercury switch, the control electrode is connected to the anode. The switch is opened by transferring the control electrode to the cathode. Two rectifier tubes are connected in a reverse parallel arrangement so as to conduct current in both directions. After the circuit has been closed by the mercury switch, the switch may be short-circuited by a knife switch until the circuit is to be opened.

One of the advantages of this form of switch over other types is that this switch always opens the circuit when the current is zero and thus produces no switching transients.

The rectifiers described may likewise be used as high-voltage switches on direct-current circuits, the switch being closed by connecting the control electrode to the anode and opened by transferring the control electrode to the cathode and connecting in parallel with the rectifier a high-voltage condenser, charged to the applied voltage and poled in opposition thereto across the rectifier, so as to reduce the current through the rectifier to zero.

Acknowledgments

The majority of the tests and the experimental rectifier designs described herein were made in the Physics Department, University of Washington, with the collaboration of Professors Joseph E. Henderson and Donald H. Loughridge to whom the writer is deeply indebted. The writer also wishes to express his appreciation of the assistance rendered by his son, T. Marx Libby, in obtaining much of the test data.

Bibliography

(1) F. Penning, *Proc. Royal Akad.*, (Amsterdam), vol. 34, (1931).
(2) T. L. R. Ayers, *Phil. Mag.*, vol. 45, p. 363, (1923).
(3) L. Smede, *Elec Jour.*, vol. 25, p. 403, (1928).
(4) Hull and Brown, *Trans. A.I.E.E.*, vol. 50, pp. 747–753, (1931).

A Distortion-Free Amplifier*

P. O. PEDERSEN†, FELLOW, I.R.E.

Summary—*Distortion in tube amplifiers may be eliminated by using an auxiliary amplifier in which a fraction of the main-amplifier input voltage combined with a fraction of the distorted main-amplifier output voltage produces a correcting component which, combined with the total output, restores this to the same shape as the input.*

I. Introduction and General Theory

THE generally known amplifiers are afflicted with various deficiencies as (1) the *nonlinear* distortion that is mainly due to the curvatures of the tube characteristics; (2) the dependence of the amplification on the voltage of the power sources used; (3) amplifier noise; (4) and finally, induction from outside sources into the amplifier itself which may cause disturbances.

These deficiencies may most seriously affect amplifiers which are to handle wide frequency bands, or when several frequency bands belonging to different signal circuits (talking channels) are to be handled by one amplifier.

A considerable improvement is attained in later years by the widely used amplifiers with negative feedback, about which already exists a very comprehensive literature. This solution is not perfectly ideal though. The following deficiencies may be mentioned: (1) the nonlinear distortion is but partly eliminated; (2) the feedback principle itself involves an inevitable difference in time (phase displacement) between the input voltage and the feedback voltage which is inconvenient for a correct reproduction of rapid current and voltage variations; (3) the feedback may cause instability problems; (4) the amplification is reduced by the feedback.

* Decimal classification: R363.1. Original manuscript received by the Institute, July 10, 1939.
† Principal, Technical University of Denmark, Copenhagen, Denmark.

A couple of years ago the author[1] became interested in designing an amplifier along different lines in which these deficiencies should be eliminated or at least reduced.

The amplifier system to be described aims at avoiding or at least reducing the deficiencies quoted: (1) by reducing feedback to a value which is of little or no significance; (2) by combining the output from the main amplifier with the output from an auxiliary amplifier whose input voltage is determined by the

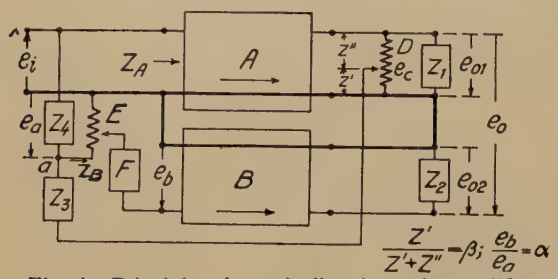

Fig. 1—Principle schematically. A = main amplifier, B = auxiliary amplifier.

difference between (a) a certain, constant, or frequency-dependent fraction of the main-amplifier output voltage and (b) the main-amplifier input voltage; (3) by arranging the transmission time through the main amplifier to the input terminals of the auxiliary amplifier to be equal, or at least very nearly equal, to the time through the direct path from the main-amplifier input terminals to the auxiliary-amplifier input terminals.

In this manner we obtain an amplifier system, Fig. 1, that is almost completely distortion-free, so that the ratio F between the total output voltage $e_0(t-\tau)$ and the input voltage $e_i(t)$, that is, the amplification, will very nearly be constant

$$F = \frac{e_0(t-\tau)}{e_i(t)} = \text{constant}, \qquad (1)$$

independent of the amplitude and the shape of the input voltage; τ being the transmission-delay constant of the amplifier system.

If (1) is satisfied then both the *nonlinear* and the *linear* distortion have been eliminated.

There may, however, be cases where it is desirable to eliminate only the nonlinear distortion without disturbing the linear distortion which does not give rise to other frequencies, cause cross modulation or the like. In this case the condition (1) is changed to

$$F(t) = \frac{e_0(t-\tau(t))}{e_i(t)} \qquad (2)$$

[1] Application for Danish patent filed March 16, 1938. After a preliminary experimental investigation of this new amplifier principle, which verified its merits, it was found that a U.S.A. patent No. 2,043,587 issued in 1936 to W. W. Macalpine, was based on similar principles. In consequence hereof I dropped the patent case; but since the U.S.A. patent does not give either a theoretical foundation nor an experimental verification of the correctness of its principle and, since I have found no such material published elsewhere, a brief account of my investigations, as a whole in accordance with the said Danish patent application, may be of sufficient interest to justify its publication.

where $F(t)$ and $\tau(t)$ are dependent on the curve form of $e_i(t)$ but independent of its amplitude in that sense that $F(t)$ and $\tau(t)$ are the same functions of t for the input voltages $e_i(t)$ and $ae_i(t)$, where a is any number different from 1.

The principle of the amplifier system is shown in Fig. 1 while Figs. 2 and 3 are simplified diagrams to be used for calculating the input voltage of the auxiliary amplifier and of the magnitude of the feedback, respectively. In these figures, Z_3 is equal to (Z_3+Z') of Fig. 1.

Applying the symbols[2] used in Fig. 2 we have

$$i_1 = i_2 + i_3, \quad i_3 = \frac{e_a}{Z_B}, \quad i_1 = \frac{e_i - e_a}{Z_4}, \quad i_2 = \frac{e_a + e_c}{Z_3} \qquad (3)$$

where Z_B is the input impedance of the auxiliary amplifier measured from the point a. Hence we get

$$e_a = \frac{Z_3 Z_B}{Z_3 Z_4 + Z_3 Z_B + Z_4 Z_B}\left(e_i - \frac{Z_4}{Z_3} e_c\right). \qquad (4)$$

If in this we put $Z_4/Z_3=n$, $Z_3/Z_B=p$ then (4) may be written

$$e_a = \frac{1}{1+n+np}(e_i - ne_c) = K(e_i - ne_c) \qquad (5)$$

where

$$K = \frac{Z_B}{Z_B(1+n)+nZ_3} = \frac{1}{1+n+np}. \qquad (6)$$

In most cases it will be advantageous that the ratio n between the impedances Z_4 and Z_3 be constant, independent of frequency, and the same should be aimed at for the factor K. There are, however, cases where it is desirable that these factors be dependent on frequency in a predetermined manner. Such a dependency may be obtained by a suitable choice of the impedances Z_3, Z_4, and Z_B.

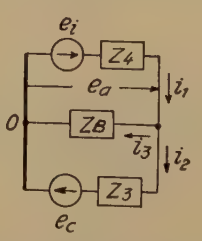

Fig. 2—Simplified diagram for calculating the input voltage of the auxiliary amplifier. The impedance Z_3 in this figure is equal to (Z_3+Z') in Fig. 1.

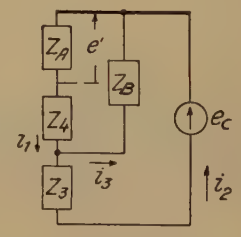

Fig. 3—Simplified diagram for calculating the magnitude of the feedback. Z_3 in this figure is equal to (Z_3+Z') in Fig. 1.

The potentiometer E varies the fraction α of the voltage e_a which should be supplied to the auxiliary amplifier. Generally the conditions will be so selected that α will be a constant value, independent of frequency, but, if desirable, it may be made dependent on frequency.

[2] In all formulas, in accordance with Figs. 2 and 3, Z_3 signifies the sum of (Z_3+Z') in Fig. 1. In most cases $Z_3 \gg Z'$, so that the difference between Z_3 and (Z_3+Z') is rather small.

F is used for adjusting the phase of the input voltage to the auxiliary amplifier in order to secure a desired phase relation between its output voltage e_{02} and the output voltage e_{01} of the main amplifier. Only the finer phase adjustment is carried out in this manner though, larger phase shifts of about 180 degrees are done by other means as by using an odd or an even number of valves or by suitable transformers.

The impedances, Z_3 and Z_4, are chosen so that the transmission time from the input terminal x through the main amplifier, the potentiometer D, and the impedance Z_3 to the point a is very nearly equal to the transmission time from the terminal x through the impedance Z_4 to the point a. Further, Z_4 is so chosen that

$$\left|\frac{Z_4}{Z_A}\right| = |nm| \gg 1, \tag{7}$$

where Z_A is the input impedance of the main amplifier[3] and $Z_3/Z_A = m$. When (7) is satisfied the feedback will be insignificant as is clearly shown in Fig. 3. Using the symbols from that figure we have

$$\begin{aligned} &i_1 = i_2 + i_3, \quad i_2Z_3 + i_1(Z_A + Z_4) = e_c \\ &i_2Z_3 - i_3Z_B = e_c \\ &e' = i_1Z_A, \end{aligned} \tag{8}$$

whence the main-amplifier input voltage corresponding to the voltage e_c is determined by

$$e' = \frac{e_c}{(mn+1)(1+p)+m}. \tag{9}$$

In most cases the condition will be so chosen that $|ne_c|$ is only very little different from $|e_i|$ whereby the working interval of the auxiliary amplifier will be very small, and consequently the amplification factor of the auxiliary amplifier will be approximately constant. By inserting $|ne_c| = |e_i|$ in (9) we get a feedback determined by

$$\left|\frac{e'}{e_i}\right| = \frac{1}{|n[(mn+1)(1+p)+m]|}, \tag{10}$$

and by choosing suitably large values of $|m|$ and $|n|$ it is always possible to obtain a condition where

$$\left|\frac{e'}{e_i}\right| \ll 1, \tag{11}$$

so that the feedback will be negligible.

The output voltage e_{01} of the main amplifier may be expressed by

$$e_{01} = F(e_i) + N + V, \tag{12}$$

where $F(e_i)$ is the output voltage of the main amplifier, which is generally dependent on the design and setting of the amplifier, on the amplitude and shape of the input voltage, and also on the impedances connected to the output terminals. $F(e_i)$ will generally show both linear and nonlinear distortion. N denotes the output voltage resulting from amplifier noise and V the voltage resulting from variation in the battery voltages etc., as well as from induction by other circuits into the main amplifier.

At the potentiometer D a certain fraction β of e_{01} is branched off, that is,

$$e_c = \beta e_{01}, \tag{13}$$

where β may be constant or dependent on the frequency.

The voltage e_b put into the auxiliary amplifier is according to (5) determined by

$$\begin{aligned} e_b = \alpha e_a &= \alpha K[e_i - \beta n e_{01}] \\ &= \alpha K[e_i - \beta n(F(e_i) + N + V)]. \end{aligned} \tag{14}$$

The output voltage e_{02} of the auxiliary amplifier is determined by

$$e_{02} = f(e_b) = f\{\alpha K[e_i - \beta n(F(e_i) + N + V)]\}, \tag{15}$$

here assuming the auxiliary amplifier to be so well shielded that we may waive attention to induction from outside sources, and further to be so designed that the inside noise at a relatively small load is insignificantly small.

The total output e_0 is then

$$\begin{aligned} e_0 = e_{01} + e_{02} = &[F(e_i) + N + V] \\ &+ f\{\alpha K[e_i - \beta n(F(e_i) + N + V)]\}. \end{aligned} \tag{16}$$

By suitable choice of the properties of the auxiliary amplifier the values of the function f, as well as of the parameters α, β, n, K can be made constant or in a suitable manner dependent on frequency. Then we are within wide limits able to give the total output voltage e_0 any desired dependency on the input voltage e_i.

The interval within which the auxiliary amplifier is supposed to introduce corrective action is generally very small and we can arrange the auxiliary amplifier so that its amplification is constant with very good approximation within the active interval. We then have

$$e_0 = \alpha bKe_i + (1 - \alpha bK\beta n)(F(e_i) + N + V). \tag{17}$$

Also in this case we can to a great extent secure a desired dependency of the total output voltage e_0 on the input voltage e_i.

In most cases complete proportionality between the total output voltage and the input voltage, or between the input voltage and the output current, or between the input voltage and a total number of ampere turns, is desirable.

Considering a distortion-free amplifier we must, according to (17), have

$$\alpha bK\beta n = 1, \tag{18}$$

[3] No attention has here been paid to the impedance Z_i of the voltage source connected to the input terminals of the main amplifier, but since this impedance, as far as the question of feedback is concerned, is in parallel to Z_A, its presence will tend further to reduce the feedback.

then

$$e_0 = \alpha b K e_i = \frac{e_i}{\beta n}. \tag{19}$$

The resulting amplification is consequently

$$F = \alpha b K = \frac{1}{n\beta}. \tag{20}$$

The parameters α, β, b, n, and K can be constant, independent of frequency, positive or negative, or two

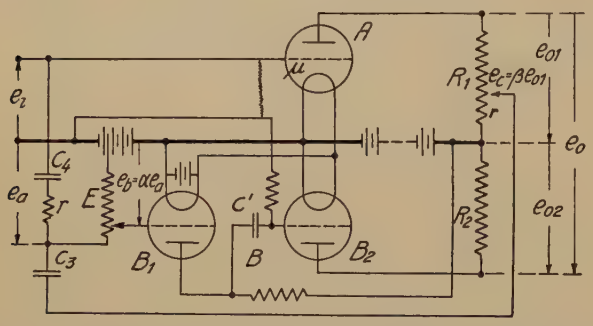

Fig. 4—Arrangement for distortion-free voltage amplification, A = main amplifier, B = auxiliary amplifier.

or more may be dependent upon frequency, but their product must, using the positive directions of voltages shown in Fig. 1, always be positive and equal to 1 if the system shall act as a distortion-free voltage amplifier.

If here we choose $n=1$ then

$$F = \frac{e_0}{e_i} = \frac{1}{\beta} = \frac{Z'+Z''}{Z'}, \tag{21}$$

where Z' and Z'' are the two sections of the potentiometer D (see Fig. 1). If the ratio Z''/Z' is constant and independent of frequency, then the same will apply to the amplification. Z' and Z'' may be pure ohmic resistances or capacitances. If the latter are free of losses the amplification will in both cases be independent of frequency. Z' and Z'' may also be more complex impedances that may give F any desired dependence on frequency.

If n is different from 1 and is a real constant, independent of frequency, then according to (19),

$$F = \frac{1}{n\beta} = \frac{Z'+Z''}{nZ'}. \tag{22}$$

II. Example as to the Design of a Distortion-Free Amplifier

An example of an arrangement for distortion-free voltage amplification is shown in Fig. 4. The main amplifier A consists of a single valve having the amplification factor μ and, see Fig. 5, a static characteristic acb whose point c is representing the grid voltage e_{g0} and the anode current i_{a0}. The input voltage e_i is reckoned from e_{g0} and the variable anode current i_a from i_{a0}. Assume that the input voltage varies between $\pm e_{i0}$. The maximum voltages, that will act upon the auxiliary amplifier, will depend on the amplitude e_{i0} of the input voltage, on the shape of the characteristic, and on the resulting amplification F. For the sake of simplicity put $n=1$ which in Fig. 4 corresponds to the condition that $C_3=C_4$ and $r=\beta R_1$. According to (21) we then get $F=1/\beta$.

If the main amplifier alone should produce this amplification at the operating point c then the plate resistance ρ_{00} at this point would be determined by

$$F = \frac{1}{\beta} = \frac{\mu R_1}{\rho_{00}+R_1}, \tag{23}$$

or

$$\rho_{00} = (\beta\mu - 1)R_1. \tag{24}$$

If the slope of the characteristic at this point corresponds to the straight line cc' then at an arbitrary point x on the characteristic we get an amplification F_x determined by

$$F_x = \frac{de_{01}}{de_i} = \frac{\mu R_1}{\rho_x + R_1}, \tag{25}$$

where ρ_x is the plate resistance of the valve in the point x; that is,

$$\frac{1}{\rho_x} = \frac{1}{\mu}\left(\frac{di_a}{de_i}\right)x. \tag{26}$$

The share Δe_{01x} of that part of the voltage e_{01} which is to be compensated for, which is the voltage interval

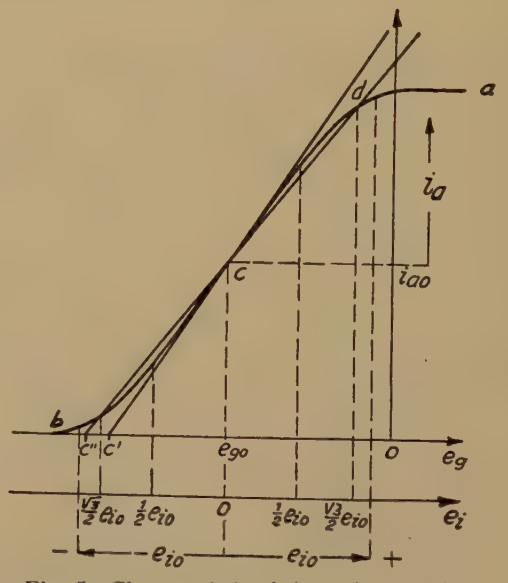

Fig. 5—Characteristic of the main amplifier.

from e_{ix} to $(e_{ix}+de_{ix})$, is accordingly

$$\Delta e_{01x} = (F_x - F_0)de_{ix} = \mu R_1 \frac{\rho_{00}-\rho_x}{(\rho_x+R_1)(\rho_{00}+R_1)}de_{ix}. \tag{27}$$

If the amplification factor of the auxiliary amplifier is b then the corresponding contribution to the input

voltage Δe_{bx} of the auxiliary amplifier at the point x will be

$$\Delta e_{bx} = \frac{\Delta e_{01x}}{b} = \frac{\mu R_1}{b} \frac{\rho_{00} - \rho_x}{(\rho_x + R_1)(\rho_{00} + R_1)} de_{ix}. \quad (28)$$

Since ρ_x does not vary much within the part of the characteristic used we have, with approximation

$$\Delta e_{bx} \cong \text{constant } (\rho_{00} - \rho_x) de_{ix}. \quad (29)$$

Consequently β should be so chosen that ρ_{00}, determined by (24), on the average deviates as little as possible from the plate resistance ρ_x over the useful part acb of the characteristic[4] since otherwise unnecessarily large compensation voltages will be obtained.

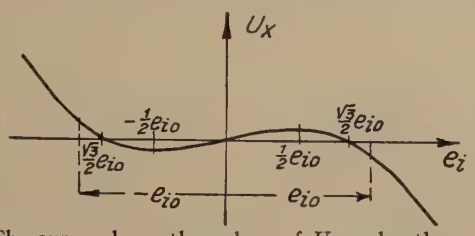

Fig. 6—The curve shows the values of U_x under the assumption that the maximum deviation in positive and negative directions are of equal magnitude.

If the equation of the characteristic referred to the point c is

$$i_a = A_1 e_i - A_3 e_i^3, \quad (30)$$

then

$$\frac{1}{\rho_x} = \frac{1}{\mu} \frac{di_a}{de_i} = \frac{1}{\mu} (A_1 - 3A_3 e_{ix}^2) \quad (31)$$

or

$$\rho_x = \frac{\mu}{A_1 - 3A_3 e_{ix}^2}.$$

If we put $\rho_{00} = \mu/A_0$ then

$$\frac{1}{\mu}(\rho_x - \rho_{00}) de_{ix} = \frac{A_0 - A_1 + 3A_3 e_{ix}^2}{A_0(A_1 - 3A_3 e_{ix}^2)} de_{ix} = \Delta U_x. \quad (32)$$

If the applied part of the characteristic is so nearly straight that $3A_3 e_{i0}^2$ is much smaller than A_1, we may apply the following approximate expression for the increase ΔU_x in the input voltage of the auxiliary amplifier, instead of (32),

$$\Delta U_x = (\rho_x - \rho_{00}) de_{ix} \cong \frac{A_0 - A_1 + 3A_3 e_{ix}^2}{A_0 A_1} de_{ix}. \quad (33)$$

Here both ΔU_x and U_x according to (29) and (33) should be multiplied by a constant dependent on the system. It follows that

$$U_x = \int_0^{e_{ix}} \Delta U_x = \frac{1}{A_0 A_1} \int_0^{e_{ix}} (A_0 - A_1 + 3A_3 e_{ix}^2) de_{ix} = \frac{1}{A_0 A_1} [(A_0 - A_1) e_{ix} + A_3 e_{ix}^3]. \quad (34)$$

According to the foregoing U_x is very nearly proportional to the input voltage of the auxiliary amplifier. It follows that

$$\frac{dU_x}{de_{ix}} = 0 \text{ for } e_{ix} = \pm \sqrt{\frac{A_1 - A_0}{3A_3}}, \quad (35)$$

$$\left.\begin{aligned} \text{and} \quad U_{x\max} &= + \frac{2}{3A_0 A_1} \frac{(A_1 - A_0)^{3/2}}{(3A_3)^{1/2}} \\ \text{for} \quad e_{ix} &= - \sqrt{\frac{A_1 - A_0}{3A_3}}, \\ \text{and} \quad U_{x\min} &= - \frac{2}{3A_0 A_1} \frac{(A_1 - A_0)^{3/2}}{(3A_3)^{1/2}} \\ \text{for} \quad e_{ix} &= + \sqrt{\frac{A_1 - A_0}{3A_3}}, \end{aligned}\right\} \quad (36)$$

while

$$U_x = 0 \text{ for } e_{ix} = 0 \text{ and } e_{ix} = \pm \sqrt{\frac{A_1 - A_0}{A_3}}. \quad (37)$$

When U for $\pm e_{i0}$ has the same absolute value as U_{max} and U_{min}, then the following equation is obtained for determining correlated values of $(A_1 - A_0)$ and e_{i0}:

$$(A_1 - A_0)^{3/2} + \tfrac{3}{2}^{3/2} A_3^{1/2} e_{i0} (A_1 - A_0) - \tfrac{3}{2}^{3/2} A_3^{3/2} e_{i0}^3 = 0, \quad (38)$$

which is satisfied by

$$A_1 - A_0 = \tfrac{3}{4} A_3 e_{i0}^2 \text{ or } e_{i0} = 2\sqrt{\frac{A_1 - A_0}{3A_3}}, \quad (39)$$

then

$$\rho_{00} = \frac{\mu}{A_0} = \frac{\mu}{A_1 - \frac{3}{4} A_3 e_{i0}^2}. \quad (40)$$

The corresponding values of U_x are shown in Fig. 6.

From the foregoing it appears that a value of ρ_{00} determined by (40) will be the most favorable, namely, the one that will give the auxiliary amplification the smallest maximum amplitudes.

From (40)

$$n\beta\mu = 1 + \frac{1}{R_1(A_1 - \frac{3}{4} A_3 e_{i0}^2)}. \quad (41)$$

The value of ρ_{00} determined by (40) corresponds to the straight line dcc'' through c, that cuts the characteristic (30) at points corresponding to the voltages $\pm \frac{\sqrt{3}}{2} e_{i0}$.

III. Calculation of the Resulting Characteristic and of the Reduction of the "Klirr-Factor"

We shall now investigate how the system will work when the characteristics of both the main and the auxiliary amplifier are curved and determined by the equations, respectively,

$$e_{01} = a_1 e_i + a_2 e_i^2 - a_3 e_i^3 + a_4 e_i^4 + a_5 e_i^5 \cdots \quad (42)$$

and

$$e_{02} = b_1 e_b + b_2 e_b^2 - b_3 e_b^3 + b_4 e_b^4 + b_5 e_b^5 \cdots. \quad (43)$$

[4] If $n = 1$ then $\rho_{00}' = (n\beta\mu - 1)R_1$ should in maximum deviate as little as possible from the values of ρ_x.

We shall assume the system to be adjusted so that the resulting amplification is equal to that of the main amplifier at small input voltages, that is,

$$\left(\frac{e_0}{e_i}\right)_{e_i \to 0} = a_1. \tag{44}$$

This adjustment is not the most favorable for larger values of the input voltage, but the following calculations will be much simpler and clearer under this assumption than for more favorable adjustments of the voltage amplitudes.

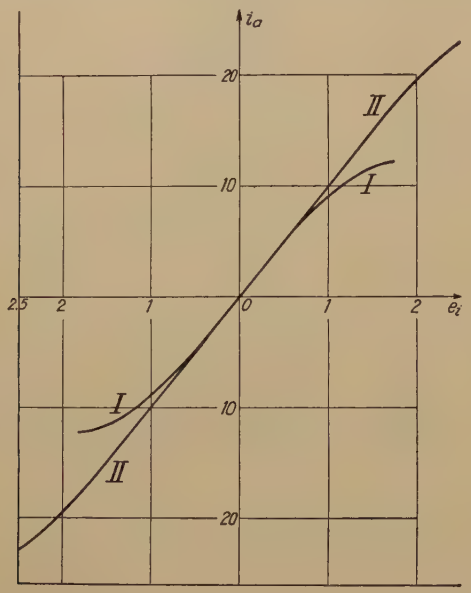

Fig. 7—Curve *I* shows the main-amplifier characteristic: $10e_i - e_i^3$, and curve *II* the resulting characteristic: $10e_i - (1/10^3)e_i^9$.

In accordance with (44) the input voltage e_b of the auxiliary amplifier is so adjusted that

$$e_b = \frac{1}{b_1}(a_1 e_i - e_{01})$$

$$= \frac{1}{b_1}[-a_2 e_i^2 + a_3 e_i^3 - a_4 e_i^4 - a_5 e_i^5 - \cdots]. \tag{45}$$

The resultant output voltage e_0 is consequently

$$e_0 = e_{01} + e_{02}$$

$$= a_1 e_i + \frac{b_2}{b_1^2}[-a_2 e_i^2 + a_3 e_i^3 - a_4 e_i^4 - a_5 e_i^5 - \cdots]^2$$

$$- \frac{b_3}{b_1^3}[-a_2 e_i^2 + a_3 e_i^3 - a_4 e_i^4 - a_5 e_i^5 - \cdots]^3$$

$$+ \frac{b_4}{b_1^4}[\ ]^4 + \frac{b_5}{b_1^5}[\ ]^5 + \cdots. \tag{46}$$

Generally the adjustment of the auxiliary amplifier will be so chosen that $b_2 = 0$; that is, the characteristic has its inflection point at the starting point. In that case (46) will become

$$e_0 = e_{01} + e_{02}$$

$$= a_1 e_i - \frac{b_3}{b_1^3}[-a_2 e_i^2 + a_3 e_i^3 - a_4 e_i^4 - \cdots]^3$$

$$+ \frac{b_4}{b_1^4}[\ ]^4 + \cdots$$

$$= a_1 e_i + \frac{a_2^3 b_3}{b_1^3} e_i^6 - 3\frac{a_2^2 a_3 b_3}{b_1^3} e_i^7 \cdots, \tag{47}$$

so that the nonlinear part of the resulting characteristic in this case has for its first term e_i^6.

If the adjustment of the main amplifier is also chosen so that $a_2 = 0$ then (46) becomes

$$e_0 = e_{01} + e_{02}$$

$$= a_1 e_i - \frac{b_3}{b_1^3}[+a_3 e_i^3 - a_4 e_i^4 - a_5 e_i^5 \cdots]^3$$

$$+ \frac{b_4}{b_1^4}[\ ]^4 + \cdots$$

$$= a_1 e_i - \frac{a_3^3 b_3}{b_1^3} e_i^9 + 3\frac{a_3^2 a_4 b_3}{b_1^3} e_i^{10}$$

$$+ 3\frac{a_3^2 a_5 b_3}{b_1^3} e_i^{11} + \cdots. \tag{48}$$

The nonlinear part of the resulting characteristic has under these assumptions for its first term e_i^9.

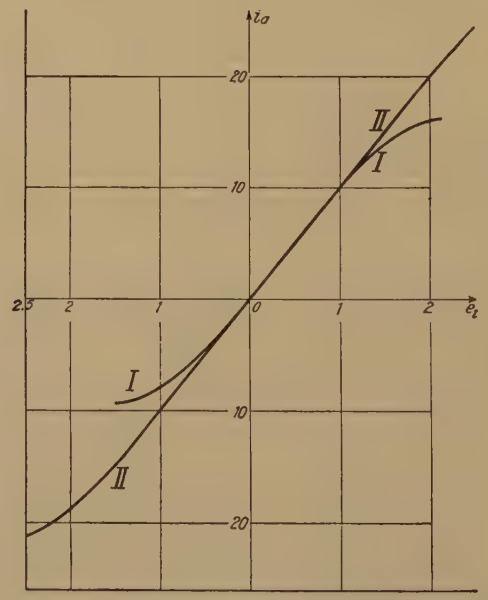

Fig. 8—Curve *I* shows the main-amplifier characteristic: $10e_i + e_i^2 - e_i^3$ and curve *II* the resulting characteristic: $10e_i + (e_i^2 - e_i^3)^3/10^3$.

If the auxiliary amplifier is a "distortion-free" amplifier of this latter type, while a new main amplifier is adjusted to $a_2 = 0$, then the nonlinear part of the resulting characteristic of such an amplifier system would have for its first term e_i^{27}.

In order to illustrate this straightening out of the resulting characteristic we shall calculate for a few

simple cases the resulting characteristics. We assume the auxiliary-amplifier characteristic in both cases to be given by

$$e_{c2} = b_1 e_b - b_3 e_b^3 = 10 e_b - e_b^3, \tag{49}$$

while the main-amplifier characteristic in the first case is determined by curve *I* of Fig. 7.

$$e_{01} = a_1 e_i - a_3 e_i^3 = 10 e_i - e_i^3 \tag{50}$$

and in the second case by curve *I* of Fig. 8,

$$e_{01} = a_1 e_i + a_2 e_i^2 - a_3 e_i^3 = 10 e_i + e_i^2 - e_i^3. \tag{51}$$

The resulting characteristics consequently will be

$$e_0 = 10 e_i - \frac{1}{10^3} e_i^9, \tag{52}$$

and

$$e_0 = 10 e_i + \frac{1}{10^3} (e_i^2 - e_i^3)^3 \tag{53}$$

corresponding to the curves *II* in Figs. 7 and 8, respectively.

It may be of some interest to see whether other adjustments of the resulting amplification could be more favorable. Suppose instead of having the auxiliary-amplifier voltage adjusted according to (45) we put

$$e_b = \frac{1}{b_1} [(a_1 - x a_3) e_i - e_{01}]. \tag{54}$$

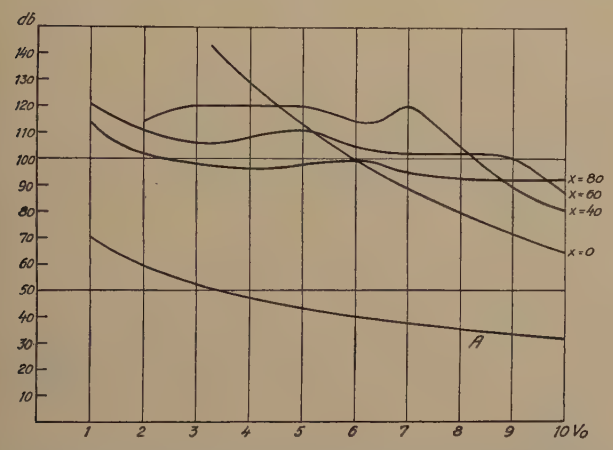

Fig. 9—Value of the "klirr-factor" for the resulting amplification, given in decibels below the linearly amplified fundamental note $(a_1 - x a_3) V_0 \sin \omega t$.

Inserting this expression in the formula for e_0 we get

$$e_0 = e_{01} + e_{02} = (a_1 - x a_3) e_i + \frac{a_3^3 b_3}{b_1^3} (x e_i - e_i^3)^3. \tag{55}$$

Here the distortion D is represented by the last term

$$D = \frac{a_3^3 b_3}{b_1^3} (x e_i - e_i^3)^3. \tag{56}$$

If we put

$$e_i = V_0 \sin \omega t, \tag{57}$$

we get

$$D = \frac{a_3^3 b_3}{b_1^3} [x^3 V_0^3 \sin^3 \omega t - 3x^2 V_0^5 \sin^5 \omega t + 3x V_0^7 \sin^7 \omega t - V_0^9 \sin^9 \omega t] \tag{58}$$

$$= \frac{a_3^3 b_3}{b_1^3} V_0^3 \{E_1 \sin \omega t + E_3 \sin 3\omega t + E_5 \sin 5\omega t + E_7 \sin 7\omega t + E_9 \sin 9\omega t\}. \tag{59}$$

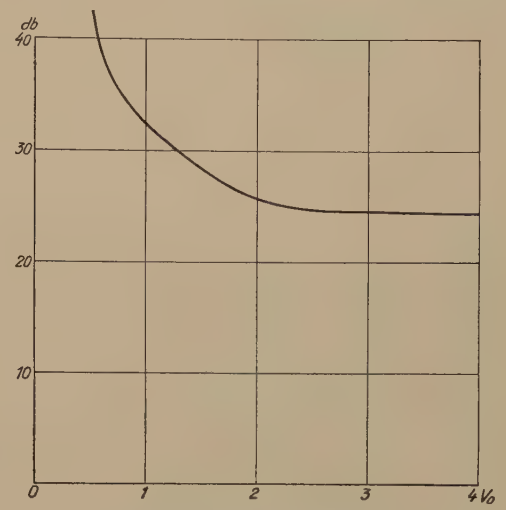

Fig. 10—Reduction of the "klirr-factor" with the arrangement shown in Fig. 4.

The "klirr-factor" k is then determined by[5]

$$k = \frac{a_3^3 b_3}{(a_1 - x a_3) b_1^3} \sqrt{E_1^2 + E_3^2 + E_5^2 + E_7^2 + E_9^2}. \tag{60}$$

In Fig. 9 the ordinate gives the "klirr-factor" in decibels below the fundamental note, that is $-20 \log_{10} k$, as a function of V_0 and for $a_1 = b_1 = 2.3$, for $a_3 = b_3 = 1/400$ as well as for $x = 0$, 40, 60, and 80. Curve *A* represents the "klirr-factor" for the main amplifier operating separately. For $x = 0$, corresponding to the "klirr-factor" determined by (45), the curve declines smoothly with increasing values of V_0; here curve *A* gives in a corresponding manner the "klirr-factor" for the main amplifier. For $V_0 = 3.5$ volts the difference between the two curves, i.e., the reduction of the "klirr-factor," is about 90 decibels, and about 32 decibels for $V_0 = 10$ volts. For the other values of x the curves are somewhat irregular, but as a whole more flat than for $x = 0$; and it has been confirmed that the higher the maximum amplitude of V_0 the higher the value of x that should be chosen. It is further seen that with the assumptions applied a reduction of 40 to 60 decibels, or even more, in the "klirr-factor" may be obtained.

There has been no opportunity so far for a thorough experimental investigation of the system, but preliminary tests with the arrangement shown in Fig. 4

[5] We have here included the amplitude to sin ωt, although this is not measured by the common "klirr-factor" bridges. Since however, this amplitude increases with the 3rd and higher powers of V_0 it does rightly belong to the nonlinear distortion.

gave the reduction of the "klirr-factor" shown in Fig. 10, using casually chosen valves type Philips A-415 for A and B, and for valve B_1 type Philips A-425.

IV. Conclusion

The above is to be considered only as preliminary communication. I have not included anything about the conditions for applying reactive output impedances or for using output transformers, which offer the advantage that one of the valves in the auxiliary amplifier may be omitted. My experimental investigations of these points are not sufficiently advanced.

Acknowledgment

I thank Mr. J. P. Christensen, E. E., Mr. A. Mortensen, E. E., and Mr. J. Oskar Nielsen, E. E., for valuable assistance in carrying out experiments and calculations.

Frequency Modulator*

C. F. SHEAFFER†, Associate, I.R.E.

Summary—*The frequency deviation obtainable in a reactance-tube frequency-modulator—oscillator combination is limited by two resistances which shunt the oscillator tank. The first is due to the plate resistance of the reactance tube and the second, to the fact that the voltage on the reactance-tube's grid is less than 90 degrees out of phase with the plate voltage. A method is deduced from a simple mathematical analysis whereby the phase of the reactance-tube grid voltage may be adjusted for cancellation of these two effects. This eliminates the tendency of the reactance tube to amplitude-modulate the oscillator output, makes possible the use of somewhat higher reactance values in the oscillator tank, and permits the satisfactory use of more powerful reactance tubes. The principle is of importance only where wide frequency deviation may be required without resorting to frequency multiplication, but will possibly find many uses as the art of frequency-modulated-wave transmission and reception progresses.*

THE use of the so-called reactance tube as a means of controlling the frequency of an oscillator has been discussed by several authors.[1,2] Its use as a frequency modulator has also been reported.[3] This paper is concerned with the development

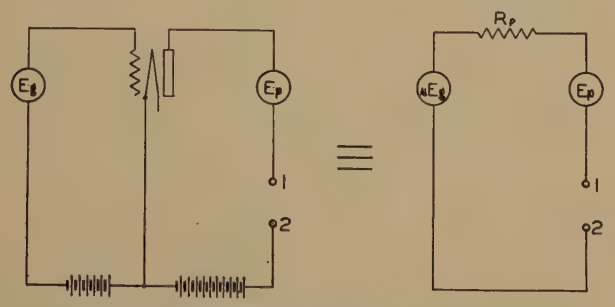

Fig. 1—Circuits which are assumed to have equivalent impedances at terminals 1 and 2.

of a more-satisfactory means of producing wide-deviation frequency modulation, or frequency control. There are perhaps several possible uses for a wide-deviation frequency modulator, however the one which interested the author was the exploration of several frequency-modulation transmitter-frequency-stabilizing schemes which require the production of wide-deviation frequency modulation without resorting to frequency multiplication.

Experiments conducted by the author have resulted in the deriving of a suitable means of using the higher-powered vacuum tubes of the pentode, or beam type, or if necessary, even using two or more such tubes in parallel for producing the controllable reactance. Reasonably wide frequency deviation may be obtained by the system without making the oscillator unduly unstable, or subject to amplitude modulation.

The procedure followed is perhaps best explained by the following mathematical representation of the factors considered.

Referring to Fig. 1, it is seen that the impedance looking into the plate of a vacuum tube may be assumed under certain conditions to be dependent upon three values: the plate resistance, the plate voltage, and the value and nature of the grid excitation. The resulting impedance will be the ratio of the plate voltage to plate current.

$$Z_{in} = E_p/I_p \tag{1}$$

If we now assume the grid voltage to be of the same frequency as the plate voltage and to have some fixed phase relation with it we may write the equation for the plate current

$$I_p = \frac{E_p + ukE_p\angle\theta}{R_p} \tag{2}$$

where k is the ratio of grid voltage to plate voltage. The admittance looking into the plate is therefore

$$Y = \frac{1}{R_p} + \frac{uk}{R_p}\cos\theta + \frac{juk}{R_p}\sin\theta. \tag{3}$$

The presence of two real terms, one of which may be made negative at will, at once suggests the possibility of canceling these two terms so as to leave only the susceptance term. The conditions required by (3) for doing this are

$$\cos\theta = 1/uk. \tag{4}$$

* Decimal classification: R355.8×R414. Original manuscript received by the Institute, September 25, 1939.

† Tulsa Broadcasting Company, Tulsa, Okla.

[1] D. E. Foster and S. W. Seeley, "Automatic tuning, simplified circuits, and design practice," Proc. I.R.E., vol. 25, pp. 289–313; March, (1937).

[2] Charles Travis, "Automatic frequency control," Proc. I.R.E., vol. 23, pp. 1125–1141; October, (1935).

[3] I. R. Weir, "Field tests of frequency and amplitude modulation with U.H.F. waves," *Gen. Elec. Rev.*, May and June.

The remaining term, therefore, would be

$$Y = j \frac{uk}{R_p} \sin \theta,$$

or equivalent to a reactance

$$X = -j \frac{R_p}{uk \sin \theta} \cdot \tag{5}$$

It is apparent that if the conditions of (4) can be met in a reactance-tube circuit, the shunting effect of the tube's plate resistance can be neutralized. To understand why it would be desirable to do this it is necessary to examine the conditions which we may consider essential for proper operation of the complete modulator unit. The ability of the reactance tube to change the frequency of the oscillator is dependent upon its ability to produce low values of reactance and upon the reactance values of the tuned circuit. Increasing the ratio L/C of the tuned circuit will increase the frequency-variation range of the modulator. The distributed capacitance of the coil together with associated circuit capacitances limits this means of increasing the modulation range. Furthermore the oscillator is less stable with high values of L/C. Because of these facts, if a wide modulation range is necessary, it must be attained by using a power reactance tube. The plate resistance of such a tube will ordinarily reach values sufficiently low to choke the oscillator during positive swings of modulating grid voltages. It is possible, therefore, for this varying plate resistance to amplitude-modulate the oscillator quite severely. Meeting the conditions of (4) will eliminate the effect of the plate resistance and therefore do away with amplitude modulation. This will, of course, increase the usable reactance range of the reactance tube.

Fig. 2 shows a schematic of the conventional reactance-tube oscillator circuit. The grid excitation for the reactance tube is obtained from the plate circuit through a resistance whose value is made high in comparison to the reactance of the grid shunt capacitance. Under these conditions the phase of the grid voltage is retarded approximately 90 degrees. This causes the plate current to lag the plate voltage thus producing the so-called reactance.

To obtain the phase required by (4) it is only necessary to alter the feedback-resistor connection as shown by the dotted line in Fig. 2. With this connection the phase will be greater than 90 degrees and will approach 180 degrees as R is reduced. A value of R may then be selected which will meet the required conditions.

It is also interesting to note that the power dissipated in the reactance-tube's plate will be less in the resistance-neutralized circuit. This is clearly indicated in the following equation which gives the average power dissipated over the oscillator cycle:

$$P(a_v) = E_b I_b + \frac{E_p I_p \cos \theta}{2} \cdot \tag{7}$$

Thus when the phase is 90 degrees the power dissipated is $E_b I_b$. Now as the angle is increased past 90 degrees, the second term in (7) becomes negative and the value of I_b is also reduced. The dissipation in the reactance-tube plate therefore varies quite radically with angle changes in the region of 90 degrees when E_p is comparable with E_b. The effect would, of course, diminish progressively with reduction of the ratio E_p/E_b. The power wasted in the circuit meeting the requirements of (4) is therefore comparatively less than that which would be wasted in the conventional circuit.

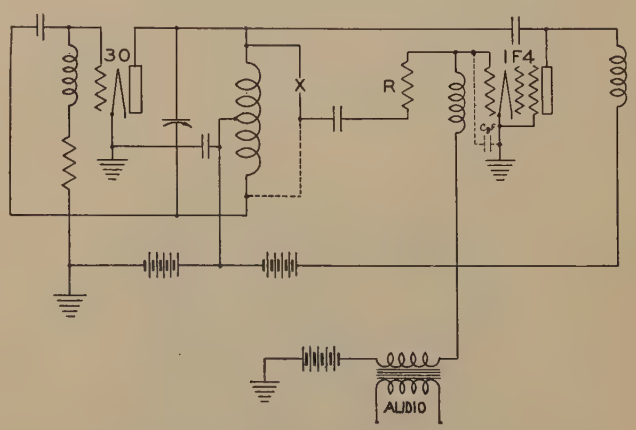

Fig. 2—Experimental frequency modulator

The circuit of Fig. 2 was set up on a frequency of 2000 kilocycles and adjusted for plate-resistance neutralization by adjusting the value of R while observing the effect of modulation on an oscilloscope screen. A receiver with a band-spread dial was used to measure the frequency variation. Calibration of the dial was accomplished by frequency modulating the oscillator with 15 kilocycles and plotting the dial reading versus side frequencies. The maximum obtainable frequency variation, with a particular setting of the tuned circuit, was ± 75 kilocycles. This was possible without the slightest indication of amplitude modulation.

The circuit was then connected in the conventional manner, and with the same tuned-circuit adjustment, optimum operating conditions gave a frequency variation of ± 55 kilocycles with 50 per cent amplitude modulation.

These results seemed representative of several tests made at various frequencies up to 4000 kilocycles and using both pentode and triode oscillator tubes. The contrast may be expected to be even greater with the use of reactance tubes possessing lower plate resistance.

It seems therefore that neutralization of the reactance-tube's plate resistance affords a worth-while advantage to devices requiring a wide frequency-variation range in that it eliminates the detrimental effect of the first two terms of (3) and by doing this increases the variation range free from amplitude variation.

Cosmic Static*

GROTE REBER†, ASSOCIATE, I.R.E.

Introduction

IN 1932 Jansky[1] published the first of a series of papers[2,3,4] indicating that a certain type of static appears to come from space and in particular from the plane of the Milky Way. Very few other[5] data are available on the disturbance. Various[6] hypotheses have been advanced to account for the phenomenon but all have failed under quantitative calculation.

160-Megacycle Tests at Wheaton, Illinois

The writer became interested in this work about three years ago. It was decided to make measurements at various frequencies with equipment of high resolving power. The apparatus shown in Fig. 1 is really a transit telescope adapted to work at radio frequencies. The mirror is 31 feet in diameter and has a focal length of 20 feet. Details of operation have been given elsewhere.[7]

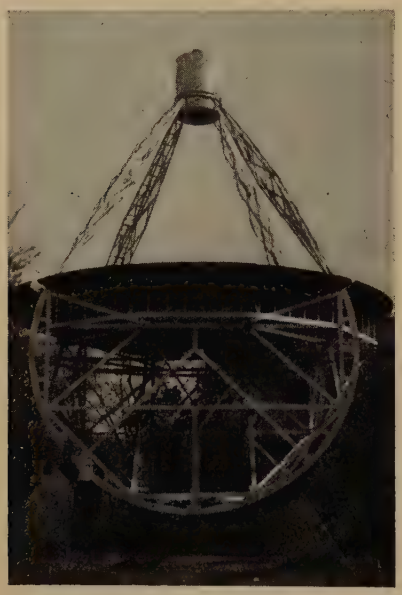

Fig. 1—Antenna system used for the investigation of cosmic static.

The output of the amplifier is indicated by the meter at the right of Fig. 2. When no radiation is present the reading is constant at some predetermined level. Any radiation captured will cause the meter to move in a downward direction. Readings are taken visually at minute intervals. A typical set of points is shown in Fig. 3. The dotted line across the dip in the curve is the condition that would have obtained had no radiation been intercepted. The input to the receiver is

$$\text{input} = \left[\left(\frac{\text{reference}+\text{deflection}}{\text{reference}}\right)^2 - 1\right] 8\times10^{-18} \text{ watt/kc band} \quad (1)$$

where "reference" is the number of microamperes corresponding to 8×10^{-18} watt per kilocycle band[4,8] and

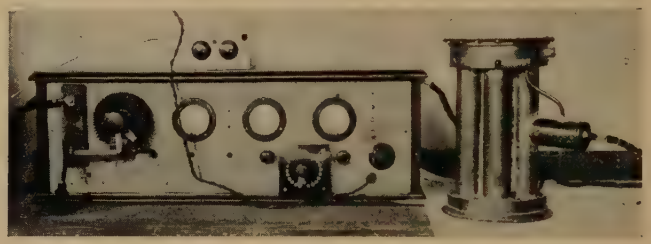

Fig. 2—Control and indicating equipment. The amplifier is shown at right.

"deflection" is the number of microamperes represented by the dip in the curve. The maximum recorded input is 15 per cent of the reference-level power and the band width of the receiver is about 10^3 kilocycles. The available input power, therefore, is 1.2×10^{-15} watt. The drum efficiency is 50 per cent, reflector efficiency

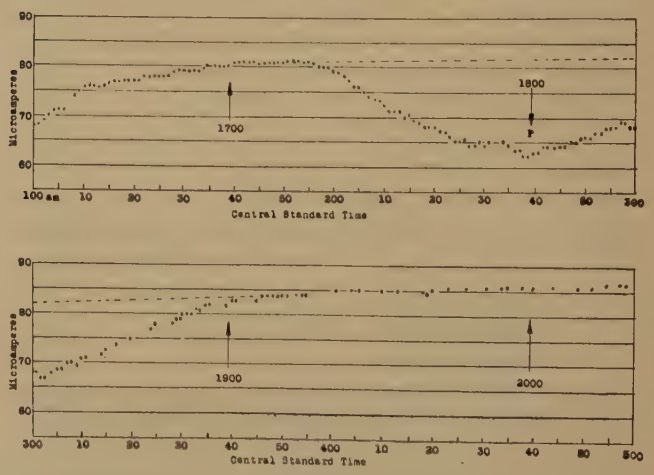

Fig. 3—Microamperes versus C.S.T. on May 11, 1939, for declination −20 degrees. Hours right ascension indicated by arrows. *P* marks the plane of the Milky Way. Galactic longitude for this declination is 337.2 degrees. The at first rapid, and later gradual, increase of reading is due to the warming up of the equipment.

* Decimal classification: R114. Original manuscript received by the Institute, September 8, 1939.

† Wheaton, Ill.

[1] K. G. Jansky, "Directional studies of atmospherics at high frequencies," Proc. I.R.E., vol. 20, pp. 1920–1932; December, (1932).

[2] K. G. Jansky, "Electrical disturbances of extraterrestrial origin, Proc. I.R.E., vol. 21, pp. 1387–1398; October, (1933).

[3] K. G. Jansky, "A note on the source of interstellar interference," Proc. I.R.E., vol. 23, pp. 1158–1163; October, (1935).

[4] K. G. Jansky, "Minimum noise levels obtained on short-wave radio receiving stations," Proc. I.R.E., vol. 25, pp. 1517–1530; December, (1937).

[5] H. T. Friis and C. B. Feldman, "A multiple unit steerable antenna for short-wave reception," Proc. I.R.E., vol. 25, pp. 841–917; July, (1937); *Bell Sys. Tech. Jour.*, vol. 16, pp. 337–419; July, (1937).

[6] Greenstein and Whipple, "The origin of interstellar radio disturbances," *Proc. Nat. Acad. Sci.*, vol. 23, pp. 177–181; March, (1937).

[7] G. Reber, "Electric resonance chambers," *Communications*, vol. 18, pp. 5–8; December, (1938).

[8] F. B. Llewellyn, "Limits to Amplification," *Bell Sys. Tech. Jour.*, vol. 14, pp. 85–95; January, (1935).

85 per cent, and area of mirror 7×10^5 square centimeters. This gives a maximum radiation intensity of 4×10^{-21} watt per square centimeter or equivalent to the energy arriving from a star of 22.1 balometric magnitude which indicates some of the technical difficulties encountered.

The acceptance cone of the mirror is about 3 degrees in diameter so the maximum absolute intensity of radiation becomes 4.5×10^{-25} watt per square centimeter per circular degree per kilocycle band. When intensity is plotted versus galactic longitude the points of Fig. 4 result. The rest of the directions around the Milky Way will be measured during the coming year as they arrive in good position.

The amplifier of Fig. 2 consists of five stages of acorn tubes tuned by concentric lines to the signal frequency. The last stage works into a diode detector which actuates a direct-current amplifier with a microammeter in the plate circuit. An increase in input will cause an increase in bias and a resultant decrease in the microammeter reading. In actual operation the amplifier is on the end of the drum in Fig. 1 and the direct bias voltage is fed down the cable to control the equipment.

Perhaps it is well to point out that cosmic static is in no way connected with cosmic rays. The latter are high-speed particles and have no directional effect except a 1 per cent increase on the leading face of the earth as it moves through space.

Radiation of Charged Particles

Considerable material is being thrown off by the stars. This expands and tends to fill up the region between the stars with a very tenuous gas. Since the gas is at a much lower density than the best artificial vacuum the particles are relatively far apart. Under the action of starlight these atoms of gas are ionized or free electrons are ejected with a velocity dependent upon the color of the light involved. Therefore space is filled with positive particles and high-speed electrons (of a few volts energy).

These particles may encounter in a variety of ways. The one of interest here is a free-free transition; that is an electron approaches a positive charge from one direction and is acted upon to leave in another direction. In 1923 Kramers[9] deduced from classical electric theory that when an electron encounters an ion in such a free-free transition energy will be radiated at the expense of the velocity of the electron. Eddington[10] applied Kramers' theory to the material inside a star. At that time he argued a certain correction due to Einstein should not be applied to Kramers' formula. This correction takes into account the stimulation of such radiation due to the transition occurring in equilibrium with an electromagnetic field. Later Eddington[11] applied Kramers' theory to the material of interstellar space with the specific argument that the average velocity loss of an electron due to free-free transitions could not exceed 12 per cent. In 1930 Gaunt[12] rederived Kramers' formula on the basis of quantum mechanics. He decided that Kramers' work is correct for visual range, too high for the X-ray range and too low for the low frequencies. Since no application was known he did not go into the low-frequency case in detail but definitely stated Kramers' formula does not include the effect of stimulated radiation. Partly on this authority and partly to fit the theory to

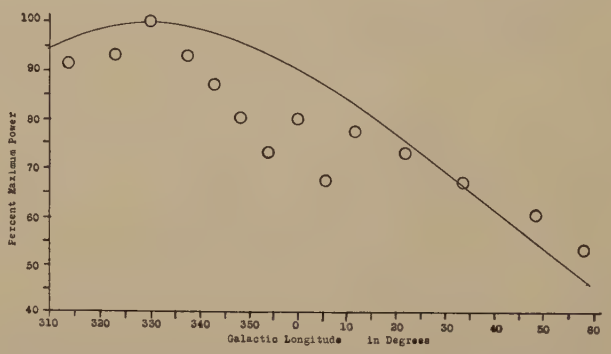

Fig. 4—Intensity versus Galactic longitude l. Circles indicate measured points. Solid line computed from equation (7).

measurements this correction is included in what follows.

Quantitative Calculations

Kramers gives the amount of energy liberated as

$$\rho = \frac{32\ \pi^2 Z^2 e^6}{3\sqrt{3}\ C^3 m^2 U} ns\Delta\nu \text{ ergs/cm}^3\text{/sec} \qquad (2)$$

where

n and s are numbers of electrons and ions per cubic centimeter
e, m, and U are the charge, mass, and velocity of the electrons
Z is the atomic number
C is the velocity of light
$\Delta\nu$ is the band width

The correction[10] for stimulated radiation may be reduced to incremental form such that true radiation becomes

$$\rho' = \frac{kT}{h\nu}\rho \text{ ergs/cm}^3\text{/sec} \qquad (3)$$

where

k is Boltzmann's constant
h is the Planck's constant
T is the effective temperature of the electromagnetic field (3.2 degrees absolute for space)
ν is the frequency in question

[9] H. A. Kramers, "Theory of the continuous X-ray spectrum," *Phil Mag.*, vol. 46, pp. 836; November, (1923).
[10] A. S. Eddington, "Absorption of radiation inside a star," Monthly Notices of Royal Astronomical Society, vol. 84, p. 104, (1924).
[11] A. S. Eddington, "Diffuse matter in interstellar space," *Proc. Royal Soc.*, vol. 111, pp. 424, (1926).
[12] Gaunt, "Continuous absorption," *Trans. Royal Soc.*, vol. 229, pp. 163, (1930).

Eddington[11] evaluated ρ as $\rho = 8.7 \times 10^{-42}\ \Delta\nu$ erg per cubic centimeter per second; therefore ρ' becomes

$$\rho' = 5\ 84 \times 10^{-31} \frac{\Delta\nu}{\nu} \text{ ergs/cm}^3\text{/sec.} \quad (4)$$

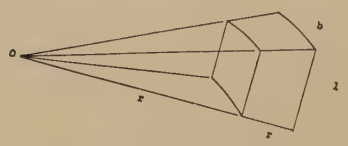

Fig. 5—Incremental volume used in calculation of radiation intensity.

Consider now the situation shown in Fig. 5. The incremental volume will be (when the angles are small)

$$\Delta V = r\Delta b\, r\Delta l \Delta r = r^2 \Delta b \Delta l \Delta r. \quad (5)$$

The incremental energy arriving at 0 from this incremental volume is

$$\Delta I = \frac{\rho'}{4\pi r^2} \Delta V = \frac{\rho'}{4\pi} \Delta b \Delta l \Delta r. \quad (6)$$

Integrating from zero to r centimeters gives an absolute intensity at 160 megacycles of $7 \times 10^{-41} r$ erg per second per square centimeter per circular degree per kilocycle band.

Astronomical Interpretation

Consider the geometry of Fig. 6 where

$$r = d \cos l + (d^2(\cos^2 l - 1) + c^2)^{1/2} \quad (7)$$

c = radius of the Milky Way
d = distance from the sun to the center
l = galactic longitude
r = distance from the earth to the edge of the galaxy.

The way r varies with l depends upon the ratio of d to c. The relation giving best fit to points is when $d = 2c/3$ and is shown by a solid line in Fig. 4. Dividing the observed maximum absolute intensity by the absolute intensity due to radiation from charged particles gives a maximum r of 6.5×10^{22} centimeters or 2.1×10^4 parsecs. The radius of the galaxy then becomes 12,600 parsecs.

Other Data

Various bright stars such as Vega, Antares, etc., have been tried but no measurable response was obtained. Repeated attempts to measure radiation from Mars were also of no avail. While some fine structure

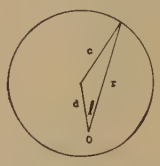

Fig. 6—Plan view of the Milky Way. Earth and sun at point O.

of radiation pattern seems to be present the existing equipment is not adequate for its accurate resolution. No conclusive measurements have been made on any of the extragalactic nebulae; however, these are to be worked on next. Tests on the sun are always under rather unfavorable conditions but if radiation occurs from this body it is of intensity below 4×10^{-24} watt-per-square-centimeter-per-kilocycle band at 160 megacycles.

In the beginning it was hoped (from the theory of black-body radiation) that the intensity would increase as the square of frequency. Therefore the first tests were made at 3300 megacycles with rather crude equipment. Nothing was found at the sensitivity limit of 10^{-20} watt per square centimeter per circular degree per kilocycle band. Better apparatus for a frequency of 900 megacycles also produced no positive results at a limit of 10^{-22} watt per square centimeter per circular degree per kilocycle band. These negative results point to a function for ρ' similar to the above.

The only other data amenable to calculation is that of Jansky's original paper. Taking into consideration the ground reflection[13] and assuming the Milky Way to have a thickness through the center of one tenth the diameter his maximum measured intensity will produce a radius of 13,100 parsecs and an eccentricity of 3/4 radius for the earth which is a good check on the inverse-frequency function of ρ'. It is also worthy of note that Plaskett in a recent paper[14] deduces a most probable radius of 15,000 parsecs for the Milky Way so these figures are in fair agreement.

[13] C. B. Feldman, "The optical behavior of the ground for short radio waves," Proc. I.R.E., vol. 21, pp. 764–801; June, (1933).
[14] J. S. Plaskett, "Modern conception of the stellar system" *Pop. Astronomy*, p. 293, May, (1939).

The Application of Feedback to Wide-Band Output Amplifiers*

F. ALTON EVEREST†, ASSOCIATE, I.R.E., AND HERBERT R. JOHNSTON‡, NONMEMBER, I.R.E.

Summary—*A mathematical analysis is made of a typical two-stage output amplifier designed for the amplification of a wide range of frequencies incorporating feedback over the two stages. In wide-band amplifiers the use of output transformers is usually ruled out due to frequency limitations, and it is found that the time constant of the feedback circuit cannot be neglected. The effect of the feedback circuit is to give rise to peaks in the response curves at both the high- and low-frequency extremities of the band. The finite time constant of the feedback circuit greatly affects the latter.*

Design curves are included giving the response and phase shift for both the low- and high-frequency regions in terms of the feedback factor, the grid-coupling time constant, and the feedback-circuit time constant for the low-frequency region, and the feedback factor and the time constants for the shunting circuits in the plate circuits of both stages for the high-frequency region. Complete derivations of all formulas are given in the two appendixes.

Introduction

DURING the last few years many papers have appeared which explain and analyze the causes for loss of gain and for the accompanying phase shift of wide-band amplifiers near their low- and high-frequency limits. These have been confined chiefly to low-level stages used mainly for voltage amplification. However, there often arises the need for amplifying signals containing components covering extremely wide frequency ranges to a level high enough to operate the electrostatic deflection plates of a cathode-ray oscillograph, to grid-modulate a television transmitter, or to perform other similar functions. In such cases, feedback over the last two stages is often helpful in minimizing distortion arising in handling relatively large signal voltages in pentodes as well as the salutary effect upon the frequency-response and phase-shift characteristics of the amplifier. It is felt that the application of feedback over the output stage and the associated driver stage of a wide-band amplifier has, perhaps, been often avoided due to a lack of understanding of the effect of the feedback circuit upon the amplifier characteristics near the high- and low-frequency extremities of the band. This paper attempts to fill this need by presenting a mathematical analysis covering both the low- and high-frequency regions which can be easily used in solving practical design problems.

I. Low Frequencies

It has previously been pointed out[1] that under certain conditions, peaks in the response curve may occur at both high and low frequencies in amplifiers using negative feedback. The authors of the article referred to assume that the feedback circuit is a resistive network. The use of negative feedback over two stages in a wide-band amplifier, however, necessitates the use of a blocking condenser to isolate the plate voltage of the second stage from the cathode circuit of the first as shown in Fig. 1, which is a schematic circuit diagram of a typical two-stage amplifier of the type under discussion. This blocking condenser has considerable effect on the amplifier characteristics at the low frequencies.

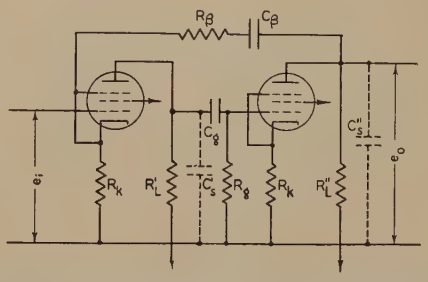

Fig. 1—A schematic wiring diagram of a typical output amplifier and driver having feedback applied across two stages.

For the low frequencies, the circuit of Fig. 1 may be simplified slightly by neglecting the shunting capacitances C_s' and C_s''. Using the familiar feedback equation, the following expression may be obtained:

$$\text{gain} = \frac{e_o}{e_i} = \frac{A}{1 - A\beta} \tag{1}$$

where

$A = e_0/e_i$, when the feedback elements C_β and R_β are omitted from their places in Fig. 1 and when R_L is shunted by the elements C_β, R_β, and R_K connected in series, and

$\beta = R_K/(R_K + R_\beta - j/\omega C_\beta)$, ($\beta$ is negative for the negative feedback circuit of Fig. 1).

A general parametric equation for the response ratio of this amplifier was developed involving two parameters, the feedback factor $A_0\beta_0$ at mid-band frequency, and the ratio T_β/T_g, involving the time constants of the feedback and grid-coupling circuits, respectively. This equation, developed in detail in Appendix A, is

$$\text{response ratio} = \frac{\omega T_\beta(\omega T_\beta - j1)}{(\omega T_\beta)^2 - p/(1-d) - j\omega T_\beta(1+p)/(1-d)} \tag{2}$$

where

response ratio = ratio of output voltage at low frequency to the output voltage at mid-band frequency,

* Decimal classification: R363. Original manuscript received by the Institute, October 4, 1939.

† Oregon State College, Corvallis, Oregon.

‡ Formerly graduate student, Oregon State College; now with Automatic Electric Company, Chicago, Illinois.

[1] F. E. Terman and Wen-Yuan Pan, "Frequency response characteristics of amplifiers employing negative feedback," *Communications*, vol. 19, pp. 5–7, 42, 44, 45; March, (1939).

$\omega = 2\pi f$,
f = frequency in cycles per second,
$T_\beta = C_\beta(R_\beta + R_K)$ = time constant of the negative-feedback network,
$T_g = C_g R_g$ = time constant of grid-coupling circuit,
$p = T_\beta / T_g$,
A_0 = amplification of amplifier at mid-band without feedback,
β_0 = feedback ratio at mid-band frequency, and
$d = A_0\beta_0$.

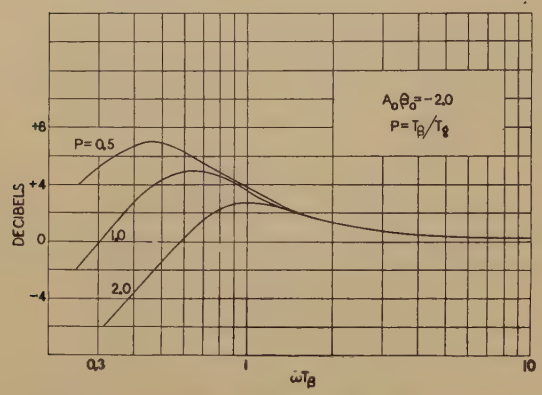

Fig. 2—Low-frequency response, feedback factor −2.0.

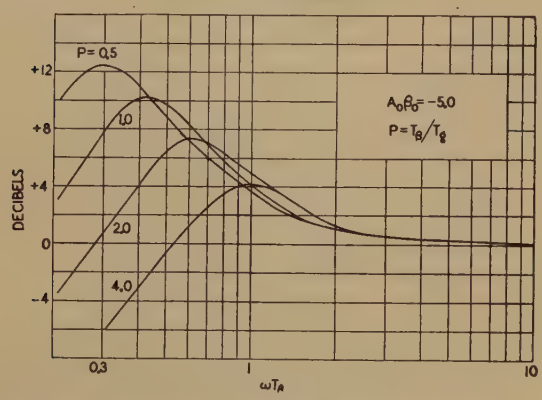

Fig. 3—Low-frequency response, feedback factor −5.0.

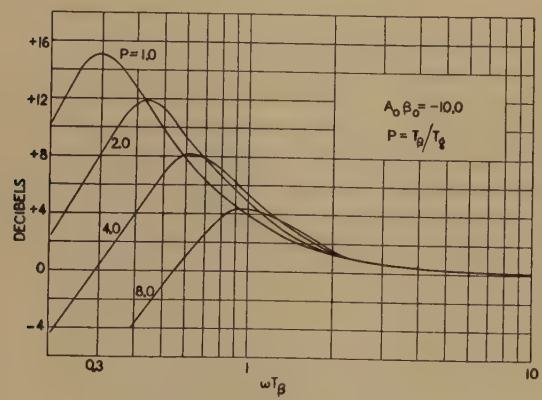

Fig. 4—Low-frequency response, feedback factor −10.0.

Figs. 2, 3, and 4 show families of curves plotted for various values of p and values of $A_0\beta_0$ of −2.0, −5.0, and −10.0, respectively. Figs. 5, 6, and 7 show the corresponding phase-shift families. These curves show the range of the variations of response and phase shift of the usual negative-feedback amplifier.

It will be noted that there exists a definite peak at the low frequencies, and this peak occurs where the rate of change of phase shift is relatively great. The

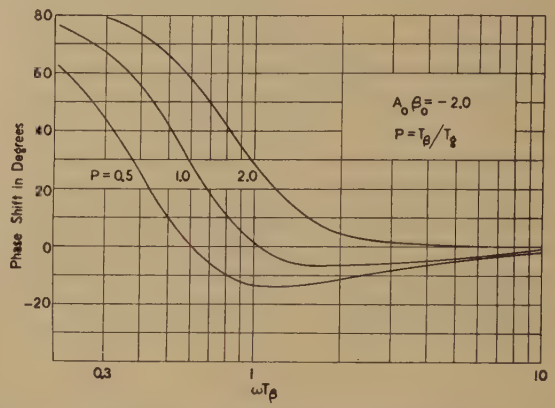

Fig. 5—Low-frequency phase shift, feedback factor −2.0.

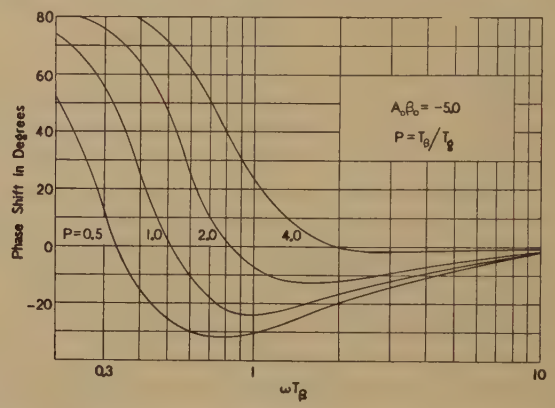

Fig. 6—Low-frequency phase shift, backfeed factor −0.5.

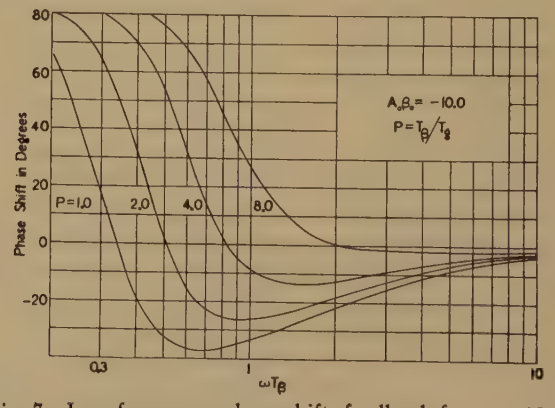

Fig. 7—Low-frequency phase shift, feedback factor −10.0.

peaks are higher as the feedback factor $A_0\beta_0$ is increased for the same value of p. For any fixed value of $A_0\beta_0$, the peaks in the low-frequency end of the band become smaller as the value of p increases. There is seen to be an optimum value of p for each value of the feedback factor $A_0\beta_0$ which makes the phase shift substantially zero out to a certain frequency, and this optimum value of p also gives only a very small peak in the region of large rate of change of phase shift.

By the use of these curves, it is possible to proportion the value of p for any feedback factor so that the phase shift is essentially zero out to a certain frequency and have only a very small peak in the low-frequency response curve below the useful range of the amplifier.

In the design of a feedback amplifier for wide-band use, the time-constant T_β is limited by the physical size of the capacitor C_β. This size must not be excessive, or stray capacitance to ground will adversely affect the high-frequency response. The resistor R_β is limited by the amount of feedback required. The cathode resistor R_K is limited by the bias requirements of the first tube. Thus, to increase p, the value of T_g must be decreased, which improves the action of the amplifier under high-amplitude shock and tends to prevent blocking.

II. High Frequencies

Fig. 8 shows a schematic diagram which is valid for the high-frequency region. The elimination of the

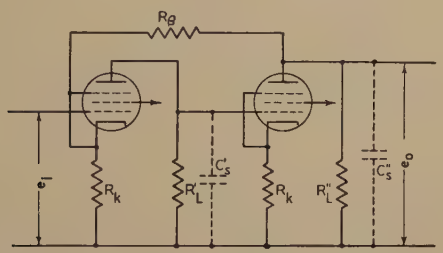

Fig. 8—Schematic circuit of two-stage feedback amplifier valid for the high-frequency region.

grid-leak resistor and plate resistance of the tube from the discussion is justified for pentode tubes used in wide-band amplifiers, because R_L is very small compared to R_g and R_p. The isolating condenser C_β is effective only in the low-frequency regions where its reactance is appreciable. Based upon these assumptions, a general parametric equation for the high-frequency response ratio is derived in Appendix B and found to be

$$\text{response ratio} = \frac{1 - A_0\beta_0}{1 - A_0\beta_0 - \dfrac{(\omega T_s')^2}{K} + j\omega T_s'\left(\dfrac{1+K}{K}\right)} \qquad (3)$$

where

A_0 = over-all amplification at mid-band frequencies without feedback,

β_0 = feedback ratio $= R_K/(R_\beta + R_K)$,

$T_s' = (R_L'C_s') =$ time constant of shunting circuit for stage 1,

$T_s'' = (R_L''C_s'') =$ time constant of shunting circuit for stage 2, and

$K = T_s'/T_s''$.

Figs. 9, 10, and 11 show high-frequency response curves for selected values of K from 0.1 to infinity for feedback factors $A_0\beta_0$ of -2.0, -5.0, and -10.0, respectively. A value of K of unity would mean that the two stages were identical as far as high-frequency response is concerned. Figs. 12, 13, and 14 present the companion phase-shift characteristics for the above figures.

It is seen that, in general, the greater the feedback factor $A_0\beta_0$, the higher the response peaks. The location of these peaks can be found by noting that for (3) to be a maximum, the denominator must be a minimum. The vector length of the denominator of (3)

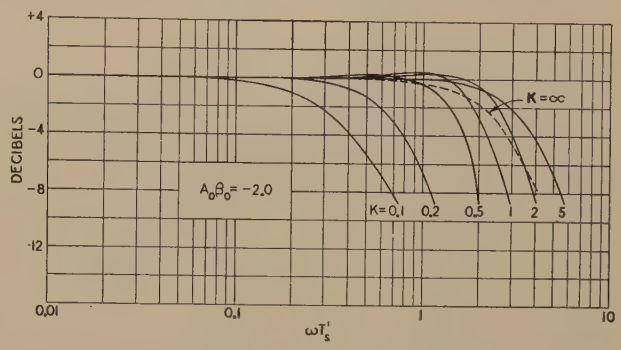

Fig. 9—High-frequency response, feedback factor -2.0.

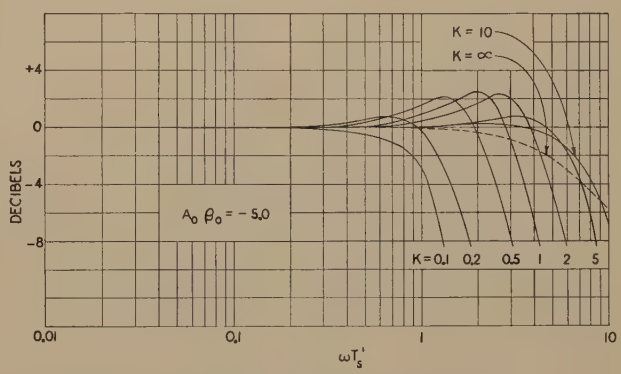

Fig. 10.—High-frequency response, feedback factor -5.0.

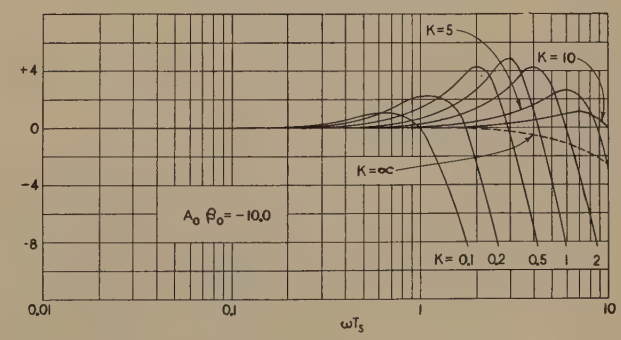

Fig. 11—High-frequency response, feedback factor -10.0.

differentiated with respect to $\omega T_s'$ and equated to zero gives the location of the peaks. The value of $\omega T_s'$ at the peaks of response is given by

$$\omega T_s' = \left[-\frac{K^2 + 2A_0\beta_0 K + 1}{2}\right]^{1/2}. \qquad (4)$$

A study of Figs. 9 to 14 inclusive also reveals that for every feedback factor there is a value of K which

will give the most nearly linear response over the widest range. To find the response peak which occurs at the highest frequency (or highest $\omega T_s'$), (4) may be differentiated with respect to K and equated to zero. The curve whose peak occurs at the largest value of $\omega T_s'$ is then given by

$$K = -A_0\beta_0. \tag{5}$$

For instance, in Fig. 10, the curve for $K=5$ satisfied (5). This curve has a slight hump, and the curves for values of K greater than 5 may also have peaks, but they will occur at lower values of $\omega T_s'$ than that for $K=5$. The peaks of the curves for values of K lower than 5 also occur at lower values of $\omega T_s'$.

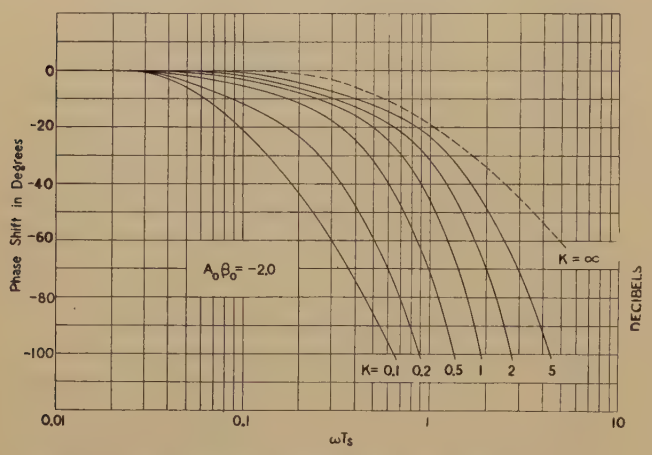

Fig. 12—High-frequency phase shift, feedback factor −2.0.

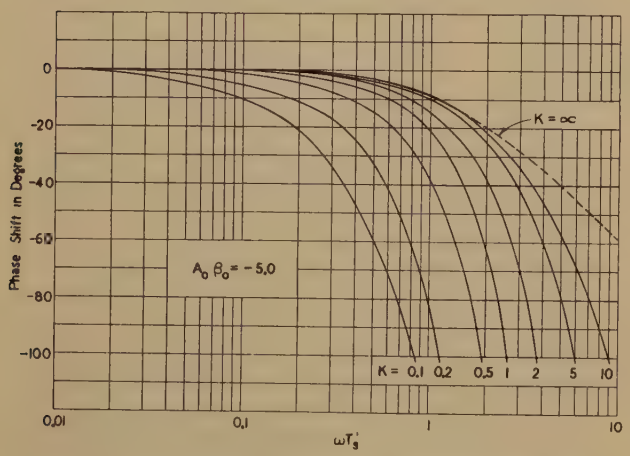

Fig. 13—High-frequency phase shift, feedback factor −5.0.

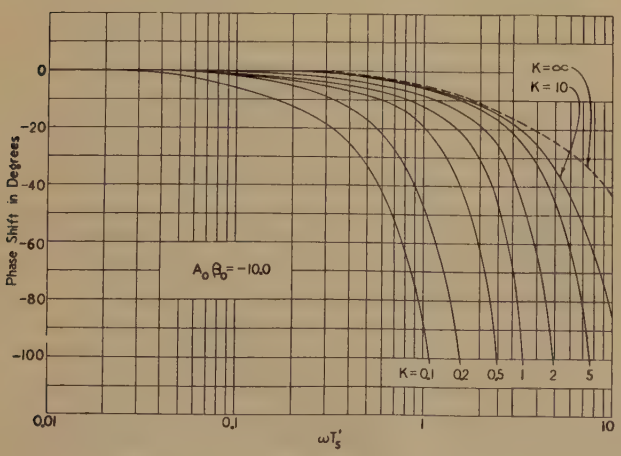

Fig. 14—High-frequency phase shift, feedback factor −10.0.

Substituting (5) in (4) gives the location of the peak that occurs at the highest value of $\omega T_s'$. This location is given by

$$\omega T_s' = \left[\frac{A_0^2\beta_0^2 - 1}{2}\right]^{1/2}. \tag{6}$$

Solving (6) for $A_0^2\beta_0^2$ and substituting (5) in (6) gives the following relationship which is very useful:

$$(A_0\beta_0)^2 = K^2 = 2(\omega T_s')^2 + 1. \tag{7}$$

T_s' is usually fixed by the fact that a certain amount of shunt capacitance is built into the amplifier, and R_L' is fixed by the driving voltage needed for the next stage. The problem is then to find a value of T_s'' that can be used and still have a satisfactory high-frequency response. A solution may be found by determining a value of $\omega T_s'$ from the value of T_s' existing and the highest frequency at which good amplification and modest phase shift are desired. This value of $\omega T_s'$ is then substituted in (7) and values of $A_0\beta_0$ and K found.

For example, assume an output amplifier whose amplification should extend to 4 megacycles with only a moderate phase shift. Assuming a value of R_L' of 4000 ohms and C_s' of 35 micromicrofarads, the value of T_s' becomes 0.14 microsecond. The corresponding value of $\omega T_s' = (2\pi)(4\times10^6)(0.14\times10^{-6}) = 3.52$. Substituting this value of $\omega T_s'$ into (7) gives a value of K of 5.08 and a value of $A_0\beta_0$ of -5.08. From the curves of Figs. 10 and 13 for $A_0\beta_0 = -5.0$, it is found that the response is uniform within plus or minus 1 decibel out to more than 6 megacycles, and that at 4 megacycles the phase shift is about 50 degrees. To accomplish this, a value of $T_s'' = T_s'/K = 0.14\times10^{-6}/5.08 = 0.0276\times10^{-6}$ must be used.

Appendix A

Derivation of the General Parametric Equation for the Phase and Gain Characteristics of a Negative-Feedback Amplifier at Low Frequencies

Fig. 1 shows the circuit diagram for the mathematical analysis of the phase and gain characteristics of a negative-feedback amplifier.

Let A_0 = mid-band amplification of amplifier with no feedback,

A = complex amplification factor of amplifier at low frequencies without feedback,

β_0 = feedback at mid-band frequencies,

β = complex expression for feedback at low frequencies,

$T_g = C_gR_g$ = time constant of grid-coupling circuit,

$T_\beta = C_\beta(R_k + R_\beta)$, time constant of feedback circuit,

R_k = cathode resistor of first tube (part of feedback circuit),
e_i = input voltage of amplifier,
e_0 = output voltage of amplifier,
$p = T_\beta/T_g$
$d = A_0\beta_0$ feedback factor
$\omega = 2\pi f$, and
$j = \sqrt{-1}$ = complex operator.

It may easily be shown that the complex amplification factor of the amplifier without feedback shown in Fig. 1 is

$$A = A_0/(1 - j/\omega T_g). \tag{1}$$

It may also be seen that the feedback ratio at low frequencies is given by the expression

$$\beta = \frac{R_k}{R_k + R_\beta - j/\omega C_\beta}. \tag{2}$$

Dividing (2) by the quantity (R_k+R_β) gives

$$\beta = \frac{R_k/(R_k + R_\beta)}{1 - j/\omega T_\beta}. \tag{3}$$

But, since $\beta_0 = R_k/(R_k+R_\beta)$, substituting this in the above expression gives

$$\beta = \frac{\beta_0}{1 - j/\omega T_\beta}. \tag{4}$$

Substituting (1) and (4) in the familiar feedback equation

$$\text{gain} = e_0/e_i = \frac{A}{1 - A\beta} \tag{5}$$

gives the expression

$$\text{gain} = \frac{A_0/(1 - j/\omega T_g)}{1 - \dfrac{A_0\beta_0}{(1 - j/\omega T_g)(1 - j/\omega T_\beta)}}. \tag{6}$$

Simplifying the above equation gives

$$\text{gain} = \frac{A_0\omega T_g(\omega T_\beta - j1)}{T_g T_\beta(\omega)^2(1 - A_0\beta_0) - 1 - j\omega(T_g + T_\beta)}. \tag{7}$$

The gain of the amplifier at mid-band frequency is given by

$$\text{gain (mid-band)} = A_0/(1 - A_0\beta_0). \tag{8}$$

The relative response of the amplifier is given by the ratio of the gain at low frequencies to the gain at mid-band frequencies:

$$\text{response ratio} = \frac{\text{equation (7)}}{\text{equation (8)}}. \tag{9}$$

Simplification results in

$$\text{response ratio} = \frac{\omega T_g(\omega T_\beta - j1)(1 - A_0\beta_0)}{T_g T_\beta(\omega)^2(0 - A_0\beta_0) - 1 - j\omega(T_g + T_\beta)}. \tag{10}$$

Dividing by T_g, multiplying by T_β, and substituting the parameters

$$p = T_\beta/T_g \text{ and } d = A_0\beta_0$$

gives the equation

$$\text{response ratio} = \frac{\omega T_\beta(\omega T_\beta - j1)(1 - d)}{(\omega T_\beta)^2(1 - d) - p - j(p+1)\omega T_\beta}. \tag{11}$$

Dividing by the quantity $(1-d)$ gives the final equation

$$\text{response ratio} = \frac{\omega T_\beta(\omega T_\beta - j1)}{(\omega T_\beta)^2 - p/(1 - d) - j\omega T_\beta(1+p)/(1-d)}. \tag{12}$$

Appendix B

Derivation of the General Parametric Equation for the Phase and Gain Characteristics of a Negative-Feedback Amplifier at High Frequencies

Fig. 8 shows the circuit diagram for the analysis of the two-stage negative-feedback amplifier at high frequencies.

Let A_0', A_0'' = amplification of stages 1 and 2, respectively, at mid-band frequencies without feedback,
$A_0 = (A_0'A_0'')$ = over-all amplification at mid-band frequencies without feedback,
A', A'' = complex amplification of stages 1 and 2, respectively, in high-frequency region without feedback,
β_0 = feedback ratio at mid-band frequencies and at high frequencies,
R_L', R_L'' = plate load resistances of stages 1 and 2, respectively,
C_s', C_s'' = total shunting capacitances of stages 1 and 2, respectively,
$T_s' = (R_L'C_s')$ = time constant of shunting circuit for stage 1,
$T_s'' = (R_L''C_s'')$ = time constant of shunting circuit for stage 2,
$K = T_s'/T_s''$ = ratio of time constant of shunting circuit of stage 1 to that of stage 2.

Assuming that R_L' and R_L'' are much smaller than R_g or the plate resistance of the tubes, it can be demonstrated that the complex amplification of stage 1 in the high-frequency region is

$$A' = \frac{A_0'}{1 + j\omega T_s'}$$

and for stage 2 is

$$A'' = \frac{A_0''}{1 + j\omega T_s''}.$$

The over-all high-frequency amplification without feedback is then given by

$$A'A'' = \frac{A_0'A_0''}{(1 + j\omega T_s')(1 + j\omega T_s'')}. \tag{1}$$

The feedback ratio at high frequencies remains the same as for mid-band frequencies, because the reactance of C_β becomes negligible. Therefore,

$$\beta_0 = \frac{R_K}{R_\beta + R_K}. \tag{2}$$

The gain in the high-frequency region using the familiar feedback equation is given by

$$\text{h-f gain} = \frac{e_0}{e_i} = \frac{(A'A'')}{1 - (A\,A'')\beta_0}. \tag{3}$$

Substituting (1) and (2) in (3) gives:

$$\text{h-f gain} = \frac{\dfrac{A_0'A_0''}{(1+j\omega T_s')(1+j\omega T_s'')}}{1-\left[\dfrac{A_0'A_0''}{(1+j\omega T_s')(1+j\omega T_s'')}\right]\left[\dfrac{R_K}{(R_\beta+B_K)}\right]},$$

which may be simplified to

$$\text{h-f gain} = \frac{A_0(R_\beta+R_K)}{(1+j\omega T_s')(1+j\omega T_s'')(R_\beta+R_K)-A_0R_K}. \tag{4}$$

But

$$\text{mid-band gain} = \frac{A_0}{1 - A_0\beta_0} \tag{5}$$

and

$$\text{response ratio} = \frac{\text{gain at h-f point}}{\text{mid-band gain}} = \frac{\text{equation (4)}}{\text{equation (5)}}, \tag{6}$$

therefore

$$\text{response ratio} = \frac{\dfrac{A_0(R_\beta+R_K)}{(1+j\omega T_s')(1+j\omega T_s'')(R_\beta+R_K)-A_0R_K}}{\dfrac{A_0}{1-A_0\beta_0}}.$$

Simplifying and dividing the numerator and denominator by $(R_\beta+R_K)$,

$$\text{response ratio} = \frac{1-A_0\beta_0}{1-A_0\beta_0-(\omega T_s')(\omega T_s'')+j(\omega T_s'+\omega T_s'')}. \tag{7}$$

Letting $K = T_s'/T_s''$ and substituting it into (7) gives the general parametric equation,

$$\text{response ratio} = \frac{1-A_0\beta_0}{1-A_0\beta_0-\dfrac{(\omega T_s')^2}{K}+j\omega T_s'\dfrac{(1+K)}{K}}. \tag{8}$$

The response ratio may be translated directly into decibels above or below the zero-decibel point corresponding to a response ratio of unity in the mid-band region.

Acknowledgment

The assistance of Messrs. William H. Huggins and Lee Coe is gratefully acknowledged, the former for his analysis leading to equations (4) to (7) of the main body of the paper, and the latter for the calculation and preparation of some of the figures. Both are students in Electrical Engineering at Oregon State College.

Antenna Arrays with Closely Spaced Elements*

JOHN D. KRAUS†, ASSOCIATE MEMBER, I.R.E.

Summary—*A number of arrays called "flat-top beam" antennas using closely spaced out-of-phase elements are described. Gain equations are developed for arrays with closely spaced horizontal elements above perfectly conducting ground.*

Curves showing the effect of spacing and loss resistance on the gain and resistance of a "flat-top beam" are presented. It is shown that at small spacings, loss resistance has an important effect on the radiating efficiency of the array. Curves illustrating the effect of height above ground on the gain and vertical radiation pattern are also given.

Introduction

RECENTLY it was shown by G. H. Brown[1] that directional antennas using parallel elements spaced less than one-quarter wavelength were capable of worth-while gains for many relations of current magnitude and phase. For convenience we may designate these arrays using spacings of less than one-quarter wavelength as antennas with "closely spaced elements."

The use of such close spacing makes possible the construction of a very compact array having a substantial gain. An array of this type which is of considerable practical interest is one in which two parallel elements are driven with equal and out-of-phase currents. Brown[1] has given data on this type in his Figs. 15 and 16 which apply to vertical quarter-wave elements above a perfectly conducting ground. An application of this array for use on the high frequencies consists of two half-wave elements oriented in a horizontal plane some distance above the ground. It is the main purpose of this paper to investigate the characteristics of this type of antenna under different conditions of spacing, height above ground, loss resistance, and so forth.

* Decimal classification: R325.1. Original manuscript received by the Institute, November 14, 1938; abridgment received, December 17, 1939. Presented in part before Detroit Section, September 23, 1938. Figs. 4, 5, and 6 were published in *Radio*, no. 236, pp. 9–19; February, (1939).

† Ann Arbor, Michigan.

[1] G. H. Brown, "Directional antennas," PROC. I.R.E., vol. 25, pp. 78–145; January, (1937).

The "Flat-Top Beam" Antenna[2-7]

A number of directional arrays using horizontal closely spaced out-of-phase elements are shown in plan view in Fig. 1. In Figs. 1A and 1B we have two closely spaced elements approximately one-half wavelength long, fed with equal and out-of-phase currents. The type at A is fed at the center and that at B from one end. The arrows indicate the direction of the antenna currents at a given instant. Practical values of the spacing S lie between 0.1 and 0.3 wavelength. The radiation pattern of these arrays is bidirectional. The free-space maximum is in the plane of the elements and at right angles to them. Minimum radiation occurs in a vertical plane, parallel to the elements.

Figs. 1C and 1E show arrays in which additional colinear sections have been added, each consisting of two half-wave elements. These arrays give a sharper horizontal radiation pattern and increased gain. The type at C can be spoken of as having two sections and that at E as having four sections. Crossovers between the sections provide the proper phasing. The types in Figs. 1C and 1E are fed in the center, while those of Figs. 1D and 1F are similar types fed from one end. Types with three sections or more than four sections are also possible.

Although these antennas are well suited for use horizontally as has been described, they can, of course, also be operated vertically. In this case the end-fed types with the feeders at the lower end are usually more convenient.

Fig. 2 shows the horizontal radiation pattern from an antenna of the type of Fig. 1A. The solid curve is

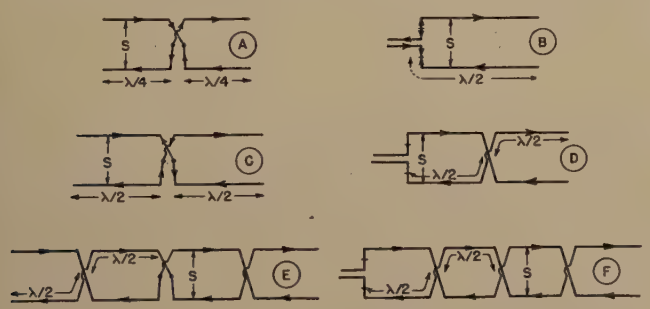

Fig. 1—Six types of "flat-top beam" antennas.

computed for free-space and the dashed curve measured. The spacing was one-eighth wavelength and the antenna was designed for operation on approximately 14 megacycles. It was situated about one wavelength above ground. Measurements were made by means of a calibrated field-strength meter located in a fixed position at a distance of about five wavelengths from the antenna. The antenna was then rotated so that the pattern could be measured. The maximum signal occurred broadside (90 degrees) and the minimum off the ends of the elements. This

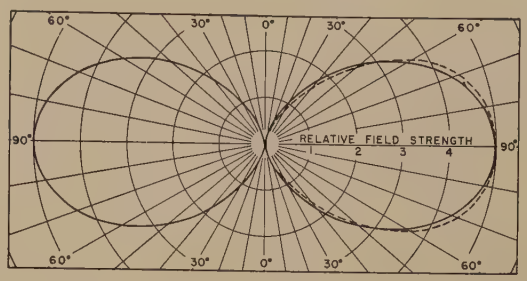

Fig. 2—Horizontal radiation pattern of a two-element array of the type shown in Fig. 1A. The elements of the antenna are horizontal and the maximum radiation is broadside to the array. The spacing S is one-eighth wavelength. The solid curve is computed and the dashed curve measured.

antenna gives approximately the same type of horizontal radiation pattern as shown in Fig. 2 over a range of frequencies from less than that of the fundamental to twice the fundamental frequency.

Loss Resistance and Spacing

A transmitting antenna is an electrical device for radiating radio-frequency power. The radiating efficiency depends on the ratio of the power radiated to the power delivered to the antenna. The fraction which is not radiated is dissipated in the loss resistance and appears chiefly in the form of heat, as for example, in the antenna conductor itself or in the insulators supporting the antenna. In other words, an antenna with a total terminal resistance R_0 may be considered to have a terminal radiation resistance R_{00} and an effective terminal loss resistance R_{0L} such that

$$R_0 = R_{00} + R_{0L}.$$

It follows, then, that

$$\text{radiating efficiency in per cent} = \frac{R_{00}}{R_{00} + R_{0L}} \times 100.$$

Since many types of short-wave antennas have radiation resistances which are large compared to any loss resistances which may be present, the efficiencies are very high. In an array with closely spaced elements, however, the radiation resistance is usually much less and a serious reduction in radiating efficiency may result from the presence of even a relatively small loss resistance. It is, therefore, of importance to investigate the effect of both spacing and loss resistance on the gain of a "flat-top beam" antenna.

With the exception of a four-element array treated at the end of this paper, the following discussion will

[2] J. D. Kraus, "Small but effective flat-top beam," *Radio*, no. 217, p. 56; March, (1937); also *Radio*, no. 220, p. 10; June, (1937).

[3] J. D. Kraus, "Rotary flat-top beam antennas," *Radio*, no. 224, p. 11; December, (1937).

[4] J. D. Kraus, "Directional antennas with closely-spaced elements," *QST*, vol. 22, p. 21; January, (1938).

[5] R. R. Sprole and J. D. Kraus, "Optional end-fire directivity with the flat-top beam antenna," *Radio*, no. 225, p. 85; January, (1938).

[6] J. D. Kraus, "Flat-top beam antennas," *Television and Short-Wave World* (London), vol. 11, p. 101; February, (1938).

[7] J. D. Kraus, "New design data on the flat-top beam antenna," *Radio*, no. 230, p. 15; June, (1938).

be limited to arrays of *two* parallel horizontal elements having an electrical length of 180 degrees. In practice, antennas are frequently made somewhat shorter than 180 degrees. However, it has been pointed out by Brown[8] that the ratio of the mutual to self-resistance of two identical antennas is quite constant over a rather wide range of lengths. The radiation resistance of the array will be slightly different when lengths other than 180 degrees are used for the elements. The gain of the array, however, when compared to a single element of the same length as the array elements will be practically unchanged. Accordingly, gain—spacing calculations

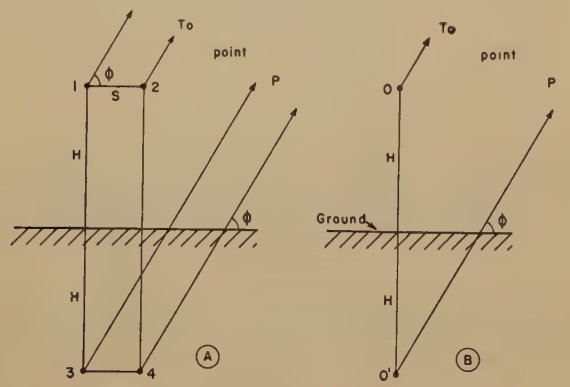

Fig. 3

made on the basis of 180-degree elements will be substantially the same as for slightly shorter or longer elements.

Height above Ground

Antennas are normally operated in proximity to the ground. It is, therefore, of interest to determine the characteristics of the horizontal two-element array operating at a height H above ground. Fig. 3A shows in end view two parallel 180-degree elements, 1 and 2, having a spacing S and a height H above ground. The quantities S and H may be expressed in a number of units. Thus,

$$S^\circ = 2\pi S_\lambda = 2\pi \frac{S_m}{\lambda_m},$$

where S° = spacing in electrical degrees,
S_λ = spacing measured in wavelengths,
S_m = spacing measured in meters, and
λ_m = wavelength measured in meters or in the same units as the spacing.

Similar designations may be written for H.

Antennas can be compared in a number of ways. The two following types of comparison are used in this paper. *First*, a horizontal antenna at a certain height above ground is compared with a half-wave antenna in free space. This gives the vertical-plane radiation pattern of the horizontal antenna above ground. *Second*, the horizontal antenna at a height H above ground is compared with a half-wave reference antenna at the same height above the same type of ground. This type of comparison is one often used experimentally.

Let us consider that the ground is perfectly conducting. It has been pointed out,[9] that for the purpose of comparing horizontal antennas more than one-quarter wavelength above ground this assumption will yield very nearly the same results as would be obtained by making the comparison over most types of actual ground. Thus, the gain at a given vertical angle of one antenna over another with both above perfectly conducting ground will be substantially the same as with both above ordinary ground.

For the purpose of analysis, the perfectly conducting ground may be replaced by an image of the antenna located as far below the surface of the ground as the real antenna is above. Referring to Fig. 3A, the image of element 1 is 3 and of 2 is 4. We wish to compare the field of the array of two elements above ground, or of the two elements and their images, at a distant point P in the plane passing through the center of the elements and perpendicular to them. This point is at a sufficient distance D from the array that the radius vectors from P to the different elements are essentially parallel. The angle which these radius vectors make with the horizontal is ϕ.

Although this discussion is chiefly concerned with the particular case when the currents in the two elements are equal and opposite in phase, the gain equations can be developed for the more general case with little additional effort. This general case applies to currents in the two elements having any desired magnitude and phase relation. Equal and out-of-phase currents will then be considered as a special case.

Gain Equations

The expression for the gain in field strength of the two-element array at any vertical angle ϕ will be derived as a function of loss resistance, spacing between the elements, height above ground, and the magnitude and phase relation of the element currents. The method will be that used by Brown.[1] We desire to find the gain of the array consisting of two closely spaced horizontal 180-degree elements above ground over a single horizontal 180-degree reference element at the same height above ground and operated at the same frequency. Since it may be desirable, however, to know also the gain of either the array above ground or the half-wave antenna above ground over a half-wave antenna in free space, the derivation is made in three steps.

First, the expression is derived for the gain of the array at a height H above ground over a half-wave antenna in free space. *Second*, the gain is computed

[8] See page 88 of footnote reference (1).

[9] Friis, Feldman, and Sharpless, "Determination of direction of arrival of short radio waves," Proc. I.R.E., vol. 22, p. 53; January, (1934).

for a single horizontal half-wave antenna at a height H above ground over a half-wave antenna in free space. *Third*, the gain of the array over the half-wave antenna at the same height above ground is obtained by taking the ratio of the gains obtained in the first and second steps. In all cases in computing the gain, equal powers are assumed in the antenna under consideration and the antenna to which the gain is referred. Also, 180-degree elements and the same form factor are assumed throughout.

Gain of Array over Free-Space Half-Wave Antenna

Let the currents in the array elements be related as follows:

$$I_2 = MI_1\angle\alpha \quad \text{or} \quad I_1 = \frac{I_2}{M}\angle -\alpha \tag{1}$$

where I_1 = root-mean-square current at current loop of element 1,
I_2 = same for element 2,
M = a fraction relating the current magnitudes, and
α = the phase angle between the currents in elements 1 and 2.

The currents in the image elements will be,

$$I_3 = -I_1 \quad \text{and} \quad I_4 = -I_2. \tag{2}$$

Writing Kirchhoff's law for each element,

$$\left.\begin{aligned} V_1 &= I_1Z_{11} + I_1Z_{1L} + I_2Z_{12} + I_3Z_{13} + I_4Z_{14} \\ V_2 &= I_1Z_{12} + I_2Z_{22} + I_2Z_{2L} + I_3Z_{23} + I_4Z_{24} \\ V_3 &= I_1Z_{13} + I_2Z_{23} + I_3Z_{33} + I_3Z_{3L} + I_4Z_{34} \\ V_4 &= I_1Z_{14} + I_2Z_{24} + I_3Z_{34} + I_4Z_{44} + I_4Z_{4L} \end{aligned}\right\} \tag{3}$$

where, V_1, V_2, etc. = the driving voltages at the terminals of the respective elements. For the purpose of analysis, we can assume that the element is driven by a generator of constant power output inserted at the current-loop point. The voltage appearing across this generator is then V. And where,

Z_{11}, Z_{22}, etc. = self-impedances of the elements,
Z_{12}, Z_{13}, Z_{14}, etc. = mutual impedances between elements, and

Z_{1L}, Z_{2L}, etc. = loss impedances of the elements.

The losses of each element may consist of several parts, the copper loss, the dielectric loss, and so forth. The effect of the losses on the mutual impedances is considered as being negligible. It is further assumed that the real part of the loss impedance is independent of the spacing, height of the elements, and so forth.

Substituting from (1) and (2) in (3), we obtain

$$\left.\begin{aligned} V_1 &= I_1[Z_{11} + Z_{1L} + M|Z_{12}|\angle(\alpha+\beta_{12}) - Z_{13} - M|Z_{14}|\angle(\alpha+\beta_{14})] \\ V_2 &= I_2\left[\frac{|Z_{12}|}{M}\angle(-\alpha+\beta_{12}) + Z_{22} + Z_{2L} - \frac{|Z_{23}|}{M}\angle(-\alpha+\beta_{23}) - Z_{24}\right] \\ V_3 &= I_3[-Z_{13} - M|Z_{23}|\angle(\alpha+\beta_{23}) + Z_{33} + Z_{3L} + M|Z_{34}|\angle(\alpha+\beta_{34})] \\ V_4 &= I_4\left[-\frac{|Z_{14}|}{M}\angle(-\alpha+\beta_{14}) - Z_{14} + \frac{|Z_{34}|}{M}\angle(-\alpha+\beta_{34}) + Z_{44} + Z_{4L}\right] \end{aligned}\right\} \tag{4}$$

where

β_{12}, β_{23}, etc. = phase angles of the mutual impedances.

But

$$Z_{12} = R_{12} + jX_{12}$$

and

$$R_{12} = |Z_{12}|\cos\beta_{12}$$

and

$$X_{12} = |Z_{12}|\sin\beta_{12}, \text{ etc.}$$

Likewise

$$Z_{11} = R_{11} + jX_{11}, \text{ etc.}$$

where

R_{11} = self-resistance of element 1, and
X_{11} = self-reactance of element 1.

Expanding (4)

$$\left.\begin{aligned} V_1 &= I_1[R_{11} + R_{1L} + M|Z_{12}|\cos(\alpha+\beta_{12}) - R_{13} - M|Z_{14}|\cos(\alpha+\beta_{14}) \\ &\quad + j\{X_{11} + X_{1L} + M|Z_{12}|\sin(\alpha+\beta_{12}) - X_{13} - M|Z_{14}|\sin(\alpha+\beta_{14})\}] \\ V_2 &= I_2\left[R_{22} + R_{2L} + \frac{|Z_{12}|}{M}\cos(-\alpha+\beta_{12}) - R_{24} - \frac{|Z_{23}|}{M}\cos(-\alpha+\beta_{23})\right. \\ &\quad \left. + j\left\{X_{22} + X_{2L} + \frac{|Z_{12}|}{M}\sin(-\alpha+\beta_{12}) - X_{24} - \frac{|Z_{23}|}{M}\sin(-\alpha+\beta_{23})\right\}\right] \end{aligned}\right\} \tag{5}$$

and there are two similar expressions for V_3 and V_4.

Let P be the power delivered to the array consisting of elements 1 and 2. An equal power, in this analysis, is present in the image of the array. Each element alone has a power input equal to the product of its current squared and the resistive or real component of its impedance as given in (5). The total power in all four elements is $2P$. In addition, by symmetry we can write

$$\left.\begin{aligned} R_{11} &= R_{22} = R_{33} = R_{44} \\ R_{12} &= R_{34},\ R_{13} = R_{24},\ \text{etc.} \\ R_{1L} &= R_{2L} = R_{3L} = R_{4L} \end{aligned}\right\}. \tag{6}$$

Substituting from (6) in (5) and adding up the power in all four elements, we obtain

$$2P = I_1^2[2R_{11} - 2R_{13} + 2M^2R_{11} - 2M^2R_{13} + 2R_{1L} + 2M^2R_{1L} + 4MR_{12}\cos\alpha - 4MR_{14}\cos\alpha] \tag{7}$$

and the current in element 1 is

$$I_1 = \sqrt{\frac{P}{(R_{11} + R_{1L} - R_{13})(M^2 + 1) + 2M\cos\alpha(R_{12} - R_{14})}}. \tag{8}$$

Since the relation of the currents in all of the elements is known, it is possible by means of (8) to obtain the current in each element when the R's are known. Then in order to find the field strength F at the point P, the fields due to the currents in each of the elements are added vectorially. The point P is at a large distance D in a direction making an angle ϕ with the horizontal. Performing this addition and expressing the currents in terms of I_1 gives

$$F = kI_1\left|\ [1 + M\angle(\alpha + S^\circ\cos\phi) - 1\angle(2H^\circ\sin\phi) - M\angle(\alpha + S^\circ\cos\phi + 2H^\circ\sin\phi)]\ \right| \tag{9}$$

where k = a constant involving the distance D, the frequency, and form factor.

Let us now consider a 180-degree element in free space. The field strength from this antenna will be constant in all directions in the plane passing through the center of the element and perpendicular to it. For a power input P to the antenna, the field strength F' at a distance D in this plane is

$$F' = k\sqrt{\frac{P}{R_{00} + R_{0L}}}. \tag{10}$$

where

k = same constant as in (9),

R_{00} = self-resistance of the element, and

R_{0L} = loss resistance of the element.

Putting the value of I_1 from (8) in (9) and dividing this result by (10) gives the *gain in field strength of the two-element array* at any vertical angle ϕ and height H above ground over the field from a single element in free space as follows:

$$\text{gain (A.A.G.)}^{10} = \sqrt{\frac{R_{00} + R_{0L}}{(R_{11} + R_{1L} - R_{13})(M^2 + 1) + 2M\cos\alpha(R_{12} - R_{14})}} \cdot \left|\ [1 + M\angle(\alpha + S^\circ\cos\phi) - 1\angle(2H^\circ\sin\phi) - M\angle(\alpha + S^\circ\cos\phi + 2H^\circ\sin\phi)]\ \right|. \tag{11}$$

This expression completes the first step in deriving the gain equations. Before proceeding with the second step let us examine several of the equations already obtained, for the case of a "flat-top beam" antenna where $M = 1$ and $\alpha = 180$ degrees. For this case, (8) becomes

$$I_1 = \sqrt{\frac{P}{2(R_{11} + R_{1L} + R_{14} - R_{12} - R_{13})}}. \tag{12}$$

This expression gives the current in either element of a two-element array having equal and out-of-phase currents as a function of spacing, height, loss resistance, and power input P. Sources for the R's will be mentioned later. The total resistance R_1 of each element is

$$R_1 = R_{11} + R_{1L} + R_{14} - R_{12} - R_{13}. \tag{13}$$

When R_{1L} is zero, (13) gives the radiation resistance of each element. As the array is elevated to large heights R_{13} and R_{14} become very small and with the array in free space are zero.

Two curves indicating the variation of the current I_1 with spacing for 100 watts input to the array are shown in Fig. 4. One curve is for zero loss resistance

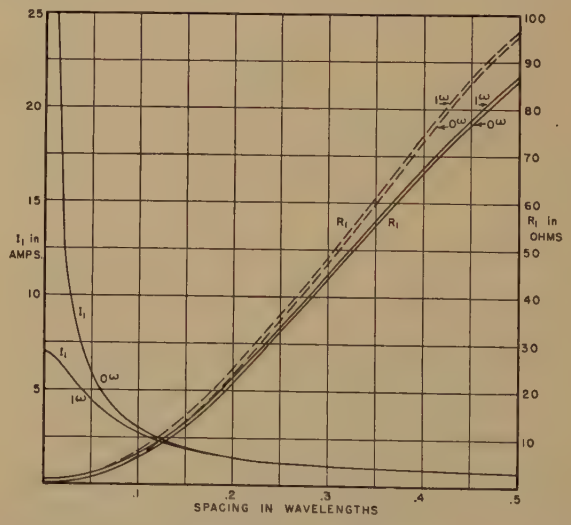

Fig. 4—Current and resistance of each element of an array of two out-of-phase elements as a function of spacing.

(0^ω) and the other for a 1-ohm loss resistance (1^ω) per element. These curves as computed from (12) show that with no losses the current reaches very high values at small spacings, but is definitely limited when a 1-ohm loss resistance is present.

The total resistance R_1 of either element as given

by (13) as a function of the spacing is also shown in Fig. 4. The two solid curves are for the case of the array in free space and the two dashed curves when the height is 0.5 wavelength above perfectly conducting ground. One curve of each pair is for zero loss resistance and the other for a loss resistance of 1 ohm. These curves indicate that as the spacing is reduced the resistance becomes very small and approaches the loss resistance as the spacing is reduced to zero. It is also apparent that the resistance of the elements with the array one-half wavelength above ground is not much different than when the array is in free space except at large spacings.

Gain of Half-Wave Antenna above Ground over Half-Wave Antenna in Free Space

Let us now proceed with the second step in obtaining the gain equations, namely, that of finding the gain of a 180-degree antenna above ground over an antenna of the same type in free space.

Fig. 3B shows a horizontal 180-degree element 0 in end view and at a height H above ground. For a perfectly conducting earth, the ground may be replaced by the image 0′ at a distance $2H$ from 0. Writing Kirchhoff's law for each element and following the same procedure as for the two-element array, we obtain

$$I_0 = \sqrt{\frac{P}{R_{00} + R_{0L} - R_{00'}}} \tag{14}$$

where

I_0 = current in element 0,
P = power delivered to element 0,
R_{00} = self-resistance of element 0,
R_{0L} = loss resistance of element 0, and
$R_{00'}$ = mutual resistance of element 0 and its image 0′.

The total resistance R_0 of element 0 is

$$R_0 = R_{00} + R_{0L} - R_{00'}. \tag{15}$$

As the element 0 is raised to large heights above the ground, $R_{00'}$ decreases to a very small value and becomes zero when the element is in free space.

The field strength at a distance D in the plane passing through the center of the element and perpendicular to it, is the vector sum of the fields from the real and image elements. This result is well known and is of the form

$$F'' = kI_0[2 \sin (H^\circ \sin \phi)]. \tag{16}$$

Substituting the value of I_0 as given in (14) in (16) and dividing this result by (10), the *gain of the half-wave antenna* above ground over the half-wave antenna in free space is obtained as follows:

$$\text{gain (H.W.A.G.)} = \sqrt{\frac{R_{00} + R_{0L}}{R_{00} + R_{0L} - R_{00'}}}\,[2 \sin (H^\circ \sin \phi)]. \tag{17}$$

This completes the second step of the derivation. When $R_{0L} = 0$ and $\phi = 90°$, (17) becomes equivalent to Brown's equation[11] (140) for the case of a flat-sheet reflector.

Gain of Array above Ground over Half-Wave Antenna above Ground

For the third step it merely remains to take the ratio of (11) to (17) which yields

$$\text{gain}\left(\frac{\text{A.A.G.}}{\text{H.W.A.G.}}\right) = \sqrt{\frac{R_{00} + R_{0L} - R_{00'}}{(R_{11} + R_{1L} - R_{13})(M^2 + 1) + 2M \cos \alpha (R_{12} - R_{14})}} \cdot \frac{\left|[1 + M\angle(\alpha + S^\circ \cos \phi) - 1\angle(2H^\circ \sin \phi) - M\angle(\alpha + S^\circ \cos \phi + 2H^\circ \sin \phi)]\right|}{2 \sin (H^\circ \sin \phi)}. \tag{18}$$

This expression gives the gain of a two-element horizontal array in which the currents have any magnitude relation as given by M or phase relation α with both elements at the same height H above ground. In order to obtain the gain of the array at one height above ground over the half-wave antenna at a different height above ground, (18) can be extended to include this case by merely putting the proper values of H° and R in the equation.

Gain of "Flat-Top Beam" Antenna

For the case of a "flat-top beam" antenna, $M = 1$ and $\alpha = 180$ degrees. Under these conditions (18) reduces to

[10] Array Above Ground. The gain is always referred to a half-wave antenna in free space except where "gain $\left(\frac{\text{A.A.G.}}{\text{H.W.A.G.}}\right)$" is used, meaning the gain of the Array Above Ground *over* the Half Wave Above Ground. "Gain" always implies the absolute magnitude.

[11] See page 123 of footnote reference (1).

$$\text{gain}\left(\frac{\text{A.A.G.}}{\text{H.W.A.G.}}\right) = \sqrt{\frac{R_{00} + R_{0L} - R_{00'}}{2(R_{11} + R_{1L} + R_{14} - R_{12} - R_{13})}} \cdot \frac{\left|[1 - 1\angle(S^\circ \cos\phi) - 1\angle(2H^\circ \sin\phi) + 1\angle(S^\circ \cos\phi + 2H^\circ \sin\phi)]\right|}{2 \sin(H^\circ \sin\phi)}. \quad (19)$$

At large heights above ground $R_{00'}$, R_{13}, and R_{14} become very small. When the array and half-wave antenna are compared in free space, it can be shown that (19) reduces to

$$\text{gain} = \sqrt{\frac{2(R_{00} + R_{0L})}{R_{11} + R_{1L} - R_{12}}} \sin\left(\frac{S^\circ}{2} \cos\phi\right). \quad (20)$$

Since $R_{00} = R_{11}$, and putting $R_{0L} = R_{1L} = 0$, we obtain

$$\text{gain} = \frac{\sqrt{2} \sin\left(\frac{S^\circ}{2} \cos\phi\right)}{\sqrt{1 - \frac{R_{12}}{R_{00}}}}. \quad (21)$$

This expression is equivalent to Brown's equation (50) for the case where $\alpha = 180$ degrees.[12]

Values of self-resistance (R_{00} and R_{11}) and mutual resistance (R_{12}, R_{13}, etc.) have been given by a number of writers. Carter,[13] Brown,[14] Rumble,[15] and Morrison[16] have published graphs from which the variation of the mutual resistance with spacing between two elements can be obtained. For small values of spacing, however, the radiation resistance of each element becomes the small difference of two large numbers, involving the self- and mutual resistances. A small inaccuracy in either of these resistances can produce a relatively large error in the radiation resistance with the result that the computed gain of the array may be considerably in error. It is not possible to read the above-mentioned graphs with sufficient exactness to compute accurately the gain of arrays with closely spaced elements. Accordingly, the mutual resistances used in the calculations in this paper were computed from the expression involving the cosine integral as given by Pistolkors.[17] For many of the computations the values of the integral were taken from Janke-Emde[18] but in some cases it was necessary to evaluate the integral functions from their series expansion.

[12] See page 94 of footnote reference (1).
[13] P. S. Carter, "Circuit relations in radiating systems and applications to antenna problems," Proc. I.R.E., vol. 20, p. 1016; June, (1932).
[14] See page 87 of footnote reference (1).
[15] A. R. Rumble, "Directional array field strengths," *Electronics*, vol. 10, p. 16; August, (1937).
[16] J. F. Morrison, "Simple method for observing current amplitude and phase relations in antenna arrays," Proc. I.R.E., vol. 25, p. 1313; October, (1937).
[17] A. A. Pistolkors, "The radiation resistance of beam antennas," Proc. I.R.E., vol. 17, pp. 562–579; March, (1929).
[18] Janke-Emde, "Tables of Functions," second edition, B. G. Teubner, Berlin, Germany, (1933).

Gain Versus Loss Resistance and Spacing

In contrast to the single half-wave antenna, a relatively small loss resistance can have a marked effect on the radiating efficiency of an array with closely spaced elements. This is shown by the curves of Fig. 5 which are computed from (20) for the case of two closely spaced half-wave elements in free space with equal and out-of-phase currents, as compared to a single half-wave element also in free space. Identical results would be obtained with vertical quarter-wave elements over perfectly conducting ground. The gain is evaluated for $\phi = 0$ degrees, in which direction the gain is a maximum.

Curves are given in Fig. 5 for loss resistances of 0, 0.25, 1, 5, and 20 ohms. With zero loss resistance it appears that the array maintains a substantial gain as the spacing between the elements is reduced to zero. However, the presence of a loss resistance as small as 0.25 ohm causes a sharp falling off of gain as the spacing approaches zero. It appears that for

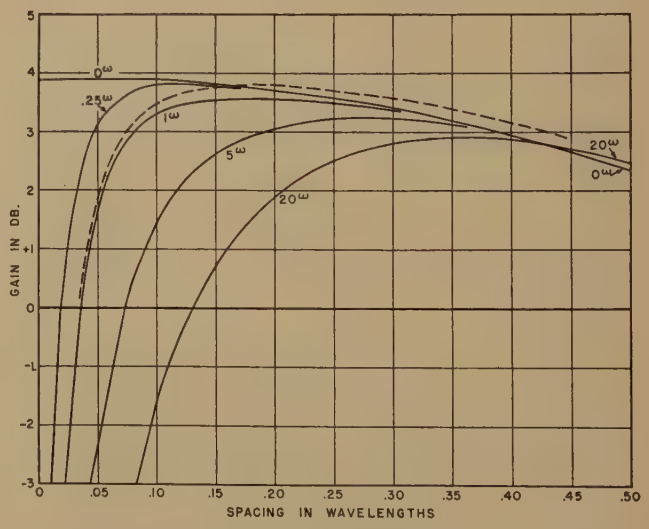

Fig. 5—Gain of two out-of-phase elements in free space as a function of spacing for various loss resistances.

practical values of loss resistance of the order of 1 ohm it is not desirable to use spacings of much less than one-eighth or one-tenth wavelength in the case of a "flat-top beam" antenna.

Unless otherwise stated, the loss resistance in each element of the array and in the comparison antenna is assumed to be the same. The solid curves of Fig. 5 are for this case. Suppose, however, that they are not the same, and that $R_{0L} = 5$ ohms and $R_{1L} = 1$ ohm. Such an assumption results in the dashed curve of Fig. 5.

Gain Versus Height

By placing $M=1$ and $\alpha=180$ degrees in (15) we have the equation for the *gain of a single-section "flat-top beam"* at a height H over a half-wave antenna in free space, as follows:

$$\text{gain (A.A.G.)} = \sqrt{\frac{R_{00}+R_{0L}}{2(R_{11}+R_{1L}+R_{14}-R_{12}-R_{13})}} \cdot \left|\left[1-1\angle(S^\circ\cos\phi)-1\angle(2H^\circ\sin\phi)+1\angle(S^\circ\cos\phi+2H^\circ\sin\phi)\right]\right|. \quad (22)$$

The gain of a half-wave antenna at the same height over a half-wave antenna in free space is given by (17).

Curves giving the gain as a function of height for the array of two out-of-phase elements (solid) and the half-wave antenna (dashed) are shown in Fig. 6. In both cases the gain is computed for vertical angles of 5, 15, and 30 degrees and is referred to a half-wave antenna in free space. The curves are obtained by evaluating (17) and (22). All curves are for zero loss resistance except the dotted curves which illustrate the effect of 0.5-ohm loss resistance per element on the gain for the $\phi=30$-degree case. The array spacing is one-eighth wavelength.

The gain of the array as a function of height for various vertical angles has been considered. The gain can also be treated as a function of vertical angle for various heights. Such information is presented in Fig. 7. The solid curves show the gain of the array above

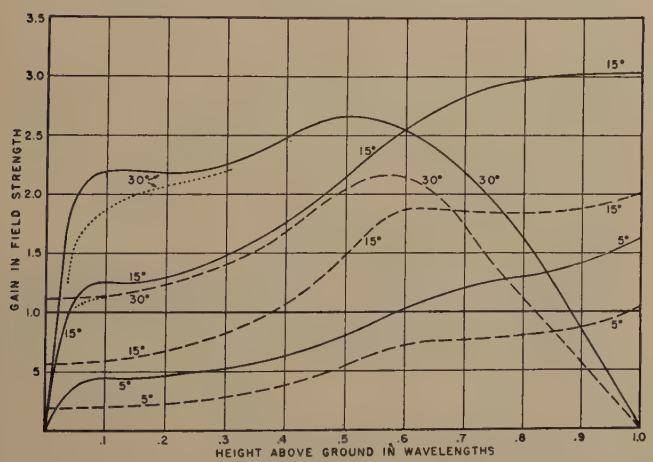

Fig. 6—The effect of height above ground on the gain of two horizontal out-of-phase elements with a spacing of one-eighth wavelength is shown by the solid curves. The gain of a single horizontal half-wave antenna is shown by the dashed curves. The gain is given for vertical angles of 5, 15, and 30 degrees and is referred to a half-wave antenna in free space. Perfectly conducting ground is assumed.

ground over a free-space half-wave antenna as a function of ϕ for heights of 0.5 and 0.75 wavelength. The dashed curves give the gain of the half-wave antenna above ground over the free-space half-wave antenna for corresponding heights.

Four-Element Array

So far, the discussion has been limited to arrays of two elements per section, that is, two elements centered in a plane perpendicular to them. The use of more than two elements in one section of a driven array can also be investigated. Consider, for example, the diamond-shaped configuration shown in Fig. 8. This consists of four parallel 180-degree elements.

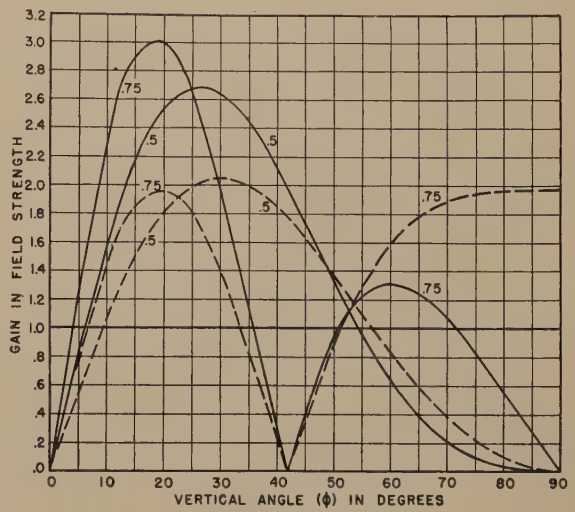

Fig. 7—The gain of an array of two horizontal out-of-phase elements over a half-wave antenna in free space for various vertical angles is shown by the solid curves. The gain of a single horizontal half-wave antenna is shown by the dashed curves. The gains are given for antenna heights of 0.5 and 0.75 wavelength above ground. The array spacing is one-eighth wavelength.

The elements 1 and 2 are separated by a distance A and the elements 3 and 4 by a distance B. Further, the elements are symmetrically disposed, so that the A axis bisects the B axis and also is bisected by it. Let us assume that the currents in elements 1 and 2 are equal and in phase and that the currents in 3 and 4 are equal to those in 1 and 2 but 180 degrees out of phase with 1 and 2. For the sake of simplicity

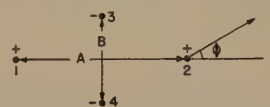

Fig. 8—Four-element array.

we shall consider the array to be in free space. The pattern perpendicular to the elements in this case would be the same as the horizontal pattern around four vertical quarter-wave elements located above perfectly conducting ground.

The *gain for* such a *four-element array* in the direction making an angle ϕ with the A axis over a half-wave antenna in free space can be shown to be

$$\text{gain} = \sqrt{\frac{R_{00}+R_{0L}}{2(2R_{11}+2R_{1L}+R_{12}+R_{34}-4R_{13})}} \cdot 2\left|\left[\cos\left(\frac{A^\circ}{2}\cos\phi\right)-\cos\left(\frac{B^\circ}{2}\sin\phi\right)\right]\right|. \quad (24)$$

The radiation pattern perpendicular to the elements of a four-element array of the type under consideration is shown in Fig. 9. The pattern is obtained by evaluating (24) for the case of $A=0.25$ and $B=0.15$ wavelength. The maximum gain is parallel to the A axis ($\phi=0$ degrees). Two minor lobes parallel to the B axis are also present. When B is zero these lobes are zero. They increase as B is increased and when B equals A they are equal to the lobes parallel to the A axis. For comparison, the

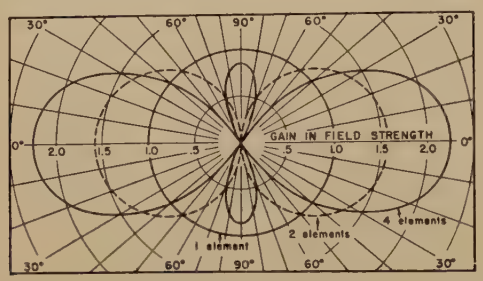

Fig. 9—Free-space radiation patterns of one-, two-, and four-element arrays, all having the same power input. The patterns are shown in the plane perpendicular to the elements.

radiation pattern of an array of two 180-degree elements is also shown. This array is of the "flat-top beam" type. A spacing of one-eighth wavelength is assumed and the plane containing the elements is parallel to the plane containing elements 1 and 2 of the four-element array. The gain of both the two- and four-element arrays is shown as the improvement over a single 180-degree element in free space having the same power input. The radiation of this free-space half-wave antenna is indicated by the circular pattern which has a gain of unity in all directions. Loss resistances are assumed to be zero for all three antennas.

Inspection of Fig. 9 shows that the four-element array has a gain at $\phi=0$ degrees of about 2.25 in field strength while the two-element array has a gain of about 1.57. These correspond to gains of about 7.0 decibels for the four-element array and 3.9 decibels for the two-element array.

The variation of the gain of the four-element array in the direction of the A axis as a function of the spacing B between elements 3 and 4 is shown in Fig.

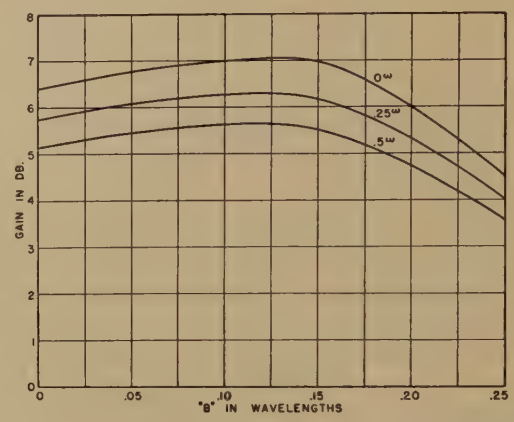

Fig. 10—Effect of variation of B on the gain of the four-element array for loss resistances of 0, 0.25, and 0.5 ohm. The value of A is 0.25 wavelength.

10. The spacing A is 0.25 wavelength. The gain is shown for loss resistances of 0, 0.25, and 0.5 ohm per element. It is apparent that the loss resistance must be made very small in order to have efficient operation of this type of array.

An experimental four-element array designed for 14-megacycle operation with $A=0.3$ and $B=0.15$ wavelength, was measured to have a gain of about 2.5 decibels over a two-element "flat-top beam" type of array. Both arrays were compared at the same height above ground in the same location and with the same power input.

Acknowledgment

The writer is much indebted to Dr. Robert M. Whitmer, of the Department of Physics of Purdue University, for his interest and counsel.

A Generalized Coupling Theorem for Ultra-High-Frequency Circuits*

RONOLD KING†, ASSOCIATE, I.R.E.

Summary—*It is proved that a distributed potential gradient of any form maintained along a parallel line is, in general, equivalent to three pairs of point generators of proper amplitudes and phases suitably arranged along the line. In the special case in which the potential gradient is characterized by cosine (direct) symmetry with respect to a central reference co-ordinate, a single pair of point generators placed at the co-ordinate of the reference point is sufficient. If the symmetry is sinusoidal (inverted) with respect to the reference co-ordinate, two pairs of symmetrically placed point generators are required.*

* Decimal classification: R 142. Original manuscript received by the Institute, October 3, 1939; revised manuscript received, November 21, 1939.

† Cruft Laboratory, Harvard University, Cambridge, Mass.

IN A recent paper[1] the general problem of coupling ultra-high frequency circuits was analyzed in detail. The following theorem was proved. Theorem: a distributed electromotive force induced in a section of a parallel line may be treated just as though it were concentrated at the center of the section, pro-

[1] Ronold King, "The application of low-frequency circuit analysis to the problem of distributed coupling in ultra-high-frequency circuits," PROC. I.R.E., vol. 27, pp. 715–724; November, (1939).

vided only it is symmetrical with respect to this center. In discussing the application of this theorem. it was stated further that in so far as the oscillation generator was concerned, the only fundamental requirement was that this must be of a form such that the components of the electric field E and of the vector potential A due to its own current and charge distribution are symmetrical with respect to the center of the oscillator. In deriving the theorem and in considering its application it was tacitly assumed

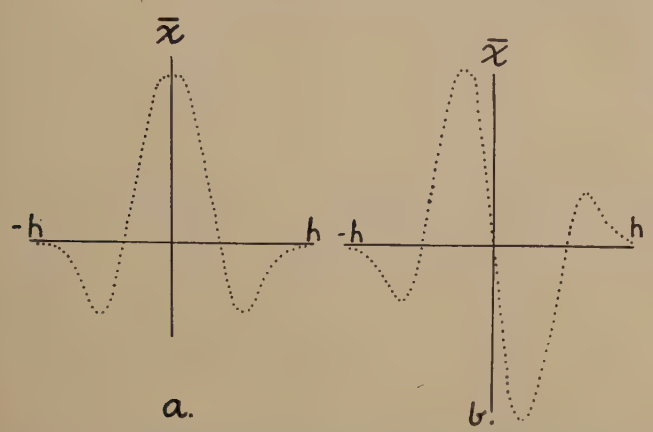

Fig. 1—Possible field distributions along one wire of a parallel line due to a coupled oscillator. a. Direct or cosine symmetrical curve. b. Inverted or sine symmetrical curve.

that the only kind of symmetry of the E and A fields which needed to be considered was a direct or cosine symmetry of the form suggested by Fig. 1a. More recently, in designing a variable oscillator for ultra-high-frequency measurements,[2] it has become evident that an inverted or sine symmetry of the type indicated in Fig. 1b may also occur. Since the coupling theorem as formulated above does not include this kind of symmetry, the question arises, how an induced potential gradient which is characterized by a sinusoidal symmetry with respect to the oscillator center may be treated analytically. It is significant to note that an answer to this question is important not only in order to permit a simple mathematical treatment of the field due to an oscillator of the type described[2] but for all kinds of oscillators which generate even harmonics in addition to a fundamental. Thus an oscillator which generates a fundamental which has a directly symmetrical field with respect to the oscillator center, may generate a second harmonic which sets up a field which is necessarily inverted in its symmetry. It appears, therefore, that a generalization of the coupling theorem to include potential gradients with inverted or sine symmetry is necessary. It will be shown now that not only this case of inverted symmetry but also the general case of a perfectly arbitrary field distribution can be treated in a simple way not envisaged in the earlier analysis.

In order to generalize the coupling theorem it is necessary to represent the induced electromotive force (given by (1–36),[3] and assumed equal and opposite in the two wires), viz.,

$$V^i = -j\omega \int_0^s A_{21x}dx \doteq \int_0^s E_{21x}dx \qquad (1)$$

by a more general series than that used in (1–43) or (1–44). Thus let the integrand in (1) be represented by a complex Fourier series of the form,

$$dV_x{}^i = \sum_{m=1}^{m} \{ [a_m \cos m\beta'(\bar{x}-x) + b_m \sin m\beta'(\bar{x}-x)] + j[c_m \cos m\beta'(\bar{x}-x) + d_m \sin m\beta'(\bar{x}-x)] \}, \qquad (2)$$

in the range

$$(\bar{x} - h) \leqq x \leqq (\bar{x} + h'). \qquad (3)$$

The interval for x defined by (3) is chosen sufficiently large on each side of the reference co-ordinate $\bar{x}$ (which may be opposite the center of the oscillator) to include the entire distance in which E and A differ significantly from zero. The amplitude factors in (2) are real, but E_x and A_x in (1) are, in general, complex. Since the imaginary part of (2) is analytically like the real part, it will be denoted by [I.P.] in the manipulation which follows.

Using the familiar relations,

$$\cosh jy = \cos y; \quad \sinh jy = j \sin y, \qquad (4)$$

(2) may be written in the following hyperbolic form:

$$dV_x{}^i = \sum_{m=1}^{n} \{ [a_m \cosh mK'(\bar{x}-x) - jb_m \sinh mK'(\bar{x}-x)] + j[\text{I.P.}] \}. \qquad (5a)$$

[3] Equation numbers of reference 1 will be preceded by a 1 as in this case. However, (1) as written above is not the same as (1–36) since the latter is in error and does not actually give the induced voltage as defined in (1–19b) with (1–13a) and (1–11c). The potential function defined by (1–36) should be expanded using (1–7, 8) to obtain

$$V = \int_0^s z^i I_2 dx + j\omega \int_0^s A_{11x}dx + j\omega \int_0^s A_{21x}dx. \qquad (a)$$

The induced voltage V^i in the secondary parallel line due to the primary oscillator is now defined as in (1–19b) to be

$$V^i = -j\omega \int_0^s A_{21x}dx. \qquad (b)$$

Under practically all conditions (b) may be expressed in terms of E_{21x} with the aid of the contour integral (1–6), written for E_{21} and A_{21}. If this is evaluated around the long rectangle formed by the parallel line, subject to the condition that the values of E_x and A_x along the two conductors be equal and opposite, one readily obtains

$$\int_0^s E_{21x}dx \doteq -j\omega \int_0^s A_{21x}dx, \qquad (c)$$

provided the contributions due to the short ends of the rectangle involving E_{21y} and A_{21y} are negligible. Since the line separation is by definition extremely small compared with its length, this will always be true except possibly when the oscillator center is moved beyond one end of the parallel line. Because one assumes in practice that the oscillator must not come near the line terminations, this is of no great significance.

It is to be noted that writing (1) for (1-36) in reference 1, in no way changes the conclusions. In fact writing E_x *or* A_x instead of E_x *and* A_x at several points in the discussion is the only additional change required.

[2] Ronold King, "A variable oscillator for ultra-high-frequency measurements," *Rev. Sci. Instr.*, vol. 10, p. 325; November, (1939).

Here,

$$K' = j\beta'. \tag{5b}$$

The range of x defined by (3) also applies to (5a).

As in the previous analysis, the current amplitude at $x=0$ in a line of length s due to a pair of equal and opposite point generators each of an electromotive-force amplitude $\frac{1}{2}V_x^e$ at the co-ordinate x in the line is, (1–27),

$$I_0=(V_x^eY_0/H)[Z_cY_s\cosh K(s-x)+\sinh K(s-x)] \tag{6a}$$

$$H=(Z_c^2Y_0Y_s+1)\sinh Ks+Z_c(Y_0+Y_s)\cosh Ks. \tag{6b}$$

The potential difference between the two wires at $x=0$ is given by

$$V_0 = I_0/Y_0. \tag{6c}$$

Here, as before, Y_0 and Y_s are, respectively, the terminal admittance at $x=0$ and $x=s$; Z_c is the characteristic impedance.

By choosing the increments dx in (1) sufficiently small, the corresponding amplitudes, dV_x^i, may be considered to be due to point generators, and (5a) may be substituted in (6a) for V_x^e. Upon integrating over the range (3) in which V^i receives significant contributions, the current at $x=0$ due to the entire distributed electromotive force is obtained. It is

$$\begin{aligned} I_0 = \frac{Y_0}{H}\sum_{m=1}^{n}\Bigg\{\Bigg[a_m\int_{\bar{x}-h}^{\bar{x}+h'}&[Z_cY_s\cosh K(s-x)\\ &+\sinh K(s-x)]\cosh mK'(\bar{x}-x)dx\\ -jb_m\int_{\bar{x}-h}^{\bar{x}+h'}&[Z_cY_s\cosh K(s-x)\\ &+\sinh K(s-x)]\sinh mK'(\bar{x}-x)dx\Bigg]\\ &+j[\text{I.P.}]\Bigg\}. \end{aligned} \tag{7}$$

Now let the following abbreviations be introduced:

$$A = \int_{\bar{x}-h}^{\bar{x}+h'}\cosh K(s-x)\cosh mK'(\bar{x}-x)dx \tag{8a}$$

$$B = \int_{\bar{x}-h}^{\bar{x}+h'}\sinh K(s-x)\cosh mK'(\bar{x}-x)dx \tag{8b}$$

$$C = \int_{\bar{x}-h}^{\bar{x}+h'}\cosh K(s-x)\sinh mK'(\bar{x}-x)dx \tag{8c}$$

$$D = \int_{\bar{x}-h}^{\bar{x}+h'}\sinh K(s-x)\sinh mK'(\bar{x}-x)dx. \tag{8d}$$

The integrations in (8) are readily performed by changing to exponential functions. The steps will not be given. Using the shorthand notation,

$$F = K + mK'; \qquad G = K - mK', \tag{9}$$

$$\begin{aligned}(f+g) &= (1/2F)(\sinh Fh+\sinh Fh')\\ &\quad+(1/2G)(\sinh Gh+\sinh Gh'),\end{aligned} \tag{10}$$

$$\begin{aligned}(f'+g') &= (1/2F)(\cosh Fh-\cosh Fh')\\ &\quad+(1/2G)(\cosh GH-\cosh Gh'),\end{aligned} \tag{11}$$

one obtains

$$A=(f+g)\cosh K(s-\bar{x})+(f'+g')\sinh K(s-\bar{x}) \tag{12a}$$

$$B=(f'+g')\cosh K(s-\bar{x})+(f+g)\sinh K(s-\bar{x}) \tag{12b}$$

$$C=(f'-g')\cosh K(s-\bar{x})+(f-g)\sinh K(s-\bar{x}) \tag{12c}$$

$$D=(f-g)\cosh K(s-\bar{x})+(f'-g')\sinh K(s-\bar{x}). \tag{12d}$$

Upon substituting (8) and (7) this becomes

$$\begin{aligned} I_0=(Y_0/H)\sum_{m=1}^{n}\Big\{&[a_m(Z_cY_sA+B)-jb_m(Z_cY_sC+D)]\\ &+j[\text{I.P.}]\Big\}. \end{aligned} \tag{13}$$

After expanding and collecting terms, using (12), one obtains

$$\begin{aligned} I_0=(Y_0/H)\sum_{m=1}^{n}\Big\{&[a_m(f+g)-jb_m(f'+g')]\\ &\cdot[Z_cY_s\cosh K(s-\bar{x})+\sinh K(s-\bar{x})]\\ &+[a_m(f'+g')-jb_m(f-g)]\\ &\cdot[Z_cY_s\sinh K(s-\bar{x})+\cosh K(s-\bar{x})]\\ &+j[\text{I.P.}]\Big\}. \end{aligned} \tag{14}$$

Since Z_c Y_s, K, and s and $\bar{x}$ are not involved in the summation over m, the following abbreviations can be written for the complex amplitude factors. It is to be noted that the term [I.P.] is like the entire preceding set of terms with c written for a, and d for b. Let

$$\begin{aligned} V = \sum_{m=1}^{n}\Big\{&[a_m(f+g)-jb_m(f'-g')]\\ &+j[c_m(f+g)-jd_m(f'-g')]\Big\}, \end{aligned} \tag{15a}$$

$$\begin{aligned} W = \sum_{m=1}^{n}\Big\{&[a_m(f'+g')-jb_m(f-g)]\\ &+j[c_m(f'+g')-jd_m(f-g)]\Big\}. \end{aligned} \tag{15b}$$

One can now write (14) in the following simple form:

$$\begin{aligned} I_0=(VY_0/H)&[Z_cY_s\cosh K(s-\bar{x})+\sinh K(s-\bar{x})]\\ &+(WY_0/H)[Z_cY_s\sinh K(s-\bar{x})+\cosh K(s-\bar{x})]. \end{aligned} \tag{16}$$

This is the general expression for the current at $x=0$ due to an induced potential gradient distributed along the line in any way which can be represented by the series (2). V and W are amplitude factors which are independent of s and $\bar{x}$. Since the terminal admittance Y_0 may include any desired length of parallel line, (16) actually gives the current at any point along the line.

In attempting to interpret (16) in a simple manner, one notes that the factor in V is of exactly the same form as (6a). It may, therefore, be represented exactly by a single pair of equal and opposite point generators each of an electromotive force $\frac{1}{2}V$ placed at the co-ordinate $\bar{x}$ in the line. It will now be shown that the

factors in W may be interpreted in terms of two opposite pairs of equal and opposite point generators each of an electromotive force $\frac{1}{2}W'$ symmetrically placed with respect to $\bar{x}$ as indicated schematically in Fig. 2. Thus, if each generator is assumed to be at an arbitrary distance x_1 from the reference point $\bar{x}$ then the contribution of the pair of generators at $\bar{x}-x_1$ is obtained from (6a) to be

$$I_{01} = (Y_0W'/H)[Z_cY_s \cosh K(s - \bar{x} + x_1) + \sinh K(s - \bar{x} + x_1)]. \quad (17a)$$

In the same way the contribution due to the equal and opposite pair at $\bar{x}+x_1$ is

$$I_{02} = -(Y_0W'/H)[Z_cY_s \cosh K(s - \bar{x} - \bar{x}_1) + \sinh K(s - \bar{x} - x_1)]. \quad (17b)$$

The total current at $x=0$ is the sum of these contributions. It is

$$I_0 = (Y_0W'/H)\{Z_cY_s[\cosh K(s-\bar{x}+x_1) - \cosh K(s-\bar{x}-x_1)] + [\sinh K(s-\bar{x}+x_1) - \sinh K(s-\bar{x}-x_1)]\}. \quad (18)$$

Using formulas 670 and 672 in Peirce, Tables of Integrals, (18) is readily transformed into

$$I_0 = (Y_0W'/H)2 \sinh Kx_1[Z_cY_s \sinh K(s - \bar{x}) + \cosh K(s - \bar{x})]. \quad (19)$$

This expression gives the current at $x=0$ due to two pairs of point generators symmetrically connected in the line with reference to the co-ordinate plane $x=\bar{x}$. A comparison of (19) with the W term in (16) shows that they are exactly alike if W' is chosen to satisfy the relation,

$$W = 2W' \sinh Kx_1. \quad (20)$$

Evidently by making W' sufficiently large, the distance x_1 of the point generators from the reference plane at x may be made as small as desired.

One may now formulate the following general coupling theorem. Theorem: The electromotive force induced in a parallel line by a coupled oscillator that

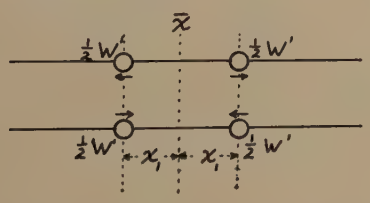

Fig. 2—Location of two opposite pairs of equal and opposite point generators.

maintains along the two wires equal and opposite potential gradients, which can be represented by complex Fourier series of the form (2), is analytically equivalent to the driving electromotive force of three pairs of point generators connected in the line in the following way. One pair of equal and opposite generators, each providing an electromotive force of amplitude $\frac{1}{2}V$, is connected in the line at the arbitrary reference plane $x=\bar{x}$. Two opposite pairs of equal and opposite generators each providing an amplitude $W/(4 \sinh Kx_1)$ are connected on opposite sides of $\bar{x}$ at equal distances x_1. V and W are defined by (15). The complete arrangement is shown in Fig. 3.

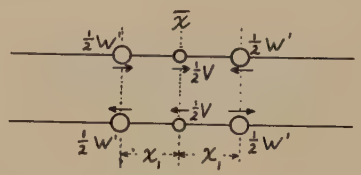

Fig. 3—Location of the three pairs of point generators required for analytical equivalence in the general case of unsymmetrical field distribution.

If the reference plane $x=\bar{x}$ is chosen at the center of the region between $(\bar{x}-h)$ and $(\bar{x}+h')$ in which the inducing fields are of significant magnitude, one has

$$h = h'. \quad (21)$$

It then follows from (11) that

$$f' = g' = 0, \quad (22)$$

$$f = (\sinh Fh)/F, \quad g = (\sinh Gh)/G. \quad (23)$$

In this case (15) reduces to

$$V = \sum_{m=1}^{n} (a_m + jc_m)(f + g) \quad (24a)$$

$$W = \sum_{m=1}^{n} (d_m - jb_m)(f - g). \quad (24b)$$

From these formulas and (2) it follows that, subject to (21), V is determined entirely from the amplitudes a_m and c_m of the cosine series, whereas W depends only upon the amplitudes b_m and d_m of the sine series. Accordingly, if the potential gradient along the parallel line is characterized by direct or cosine symmetry with respect to the plane $x=\bar{x}$ at the center of the range in which it is significant, one may set $W=0$. This means that for a directly (or cosine) symmetrical field distribution a single pair of point generators at $x=\bar{x}$ leads to an analytically equivalent solution. It is this conclusion which is formulated in the special theorem stated at the outset above and in the previous analysis.[1] It is here seen to be an important special case of a more general theorem.

If the potential gradient along the parallel line is characterized by an inverted or sine symmetry with respect to the central reference plane at $x=\bar{x}$, one may set $V=0$. In this case two opposite sets of equal and opposite point generators symmetrically placed with respect to the central plane are adequate to obtain an analytically equivalent result. This condition obtains in the oscillator already described[2] and the above analysis is the mathematical basis of arguments and statements there given.

Bridged-T Measurement of High Resistances at Radio Frequencies*

P. M. HONNELL†, ASSOCIATE, I.R.E.

Summary—*A bridged-T circuit suitable to the measurement of high resistances at radio frequencies is analyzed and a measuring set incorporating the circuit is described. The device is capable of measuring resistances ranging from 0.01 to 10 megohms with an accuracy approximating the precision of setting of the adjustable standard elements of the apparatus.*

THE exact measurement of resistances in the megohm range at radio frequencies is inherently difficult, primarily due to parasitic shunting admittances and the consequent impossibility of realizing high-resistance standards. It is usually impractical to perform such measurements by means of lattice networks and the maximum value of resistance measurable by methods utilizing tuned circuits is seriously limited by the finite Q of suitable inductances.

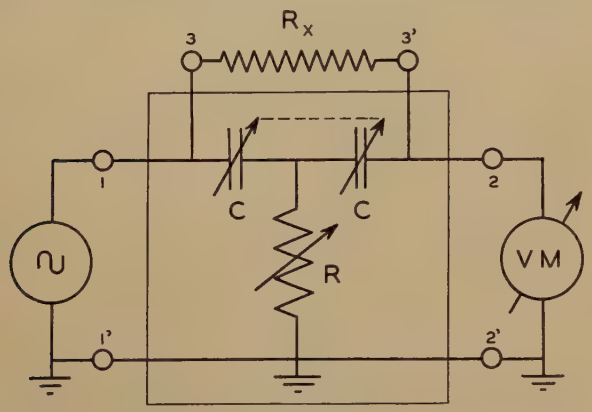

Fig. 1—Bridged-T resistance-measuring network.

The advantages of bridged-T structures in radio-frequency measurements are becoming increasingly evident, particularly from the standpoint of shielding and adjustment. The "balance" of a bridged-T is similar to that of a lattice, and is indicated by a null indicator. The calibrated voltmeter or ammeter, necessary with tuned-circuit methods, is therefore not required.

A bridged-T circuit suitable for high-resistance measurements is shown in Fig. 1, in which R_x is the unknown resistance under measurement, $C-C$ is a double-section ganged capacitance standard, and R is a low-resistance standard. This circuit not only exhibits the advantages of bridged-T networks, but also determines the unknown resistance in terms of the most accurate radio-frequency standards obtainable, air dielectric condensers and resistors ranging up to 100 ohms.

In operation, a source of voltage of known frequency is applied to the terminals 11′, and the ganged condensers and standard resistor are adjusted until a minimum output voltage is indicated across the terminals 22′. The magnitude of the unknown resistance R_x then is quite closely

$$R_x = \frac{X_c^2}{R} = \frac{1}{\omega^2 C^2 R} \tag{1}$$

ohms, with $\omega = 2\pi f$, C = farads, and R = ohms. The balance setting of the bridged-T yields only a minimum output voltage and not an absolute null, although the minimum can theoretically be made as small as desired. The absolute depth of the minimum beyond that required for precise adjustment of the variable standards is, however, more of academic than engineering importance. At the frequencies in question, all actual lattice and other measuring structures have definite balancing minima determined by factors such as finite couplings between oscillator and null indicator, etc., rather than by theoretical circuit performances. It is clear, therefore, that precision of setting is the important factor, and the bridged-T circuit here described is entirely adequate in this respect.

Bridged-T Balance Conditions

Expressing the input and output voltage and current of the bridged-T in terms of the open-circuit driving-point and transfer impedances of a four-terminal network,

$$\begin{aligned} E_1 &= Z_{11}I_1 + Z_{12}I_2 \\ E_2 &= Z_{21}I_1 + Z_{22}I_2, \end{aligned} \tag{2}$$

we obtain for the output current I_2 the following expression:

$$I_2 = \frac{-E_1 Z_{21}}{Z_{11}Z_{22} - Z_{12}Z_{21} + Z_{11}Z_{20}}, \tag{3}$$

since $E_2 = -I_2 E_{20}$ for the positive directions shown in Fig. 2, in which Z_{20} is the null-detector impedance. From (3) it is evident that for a given applied E_1, the output current I_2 would be zero and a null would result if

$$Z_{21} = 0. \tag{4}$$

The Z matrix of the bridged-T is

$$\|Z\| = \begin{Vmatrix} Z_{11} & Z_{12} \\ Z_{21} & Z_{22} \end{Vmatrix}, \tag{5}$$

and thus (4) can be evaluated by decomposition of the structure as outlined by Guillemin.[1] With the

* Decimal classification: R207×R241.5. Original manuscript received by the Institute, October 13, 1939.

† Formerly, Massachusetts Institute of Technology, Cambridge, Mass.; now, California Institute of Technology, Pasadena, Calif.

[1] E. A. Guillemin, Communication Networks, vol. II. John Wiley and Sons, New York, N. Y. (1935), p. 158, Fig. 45(b)

bridged-T circuit elements generalized as shown in Fig. 2, we obtain finally

$$\|Z\| = \begin{Vmatrix} \dfrac{z_1z_2 + z_2z_3 + z_3z_4 + z_1z_3 + z_1z_4}{z_1 + z_2 + z_4} & \dfrac{z_1z_2 + z_2z_3 + z_3z_4 + z_1z_3}{z_1 + z_2 + z_4} \\ \dfrac{z_1z_2 + z_2z_3 + z_3z_4 + z_1z_3}{z_1 + z_2 + z_4} & \dfrac{z_1z_2 + z_2z_3 + z_3z_4 + z_1z_3 + z_2z_4}{z_1 + z_2 + z_4} \end{Vmatrix}. \quad (6)$$

The condition stated in (4) which will result in $I_2=0$ can now be written

$$Z_{21} = \frac{z_1z_2 + z_2z_3 + z_3z_4 + z_1z_3}{z_1 + z_2 + z_4} = 0, \quad (4a)$$

and will obtain when

$$z_1z_2 + z_2z_3 + z_3z_4 + z_1z_3 = 0, \quad (7)$$

since the denominator of (4a) remains finite. Solving for the unknown resistance, represented by z_4, gives

$$z_4 = -z_1 - z_2 - \frac{z_1z_2}{z_3} \quad (8)$$

which, upon substitution of the proper element values from Fig. 1, yields

$$R_x = jX_c + jX_c + \frac{X_c^2}{R}. \quad (9)$$

Rewriting, we have

$$R_x = \frac{X_c^2}{R}\left(1 + j\,\frac{2R}{X_c}\right), \quad (10)$$

from which it is evident that by making the ratio of standard resistance to standard capacitive reactance (R/X_c) sufficiently small, the expression for the unknown resistance

$$R_x \approx \frac{X_c^2}{R} = \frac{1}{\omega^2C^2R} \quad (11)$$

can be made as exact as we please.[2]

A useful expression for the approximation involved is obtained if we substitute for X_c its approximate value at the balance setting, namely,

$$X_c \approx \sqrt{RR_x}$$

[2] If the condenser arms of the bridged-T do not have identical capacitances, the following expressions corresponding to (10) and (11) apply:

$$R_x = \frac{X_1X_2}{R}\left[1 + jR\left(\frac{1}{X_1} + \frac{1}{X_2}\right)\right] \quad (10a)$$

$$R_x \approx \frac{X_1X_2}{R} = \frac{1}{\omega^2C_1C_2R} \quad (11a)$$

in which C_1 and C_2 are the capacitances of the ganged condensers, and X_1 and X_2 their reactances.

in (10), thus obtaining

$$R_x \approx \frac{X_c^2}{R}\left(1 + j2\sqrt{\frac{R}{R_x}}\right). \quad (12)$$

Expressed in absolute magnitude, this reads

$$R_x \approx \frac{X_c^2}{R}\sqrt{1 + \frac{4R}{R_x}} \approx \frac{X_c^2}{R}\left(1 + \frac{2R}{R_x}\right). \quad (13)$$

The requirement that the true value of a measured resistor does not differ by more than a specified percentage from the magnitude computed on the basis of (1) is met, therefore, by keeping the ratio R/R_x

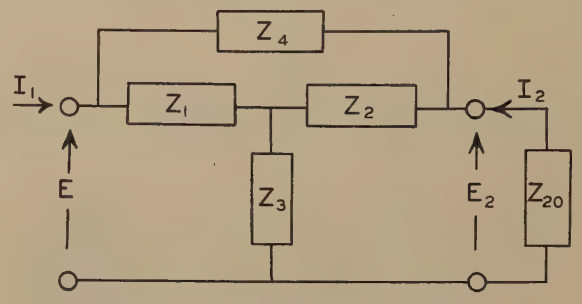

Fig. 2—Generalized network elements.

to less than one half that amount for the particular measurement. In actual measurements the ratio R/R_x can be made smaller than 5×10^{-3}, resulting in 1 per cent error, for resistances under measurement ranging from 0.01 to 0.1 megohm. For larger values of R_x, the ratio is easily maintained at less than 5×10^{-4}, with a resulting error of less than 0.1 per cent.

An interesting result arises when the output voltage indicator has an impedance which is high compared to the standard resistance and capacitance arms of the bridged-T. The ratio of output to input voltage of the measuring network, obtained by multiplying (3) by the null-indicator impedance Z_{20}, is expressible as

$$\frac{-E_2}{E_1} = \frac{Z_{20}Z_{21}}{Z_{11}(Z_{22} + Z_{20}) - Z_{12}Z_{21}}. \quad (14)$$

If $Z_{20} \gg Z_{22}$, and since $Z_{12}Z_{21}$ approximates zero near the balance settings, (14) can be approximated by

$$\frac{-E_2}{E_1} \approx \frac{Z_{21}}{Z_{11}}. \quad (15)$$

Upon substitution of the generalized element impedances from the matrix (6) in the above expression, we have

$$\frac{-E_2}{E_1} \approx \frac{z_1z_2 + z_2z_3 + z_3z_4 + z_1z_3}{z_1z_2 + z_2z_3 + z_3z_4 + z_1z_3 + z_1z_4}. \quad (16)$$

Now the adjustment of the bridged-T network for balance is accomplished by varying the condenser arms $z_1=z_2=-jX_c$, all other quantities remaining fixed. The conditions determining a minimum in the ratio $-E_2/E_1$ are therefore obtainable by differentiation of (16) with respect to the variable $-jX_c$ and

equation of the derivative to zero. The result turns out to be exactly

$$z_3 z_4 = j^2 X_c^2. \tag{17}$$

The approximate expression for R_x previously derived thus becomes exact if the null indicator is of sufficiently high impedance, since (17) is equivalent to (1). It can also be shown that under the same circumstances the maximum depth of the null obtainable in a given measurement is proportional to the ratio R/R_x; for maximum preciseness of adjustment this ratio should be kept to the smallest figure practicable.

Physical Apparatus Design

A measuring set incorporating the bridged-T circuit is illustrated in Fig. 3. This apparatus was utilized in the measurement of resistors of the type commonly

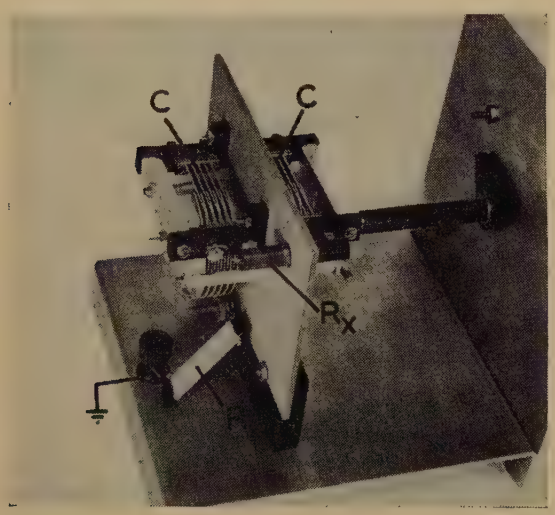

Fig. 3—Bridged-T resistance-measuring set.

found in radio receivers. The direct capacitive coupling between input and output is minimized by an electrostatic shield between the stators of the calibrated ganged condensers $C-C$ and connected to their common terminal. The direct capacitance between the terminals of the resistor R_x under measurement is likewise effectively reduced by placing the resistor through a perforation in the shield. Suitable high-frequency standard resistors R are connected between the shield and the common ground of the device.[3] Finally the entire assembly is placed in a shielding cabinet.

The source of power for measurement is conveniently obtained from a low-impedance source, preferably utilizing an oscillator—buffer-amplifier assembly to prevent frequency reactions, as exact frequency determinations are naturally demanded by (1). Either a sensitive vacuum-tube voltmeter or an exceptionally well-shielded radio receiver with an output meter is quite satisfactory as a balance indicator.

With the apparatus described, and utilizing standard resistors ranging from 1 to 100 ohms, the possible range of measurement[4] of unknown resistors was from 10^4 to 10^7 ohms, depending upon the measurement frequency. This range could have been extended to 20 megohms without difficulty.

Confirmation of Bridged-T Measurements

The results of measurements of a large number of resistors of the type illustrated were compared with measurements of the same resistors by the susceptance-variation method,[5] at frequencies of 456.0 and 3304. kilocycles per second. The agreement between the two techniques was found to be equal to the precision of setting of the calibrated standards for the range of values common to both methods. Only by careful shielding and control of residual parameters could this consistent agreement be obtained.

The feasibility of measuring the equivalent parallel resistance of tuned circuits by means of the bridged-T network has also been demonstrated by measurements confirmed with the susceptance-variation technique.

Acknowledgment

It is a pleasure to acknowledge my indebtness to Professors E. A. Guillemin and R. D. Bennett for considerable assistance in developing the theoretical and engineering aspects of this research, which was performed as a thesis project in the Department of Electrical Engineering of the Massachusetts Institute of Technology.

[3] It may be noted that the residual inductance of decade resistance boxes precludes their utilization as standard resistors.

[4] The measuring set can easily be made into a direct-reading instrument at a nominal frequency (say 1.0 megacycle per second) by calibrating the dial directly in ohms and using standard resistance values as decimal multiplying factors.

[5] D. B. Sinclair, "Parallel-resonance methods for precise measurements of high impedances at radio frequencies and a comparison with the ordinary series-resonance methods." Proc. I.R.E., vol. 26, pp. 1466–1497; December, (1938).

Characteristics of the Ionosphere at Washington, D.C., December, 1939, with Predictions for March, 1940*

T. R. GILLILAND, ASSOCIATE†, I.R.E., S. S. KIRBY†, ASSOCIATE, I.R.E., and N. SMITH†, NONMEMBER, I.R.E.

DATA on the critical frequencies and virtual heights of the ionospheric layers during December are given in Fig. 1. Fig. 2 gives the monthly average values of the maximum usable frequencies for undisturbed days, for radio transmission by way of the regular layers. The F_2 and F layers ordinarily determined the maximum usable frequencies during the day and night respectively. Fig. 3 gives the distribution of hourly values of F and F_2 data about the undisturbed average for the month.

TABLE I

IONOSPHERIC STORMS (APPROXIMATELY IN ORDER OF SEVERITY)

Day and hour E.S.T.	h_f before sunrise (km)	Minimum f_{F^0} before sunrise (kc)	Noon $f_{F_2}{}^0$ (kc)	Magnetic character[1] 00–12 G.M.T.	Magnetic character[1] 12–24 G.M.T.	Ionospheric character[2]
December						
6	330	3100	10000	0.4	0.9	0.6
7 (until 0800)	374	2000	—	1.4	0.9	0.6
8 (0000 to 1000)	352	2200	—	0.9	0.8	0.4
20 (after 1700)	—	—	—	0.0	0.2	0.2
21 (until 0600)	326	2800	—	0.9	0.8	0.2
21 (after 2000)	—	—	—	0.9	0.8	0.2
22 (until 0600)	284	5200	—	0.8	0.7	0.2
For comparison: Average for undisturbed days	298	3670	10300	0.2	0.2	0.0

[1] American magnetic character figure, based on observations of seven observatories.
[2] An estimate of the severity of the ionosphere storm at Washington on an arbitrary scale of 0 to 2, the character 2 representing the most severe disturbance.

TABLE II

SUDDEN IONOSPHERIC DISTURBANCES

Day	G.M.T. Beginning	G.M.T. End	Locations of transmitters	Relative intensity at minimum[1]
December 3	1507	1520	Ohio, Ontario, D. C.	0.05

[1] Ratio of received field intensity during fade-out to average field intensity before and after; for station WLWO, 6060 kilocycles, 650 kilometers distant.

Fig. 4 gives the expected values of the maximum usable frequencies for radio transmission by way of the regular layers, average for undisturbed days, for March, 1940.

Ionospheric storms occurred as listed in Table I. They were mild and not numerous, and their effects on high-frequency radio transmission were not great. The ionospheric storm of December 21 and 22 was characterized by F critical frequencies as much as

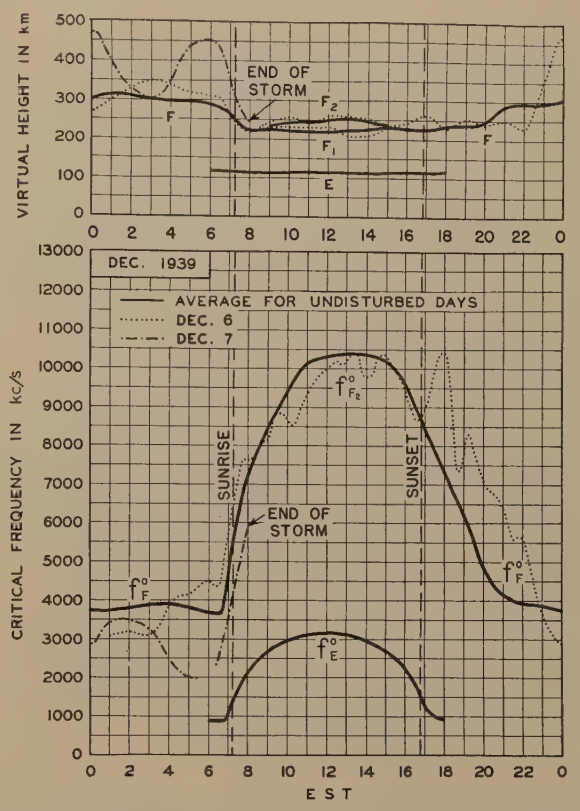

Fig. 1—Virtual heights and critical frequencies of the ionospheric layers, December, 1939. The solid-line graphs are the averages for the undisturbed days; the dotted-line graphs are for the ionospheric storm day of December 6, and the dot-dashed graphs for December 7. Reflections were too diffuse for critical-frequency measurements at 0000 December 6 and 0600 December 7.

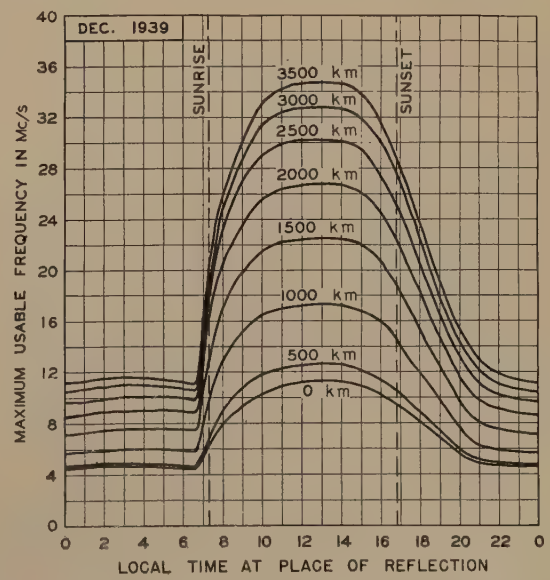

Fig. 2—Maximum usable frequencies for dependable radio transmission via the regular layers, average for undisturbed days for December, 1939.

* Decimal classification: R113.61. Original manuscript received by the Institute, January 10, 1940. These reports have appeared monthly in the PROCEEDINGS starting in vol. 25, September, (1937). See also vol. 25, pp. 823–840, July, (1937). Publication approved by the Director of the National Bureau of Standards of the U. S. Department of Commerce.
† National Bureau of Standards, Washington, D.C.

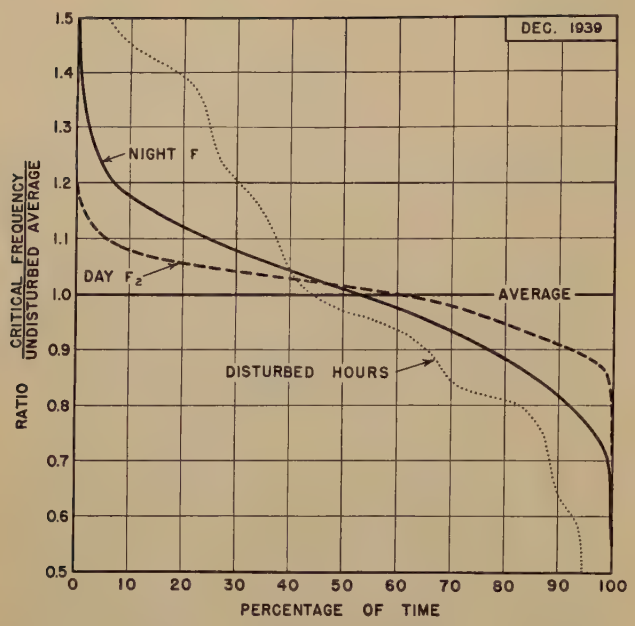

Fig. 3—Distribution of F- and F_2-layer ordinary-wave critical frequencies (and approximately of maximum usable frequencies) about monthly average. Abscissas show percentages of time for which the ratio of the critical frequency to the undisturbed average exceeded the values given by the ordinates. The solid-line graph is for 403 undisturbed night hours of observation; the dashed graph is for 208 undisturbed day hours of observation; the dotted graph is for 69 disturbed hours of observation: listed in Table I.

60 per cent greater than the monthly average, and by additional reflections with retardations greatly in excess of those of F-layer reflections. (See the report of this series for March, 1939.)[1]

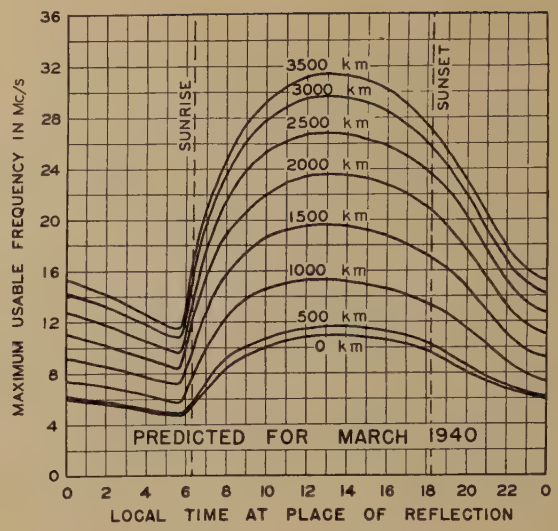

Fig. 4—Predicted maximum usable frequencies for dependable radio transmission via the regular layers, average for undisturbed days, for March, 1940.

One sudden ionospheric disturbance was observed as indicated in Table II. A prolonged period of severe low-layer absorption, for several hours during the middle of the day, was observed on December 21. Strong vertical-incidence sporadic-E reflections were observed up to 11 megacycles for 2 hours, 8 megacycles or above for 7 hours, and 6 megacycles or above for 18 hours.

[1] T. R. Gilliland, S. S. Kirby, and N. Smith, "Characteristics of the ionosphere at Washington, D.C.," March, 1938, Proc. I.R.E., vol. 27, pp. 348–350; May, (1939).

Institute News and Radio Notes

Board of Directors

The Annual Meeting of the Board of Directors was held in the Institute office on January 3. Those present were L. C. F. Horle, president; Austin Bailey, F. W. Cunningham, Alfred N. Goldsmith, Virgil M. Graham, O. B. Hanson, R. A. Heising, C. M. Jansky, Jr., F. B. Llewellyn, Haraden Pratt, B. J. Thompson, H. M. Turner, A. F. Van Dyck, H. A. Wheeler, and H. P. Westman, secretary.

Mr. Eastham was reappointed to serve as Treasurer during 1940.

Mr. Westman was appointed to continue to serve as Secretary during 1940.

Dr. Goldsmith was appointed to serve during 1940 as Chairman of the Board of Editors.

Each year five directors are appointed by the Board of Directors to serve for one year. For 1940 those appointees are W. R. G. Baker, H. C. Forbes, F. R. Lack, A. F. Van Dyck, and L. P. Wheeler.

Twenty-seven Associates and eighty-four Students were elected to membership.

President Horle, with the consent of the Board of Directors, appointed the personnel to serve on standing committees during the year.

The budget on which the Institute's financial activities will be based during 1940 was adopted.

Starting with 1941, two conventions will be held each year. The annual convention will be held in New York City during January of each year and a summer convention will be held elsewhere than in New York City during June. An exhibition of equipment will continue to be held at the annual convention but there will be none at the summer convention.

Committees

Convention Policies

The Convention Policies Committee met on December 21 and those present were H. P. Westman, chairman and secretary; R. A. Heising, president; Ralph Bown, F. W. Cunningham, L. C. F. Horle, and C. M. Jansky, Jr.

The recommendations of this committee were approved by the Board of Directors and are given in the above report on its annual meeting.

Membership

C. E. Scholz, chairman; I. S. Coggeshall, E. J. Content (representing J. R. Poppele), H. F. Dart, Coke Flannagan, L. G. Pacent, Bernard Salzberg, and J. D. Crawford, assistant secretary, attended a meeting of the Membership Committee on January 3. This meeting was devoted to a discussion of Student and Junior memberships.

Public Relations

On December 21, the Committee on Public Relations met and those present were A. F. Van Dyck, chairman; R. A. Heising, O. H. Caldwell, C. M. Jansky, Jr., B. J. Thompson, and H. P. Westman, secretary.

This was the first meeting of the committee and a substantial portion of its time was devoted to considering the basic problems of the Institute's relations with the public, particularly with those with whom engineers must associate in their professional and business activities. A preliminary report was prepared for the Board of Directors and future meetings will be held to develop more specific reommendations.

Annual Review

The nine committees listed below held meetings on the dates indicated to prepare the material on which the Annual Review for 1939 will be based. This review will be published in the March, 1940, issue of the PROCEEDINGS.

Electroacoustics

This committee met on January 9 and those present were H. S. Knowles, chairman; G. G. Muller (representing J. T. L. Brown), L. J. Sivian, and J. D. Crawford, assistant secretary.

Electronics

P. T. Weeks, chairman; R. S. Burnap, E. L. Chaffee, E. C. Homer (representing H. P. Corwith), Harley Iams (guest), Ben Kievit, Jr., F. B. Llewellyn, L. S. Nergaard (representing B. J. Thompson), R. A. Swan (representing G. D. O'Neill), J. R. Wilson, and J. D. Crawford, assistant secretary; attended a meeting of the Electronics Committee on January 5.

Subcommittee on Cathode-Ray and Television Tubes

This subcommittee of the Electronics Committee met on December 27. Those present were M. S. Glass, R. C. Hergenrother, Harley Iams, T. B. Perkins, and J. D. Crawford, assistant secretary.

Subcommittee on Large High-Vacuum Tubes

E. L. Chaffee, chairman; Robert Lord (representing Alexander Senauke), H. E. Mendenhall, I. E. Mouromtseff, E. E. Spitzer, and J. D. Crawford, assistant secretary; attended a meeting of this subcommittee of the Electronics Committee which was held on December 21.

Subcommittee on Photoelectric Devices

The Subcommittee on Photoelectric Devices of the Electronics Committee met on December 14. Those present were Ben Kievit, Jr., chairman; A. M. Glover, J. H. Miller, F. W., Reynolds (representing E. F. Kingsbury), and J. D. Crawford, assistant secretary.

Subcommittee on Small High-Vacuum Tubes

The Subcommittee on Small High-Vacuum Tubes of the Electronics Committee met on December 15 and those present were R. S. Burnap, chairman; G. W. Bain, R. H. Fidler, R. C. Hergenrother, E. C. Homer (representing H. P. Corwith), H. A. Pidgeon, and J. D. Crawford, assistant secretary.

Facsimile

Two meetings of the Technical Committee on Facsimile were held. The first on December 18 was attended by F. R. Brick, acting chairman; W. A. R. Brown, J. L. Callahan, J. V. L. Hogan, P. Mertz, C. J. Young, and J. D. Crawford, assistant secretary. Those present at the second meeting on January 4 were W. G. H. Finch, chairman; M. W. Baldwin (representing P. Mertz), J. C. Barnes, F. R. Brick (guest), J. L. Callahan, J.W. Milnor, C. J. Young, and J. D. Crawford, assistant secretary.

Radio Receivers

The Technical Committee on Radio Receivers met on December 19 and those present were D. E. Foster, chairman; R. I. Cole, L. F. Curtis (representing D. E. Harnett), D. D. Israel, C. B. McKennie (representing H. B. Fischer), and J. D. Crawford, assistant secretary.

Television

The Technical Committee on Television met on January 8. Those present were E. W. Engstrom, acting chairman; R. R. Batcher, A. B. DuMont, D. E. Foster, Stanford Goldman (representing I. J. Kaar), P. C. Goldmark, T. T. Goldsmith, Jr., A. G. Jensen, H. M. Lewis, R. E. Shelby, and J. D. Crawford, assistant secretary.

Sections

Baltimore

"Recent Advances in Frequency Modulation" was the subject of a paper by E. H. Armstrong, professor of electrical engineering at Columbia University.

A brief history and the theory of amplitude and frequency modulation introduced the subject. It was pointed out that most static eliminators are designed on the theory that the interference was different in nature from the signal for amplitude modulation. Studies have shown static to consist mainly of amplitude-modulated components with a small percentage of frequency modulation.

The frequency-modulated-wave system developed by Professor Armstrong utilizes receivers that are relatively insensitive to the amplitude-modulated components of the static.

An outline of the operation of the system shows that distortion is not dependent

on linearity of tube characteristics but on the linearity of the transformers used with the tubes.

Further advantages accrue from maintaining constant the voltages on the transmitting tubes during full modulation. Views of typical equipment demonstrated a considerable saving in space for a transmitter covering the same primary service area as compared with amplitude-modulated-wave equipment. The difference in behavior of the amplitude- and the frequency-modulated-wave systems during a thunder storm was presented by means of recordings.

December 15, 1939, C. A. Ellert, chairman, presiding.

Cincinnati

G. F. Leydorf, research engineer at WLW, presented a paper on "A High-Frequency Broadcast-Station Field-Coverage Survey." The survey was of W8XNU in Cincinnati, Ohio, which is operated on about 26 megacycles with a power of 1 kilowatt.

The measuring equipment consisted of a rotatable half-wave horizontal dipole mounted on top of an automobile and a measuring set similar to the standard type used in the broadcast band and modified to receive at the transmission frequency.

About 3000 measurements were made and plotted on a map approximately six feet square made from government topographical maps. The uniformity of field strength in adjacent locations which characterizes transmission in the standard broadcast band is not evident at the high frequencies. In the map shown, the attenuation with distance was not uniform but spotted areas of higher signal intensity were found on the sides of hills facing the station and very low signal areas on the opposite sides of the hills.

In the discussion of the paper, P. A. Young and William Alberts, who made the field survey, stated that the signal would flutter if the measuring equipment was operated while the car was in motion. Also, the signal strength varied noticeably when transport airplanes were located between the transmitter and the point of reception. Investigation disclosed that the airplane's dimensions were such as to cause resonance at the transmission frequency.

This was the annual meeting of the section and C. H. Topmiller, chief engineer of WCKY, was elected chairman; P. B. Taylor, of Wright, Field, was named vice chairman; and W. L. Schwesinger, chief transmitter engineer of WSAI, was elected secretary-treasurer.

December 20, 1939, H. J. Tyzzer, chairman, presiding.

Emporium

C. B. Jolliffe, head of the frequency Bureau of the Radio Corporation of America, presented a paper on "Government Regulation of Radio."

The various problems which face the Federal Communications Commission were first discussed and it was pointed out that a mistake on the part of the Commission can have a substantial influence on the whole radio industry. Among the problems which were discussed were those pertaining to frequency allocation, power, and service coverage. Stress was placed on the necessity of careful studies in the allocation of transmission frequencies to such services as frequency-modulated-wave broadcasting, television, police, aircraft, and marine services.

This was the annual meeting and C. R. Smith of the Hygrade Sylvania Corporation was elected chairman and H. L. Ratchford, also of the Hygrade Sylvania Corporation, was named secretary-treasurer. A dinner preceded the meeting with W. R. Jones acting as toastmaster. Brief remarks were made by each of the previous chairman of the section.

December 19, 1939, R. K. McClintock, chairman, presiding.

Montreal

J. T. Henderson, chief of the radio section of the National Research Council, presented a paper on "Cathode-Ray Direction Finders."

An outline was given of the early history of the subject following the original suggestion by Watson-Watt in England about 1915. The Research Council started active work on the subject about 1934 and descriptions were given of early models and also of long-wave fixed stations which were set up near Winnipeg and Ottawa for the directional study of atmospherics. Both loop and Adcock aerials were used. The relative advantages and disadvantages of cathode-ray and of aural null systems were described. A demonstration concluded the paper.

December 13, 1939, A. B. Oxley, chairman, presiding.

Philadelphia

"Recent Changes in Radio-Tube-Manufacturing Technique" was the subject of a paper by R. M. Wise, chief engineer of the Hygrade Sylvania Corporation.

Many of the changes in manufacturing resulted from the introduction of the loktal tubes. This type is of small size, features short connecting leads to the tube elements, is readily shielded, and is adapted to quantity-production methods. It differs from previous tubes in the substitution of a caplike header in place of the stem construction, the elimination of the usual base through the use of direct-connecting pins, and the elimination of connections through the top of the bulb.

It was pointed out that new equipment is required for bulb cutting and for header manufacture. Changes are necessary in the sealing and exhaust equipment, the latter operation being simplified. Illustrations were presented of the equipment used in manufacture and also showing constructional details of some of the tubes being produced.

December 7, 1939, R. S. Hayes, chairman, presiding.

Seattle

"Remotely Controlled Radio Receiving Systems" was the subject of papers presented by three representatives of the Pacific Telephone and Telegraph Company.

F. B. Mossman, engineer, presented a technical description of the remotely controlled radio receiver used in the ship-to-shore links to the telephone system. These receivers are unattended and usually mounted on poles located strategically in relation to the harbor and coastal craft which transmit to them. To permit operation with either weak or strong incoming signals under various conditions of noise, the noise and the signal are separately amplified, rectified, and connected to the windings of a differential polar relay. The relay operates on the differences between the noise and the signal levels, operating when the signal disappears to short-circuit the receiver output and put into operation the associated transmitter which may be located a substantial distance from the receiver. This monitoring equipment is known as a codan. Special testing equipment permitting the operation of the receiver to be checked by remote control over telephone lines was also described.

O. C. Smith, engineer, demonstrated the operation of the codan by means of an emergency portable transmitter-receiver unit.

W. A. Thies, commercial representative, presented a brief history of the Seattle installation. The transmitter is located at Puget Sound. One of the receivers is also located there and the other is at Grays Harbor on the coast. A method of operating the equipment was described and the paper concluded with the placing and completing of a call to a ship located about 450 miles northeast of Seattle. The audience was able to listen to all phases of the switching and talking.

December 14, 1939, R. O. Bach, chairman, presiding.

Membership

The following indicated admissions to membership have been approved by the Admissions Committee. Objections to any of these should reach the Institute office by not later than February 29, 1940.

Admission to Associate (A) and Student (S)

Albright, C. M., Jr., (S) 100 Ridgewood Rd., Ithaca, N. Y.

Amokasu, K., (S) Ofuna-Machi, Kanagawa-Ken, Japan.

Arner, R. C., (A) 500 S. Superior St., Angola, Ind.

Ashman, G. L., (A) 27 Gedeney Rd., Tottenham, London N.17, England.

Bailey, V. G., (S) 2205—12th St., Troy, N. Y.

Beveridge, H. N., (S) Engineering Bldg., McGill University, Montreal, Que., Canada.

Blades, J. E., (A) 458 Morris Ave., Elizabeth, N. J.

Bolster, R. O., (S) 1027 Braman, Lansing, Mich.

Branch, B. S., (S) 81 Oxford St., Cambridge, Mass.

Burks, H. B., Jr., (S) 110—21st Ave., S., Nashville, Tenn.
Carter, H. J., (A) 1336 Kennedy St., N.W., Washington, D. C.
Chambers, T. H., (S) 116 Ardmore Ave., Ardmore, Pa.
Chapin, R. S., (S) Box 382, College Station, Durham, N. C.
Clark, S. F., (A) 3924 Duvall Ave., Baltimore, Md.
Collins, E. H., (A) Albany College, 1230 S.W. Main, Portland, Ore.
Conner, R. W., (A) 509 Maryland St., Peoria, Ill.
Coolidge, A. W., Jr., (S) 210 Summer Ave., Reading, Mass.
Corbin, E. D., (A) 916 Jackson St., Fort Wayne, Ind.
Corkill, J. F., (A) 201 Beechwood Ave., Catonsville, Md.
Dana, J. J., (A) 1117 Venice Blvd., Los Angeles, Calif.
Davenport, W. B., Jr., (S) 141 S. Gay St., Auburn, Ala.
De Grey, E. H., (S) 4015 Grey Ave., Montreal, Que., Canada.
Doss, P. B., (A) c/o B. Anandam, Mgr., Mica Mines, Sydapuram P.O., S. India.
Evans, A. R., (S) 331 W. Gold St., Butte, Mont.
Fiet, O. O., (S) 2042 Quincy Ave., Ogden, Utah.
Finegold, I., (A) Y.M.C.A., Elyria, Ohio.
Gams, T. C., (S) Price Hall, Lehigh University, Bethlehem, Pa.
Gessert, E. C., Jr., (S) 927—12th St., Boulder, Colo.
Giles, T. A., (A) 113 W. Glen, Peoria, Ill.
Gross, J., (A) Box 179, Nairobi, Kenya Colony, British East Africa.
Hadley, F. P., (A) U.S.N. Radio Station, Winter Harbor, Me.
Halsall, M., (S) 2343 Morris Ave., New York, N. Y.
Hargreaves, W., (A) 39 Point Chevalier Rd., Auckland, N. Z.
Herman H., (S) 1729 Webster St., N.W., Washington, D. C.
Houston, R. H., (S) 135 S. Gay St., Auburn, Ala.
Henry Jasick, 1374 Somerset Pl., N.W., Washington, D. C.
Jessee, F. L., (A) R.F.D. 1, Paterson, N. J.
King, S., (S) 6 East Campus, Easton, Pa.
Larsen, J. F., (A) Gasvaerksvej 3, Copenhagen V, Denmark.
LaViolette, R. F., (A) 927 S. Beacon Ave., Los Angeles, Calif.
Leyland, A. J., (A) Automatic Telephone & Electric Co., Ltd., Liverpool 7, England.
Lynch, Edmund, Jr., (S) 22 N. Grandview Ave., Crafton, Pa.
Mayer, R. H., (S) Athenaeum, California Institute of Technology, Pasadena, Pa.
McCoy, R. D., (A) 30 McIntyre St., Bronxville, N. Y.
McNeill, L. P., (S) Box 3313, University of Kentucky, Lexington, Ky.
Merson, L. N., (S) 189 Mozart St., W., Montreal, Que., Canada.
Mills, C. A., Jr., (A) 223 Douglass St., Reading, Pa.
Nicolosi, J., (S) 1657-75th St., Brooklyn, N. Y.
Norvik, F. J., (S) 95 Homewood Ave., Watervliet, N. Y.
Parr, J. O., Jr., (A) 317—6th St., San Antonio, Tex.
Preston, F., (A) 760 Algonquin Ave., Detroit, Mich.
Rothstein, J., (S) 605 W. 137th St., New York, N. Y.
Rowland, D. H., (S) 721 Arlington Ave., Plainfield, N. J.
Runge, W. C., (A) 6509 N. Talman Ave., Chicago, Ill.
Satullo, A. R., (S) 3407 E. 102nd St., Cleveland, Ohio.
Schwarz, C. R., (A) 245 Schrader St., San Francisco, Calif.
Scott, G., (A) c/o Tudor Cinema, Remuera, Auckland S.E. 2, New Zealand.
Sedon, P. H., (A) 314 W. Mathew St., Jonesboro, Ark.
Shackell, S. M., (S) 801 S. First Ave., Highland Park, N. J.
Sharp, A. C., (A) Radio Station WUY, Fort Crockett, Galveston, Tex.
Smith, J. L., (A) 506 N. Orange Dr., Los Angeles, Calif.
Solbrig, A. L., (A) 20 Naussau Blvd., Malverne, L. I., N. Y.
Sugnet, R. F., (S) 112 Howard Hall, Notre Dame, Ind.
Szenert, G., (A) Tucman 950, Dto. 4, ler piso, Buenos Aires, Argentina.
Thomson, A., (S) 5571 S. E. Oak St., Portland, Ore.
Tregidga, A. C., (A) Electrical Engineering Department, Kansas State College, Manhattan, Kan.
Tucker, J. W., (S) Box 881, Virginia Polytechnic Institute, Blacksburg, Va.
Varian, R. H., (A) Box 2654, Stanford University, Calif.
Wang, C. S., (A) Research Laboratory of Electricity, Box 18, Chungking, China.
Warren, J. R., (A) 270 Stanley Ave., Hamilton, Ont., Canada.
Watters, R. L., (S) 114 Dillon Hall, Notre Dame, Ind.
Wendroff, M., (A) 2333 E. 22nd St., Brooklyn, N. Y.
Werner, I. A., (A) 121 N. Kinney St., Angola, Ind.
Yeaton, E. C., (S) 203 Lake St., Ithaca, N. Y.

Books

Simplified Filter Design, by J. Ernest Smith

Published by RCA Institutes Technical Press, 75 Varick St., New York, N. Y. 57 pages, 8½×11 inches. Price $1.00.

After a few pages of introduction and general formulas, this handbook gives the attenuation characteristics of numerous filters, both individual sections and groups of sections. There are 12 charts on individual sections and 14 on three-section filters of various band widths. Most of the space is devoted to *m*-derived filters with trap circuits.

The volume is recommended as an aid in the practical design of filters where the requirements do not justify the work involved in the synthesis of the filters from basic principles.

H. A. Wheeler
Hazeltine Service Corporation
Little Neck, L. I., N. Y.

Radio Service Trade Kinks, by Lewis S. Simon

Published by the McGraw-Hill Book Co., Inc., 330 West 42nd St., New York, N. Y. 254 plus 15 pages. 9×11¼ inches. Price $3.00.

This book gives the results of the author's experience dating back to 1921 in servicing receivers of many makes. The purpose of the volume is to state specific directions for repairing sets, as opposed to general presentation of principles. The arrangement is by specific make and model of receiver, with the common complaints, the cause, and the cure, for each model. The text proceeds alphabetically through the many lines of sets which have been sold in the United States, taking up numerous models of the various lines. In addition to the text, a total of 27 drawings are given to illustrate certain points.

The volume, therefore, has great value for the service man, but is not of special interest to the engineer unless he is concerned with service matters.

C. E. Dean
Hazeltine Service Corporation
Little Neck, L. I., N. Y.

Servicing by Signal Tracing, by John F. Rider

Published by John F. Rider, 404 Fourth Ave., New York, N. Y., 360 pages. 5¾×8¼ inches. Price $2.00.

This volume describes the signal-tracing method devised by the author, who is a well-known writer for servicemen. In this method the defective portion of a receiver is located as the first point at which the signal fails or departs from normal characteristics. At least one instrument is available having suitable sensitive vacuum-tube voltmeters for observing weak potentials at radio frequency, intermediate frequency, and audio frequency for the signal-tracing procedure. The signal-tracing method is in contradistinction to the methods of locating faults in receivers by the measurement of direct-current voltages at various points in the circuit, or by checking the direct-current resistance of various paths.

This book includes accounts of the operation of the chief types of circuits found in radio receivers. In addition, the volume has general treatments of public-address systems and television receivers. Short accounts are also given of facsimile receivers, and receivers for frequency-modulated-wave sound broadcasts. The application of the signal-tracing method in the various cases is well described. A brief chapter at the end discusses the application of the signal-tracing technique in receiver design, pointing out its convenience for locating faults, and giving a few words about its use in other design work.

One of the last chapters discusses various features of service instruments suitable for signal tracing. This chapter describes, in particular, various points of the Rider Chanalyst, an instrument designed by the author. For engineers who have not been concerned with the service field, it may be mentioned that this instrument is an ingenious arrangement including the following parts: (1) a tunable vacuum-tube voltmeter for observing the output of the superheterodyne oscillator of the receiver over most of the range in the usual all-wave design; (2) another tunable vacuum-tube voltmeter covering the intermediate-frequency and broadcast ranges; (3) an audio-frequency tube voltmeter; (4) an electronic direct-current voltmeter for observing automatic-volume-control voltages and other direct potentials; and (5) a novel wattmeter arrangement for checking the power taken from the line by the receiver under test. Four electric-eye tubes are used as reference indicators for the three signal voltmeters and the wattmeter.

The present volume is an excellent text for the serviceman, and will be of interest to engineers working in other fields who are desirous of an acquaintance with modern broadcast receivers. The same applies to the treatment of television receivers, this occupying 60 pages of the text. The subject matter throughout the book is presented in elementary terms, so that the text may be followed rapidly.

C. E. Dean
Hazeltine Service Corporation
Little Neck, L. I., N. Y.

Cathode-Ray Tubes, by Manfred von Ardenne.

(Translated from the German by G. S. McGregor and R. C. Walker.) Published in 1939 by Isaac Pitman and Sons, Ltd., London. Pitman Publishing Corp., New York, N. Y. 530 pages, 465 illustrations. Price $12.50.

This is an English translation of an elaborately prepared work on cathode rays and their applications, first written in 1933 by this well-known German scientist. While cathode-ray tubes were known and used for many years before von Ardenne entered the field, still the tubes which he produced and popularized came at the start of the present era of oscillography with its simplified operation and really brilliant traces.

During the ensuing years the technical press of Germany printed hundred of articles on the various important aspects of the art, notably in the field of electron focusing. Von Ardenne and his associates, co-operating with Leybold's (one of the pioneer concerns engaged in cathode-ray-tube manufacture) have been responsible for many of these advancements.

This book contains four sections, each taking up one phase of the problem. Chapter I is devoted to the theory and development of various types of the tube, for both general usage and special purposes. The treatment in this section is quite complete, at least insofar as low-voltage sealed-off oscillograph tubes are concerned.

The second section describes the accessories needed, since a cathode-ray tube is useless without certain associated items of equipment. Power sources, deflection amplifiers, sweep circuits, and the numerous devices which permit the study of non-electrical quantities, are described here. Screen photography, for making permanent records of oscillograms, is also taken up.

The third section treats the measurement processes, circuits, and technical equipment needed for making various tests. The fourth section is called "The Cathode-Ray Tube as an Operating Unit" and discloses certain nonoscillographic applications which have been devised utilizing various features exhibited by cathode rays. This section is mainly devoted to television, giving an up-to-date supplement to the same author's book "Television Reception." It also describes the use of a cathode-ray tube in sound film recording.

The author has provided an interesting treatise with a minimum of mathematics and particularly free from misstatements, and the translators have done a remarkable job in carrying the work into easily read English. Although this book is a translation of the original German text, the author has rewritten a large portion, so as to bring in the details of the improvements that have come about in recent years. The rewritten portion concerns mainly the section on television and certain other applications which have become important.

On page 309, one discrepancy was noticed dealing with a nomograph which shows the permissible spot-travel speed for good photographic recording. This chart does not provide a solution to the formula shown on that page. The chart solves an equation $V \alpha E^2 I$, whereas the formula shown is in the form $V \alpha EI$. However, in practice the whole problem is full of assumptions, so that the relationship between the brilliance and the first (or second) power of the anode voltage is subject to corrections. When American films, lenses, and fluorescent materials are used, neither the chart nor the formula can be taken to show more than a trend or approximation.

The book is an excellent reference for any laboratory using these instruments. It contains a great many illustrations and circuits, most of the latter with circuit constants. Several hundred bibliographical references are also included, each of which definitely takes up some specific matter referred to in the text.

R. R. Batcher
Hollis, L. I., N. Y.

A Textbook on Light, by A. W. Barton

Published by Longmans, Green and Co., 114 Fifth Ave., New York, N. Y. 417 pages plus 5-page index. 278 illustrations. Price, $3.00.

To the increasing number of radio engineers who require an elementary knowledge of the principles pertaining to light the recently published English book by A. W. Barton entitled "A Textbook on Light" will be welcome. The subject is presented by considering all of the facts and theories bearing on it, rather than by factual statements of generally accepted ideas, with the thought that this approach will help to develop the power of discrimination. While the treatment is by no means exhaustive it is adequate to meet the needs of radio engineers. It covers refraction, reflection, defects of images formed by a single lens, achromatic lenses, interference, diffraction, optical instruments, photometry, properties and theory of waves, and the corpuscular and wave theory of light.

The illustrations of Plates I and III, opposite pages 97 and 130, are most helpful in making clear the difference in the results when using an ordinary and an achromatic lens, a large and a small aperture, and also the effect of other types of distortion. It should be pointed out that the recommended illumination for various types of rooms is below what is now considered good practice in this country. The author has included a description of the classical methods of Romer, Fizeau, Foucault, and Michelson for measuring the velocity of light which always stimulates the imagination. He examines the experimental evidence for and against the corpuscular and wave theories of light and ends with a chapter entitled "The Renaissance of the Corpuscular Theory." The reviewer enjoyed reading the book and he believes others will also find it interesting and useful.

H. M. Turner
Yale University
New Haven, Conn.

Contributors

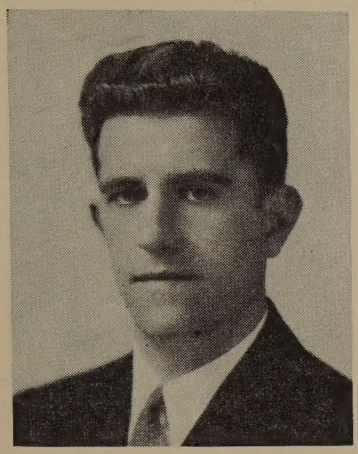

F. A. Everest

F. Alton Everest (A'38) was born on November 21, 1909, at Gaston, Oregon. He received the B.S. degree in electrical engineering from Oregon State College in 1932 and after two years of graduate work received the E.E. degree from Stanford University in 1936. For six months he worked on television development for the Don Lee Broadcasting System after which he became an instructor in electrical engineering at Oregon State college and in 1939, assistant professor. Mr. Everest is a member of Eta Kappa Nu and Sigma Xi and is an associate member of the American Institute of Electrical Engineers.

❖

Pierre M. Honnell (J'27–A'29) was born on January 28, 1908, in Paris, France. Upon graduation from the Agricultural and Mechanical College of Texas in 1930, he was commissioned in the Signal Corps Reserve, and now is a First Lieutenant. The next three years were spent as a member of the Technical Staff of Bell Telephone Laboratories. During the year 1933–1934, he attended the Technischen Hochschule in Vienna and the Conservatorie des Arts et Metiers in Paris. As research geophysicist with the Texas Company from 1934 to 1938, he was engaged in the design of seismological apparatus. For the past two years he has pursued graduate studies at the Massachusetts (M.Sc. 1938) and California Institutes of Technology. He is a member of the Society of Exploration Geophysicists and Sigma Xi.

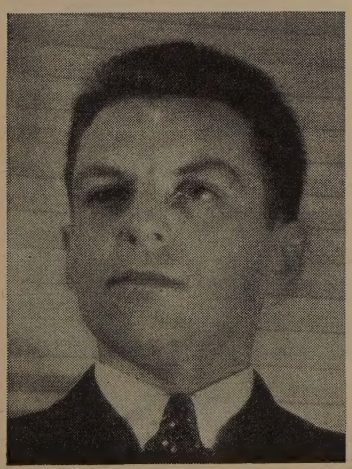

P. M. Honnell

❖

W. E. Jackson (A'29–M'34) was born on May 8, 1904, at Bridgewater, Massachusetts. He received the B. S. degree in electrical engineering from Brown University in 1925. Mr. Jackson was with the Westinghouse Electric and Manufacturing Company in 1923; the New England Telephone and Telegraph Company in 1924; a radio engineer with the General Electric Company from 1925 to 1927; radio engineer with the Department of Commerce. Air Navigation Division, Bureau of Air Commerce from 1932 to 1937; chief of the Radio Development Section, Safety and Planning Division, Bureau of Air Commerce, 1937 to date. He has been chairman of the Radio Technical Committee for Aeronautics since 1937. He is a member of Sigma Xi.

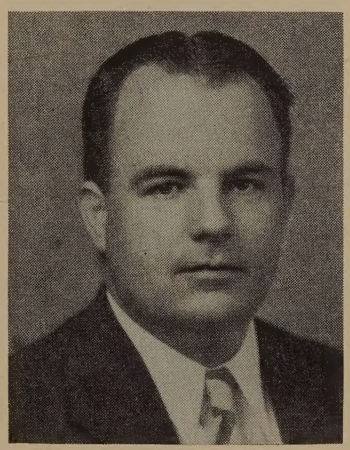

W. E. Jackson

❖

Herbert R. Johnston was born in June, 1908, at Chicago, Illinois. He was graduated from the University of Illinois with the B.S. degree in electrical engineering in 1931, later spending two years at Oregon State College as a graduate assistant in electrical engineering and receiving the M.S. degree in 1939. Mr. Johnston is a member of Tau Beta Pi, Etta Kappa Nu, and an associate member of Sigma Xi. At the present time he is employed in the Engineering Testing Department of the Automatic Electric Company of Chicago.

❖

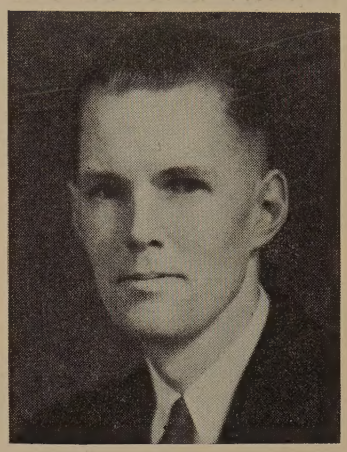

H. R. Johnston

❖

Ronold King (A'30) was born on September 19, 1905, at Williamstown, Massachusetts. He received the B. A. degree in 1927 and the M. S. degree in 1929 from the University of Rochester and the Ph.D. degree from the University of Wisconsin in 1932. He was an American-German exchange student at Munich from 1928 to 1929; a White Fellow in physics at Cornell University from 1929 to 1930; a Fellow in electrical engineering at the University of Wisconsin from 1930 to 1932. He continued at Wisconsin as a research assistant from 1932 to 1934. From 1934 to 1936 he was an instructor in physics at Lafayette College, serving as an assistant professor in 1937. During 1937 and 1938 Dr. King was a Guggenheim Fellow at Berlin. In 1938 he became instructor in physics and communication engineering at Harvard University, advancing to assistant professor in 1939.

❖

Ronold King

JOHN D. KRAUS

John D. Kraus (A'32) was born at Ann Arbor, Michigan, on June 28, 1910. He received the B.S. degree in 1930, the M.S. degree in 1931, and the Ph.D. degree in physics in 1933 from the University of Michigan. He was a research associate in the Department of Engineering Research of the University of Michigan from 1934 to 1935 and a research physicist in the Department of Physics from 1936 to 1937. From 1937 to 1938 Dr. Kraus was a research physicist with the Physicists Research Company, and since 1938 he has been engaged in independent research. He is a member of Sigma Xi, the American Physical Society, and the Acoustical Society of America.

❖

Tyng M. Libby (A'14–M'17) was born August 9, 1889 in Kingman, Kansas. He served in the United States Navy from 1906 to 1910 as a radio operator during which time he was awarded the Bailey Medal. From 1911 to 1917 he was employed in the Puget Sound Navy Yard as a radio electrician. In 1918 he went to the Todd Dry Dock and Construction Company as an electrical draftsman and left there in 1924 to enter the radio merchandising business. In 1929 he became associated with The Pacific Telephone and Telegraph Company as an Engineer, where he has been to date.

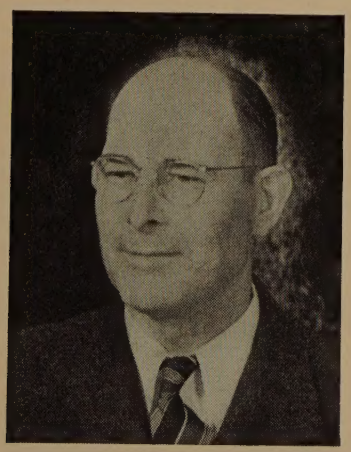

T. M. LIBBY

❖

Peder Oluf Pedersen (F'15) was born in Sig, Denmark, on June 19, 1874. He was graduated with honors in civil engineering from the Royal Technical College in 1897. In 1899 he became associated with Valdemar Poulsen in his development work on the telegraphone and later aided in the development of the Poulsen-arc system for continuous-wave wireless telegraphy and telephony.

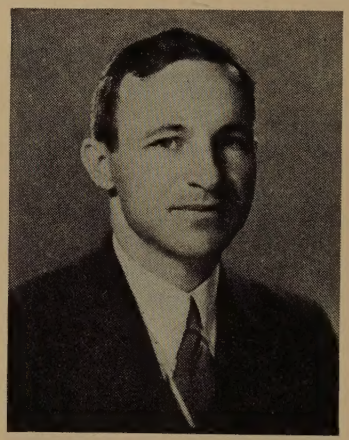

Brown Dunkins Photo Reflex

C. F. SHEAFFER

In 1909, Dr. Pederson was appointed an assistant professor of telegraphy, telephony, and radio at the Royal College at Copenhagen, becoming professor in 1912, which chair he still holds. In 1922 he was appointed principal of that college. He received the Ph.D. degree from the University of Copenhagen in 1929. In 1907 he received the Gold Medal of the the Royal Danish Society of Sciences; in 1929, the C. H. Oersted Medal; and in 1930, the Institute Medal of Honor. Dr. Pedersen is a member of numerous technical societies and was vice president of the Institute during 1939.

❖

Grote Reber (A'33) was born on December 22, 1911. He received the B.S. degree from Armour Institute of Technology in 1933. He was a radio engineer for General Household Utilities in 1933 and 1934 and was with the Stewart Warner Corporation from 1935 to 1937. Mr. Reber attended the University of Chicago during 1938, and in 1939 he went with the Research Foundation of Armour Institute of Technology. He is an associate member of the American Rocket Society and the Chicago Astronomical Society.

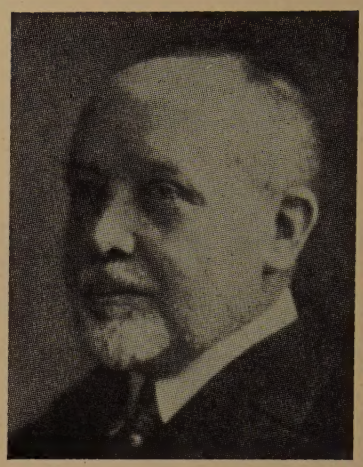

P. O. PEDERSEN

❖

Charles F. Sheaffer (A'36) was born at Shawnee, Oklahoma, on December 31, 1907. Since 1923 he has been active as a radio amateur and experimenter. From 1927 to 1934 he was chief engineer of the Oklahoma Broadcasting Company. Since 1934 Mr. Sheaffer has been a member of the engineering staff of the Tulsa Broadcasting Company, operators of KTUL.

❖

For biographical sketches of T. R. Gilliland, S. S. Kirby, and N. Smith, see the PROCEEDINGS for January, 1940.

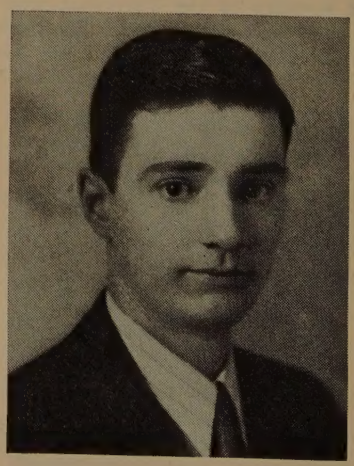

GROTE REBER